KONINKLIJKE NEDERLANDSE AKADEMIE VAN WETENSCHAPPEN

PROCEEDINGS

SERIES B

PHYSICAL SCIENCES

VOLUME LXIII - No. 5

NORTH-HOLLAND PUBLISHING COMPANY - AMSTERDAM - 1960

The complete Proceedings consist of three Series, viz.:

SERIES A: MATHEMATICAL SCIENCES

SERIES B: PHYSICAL SCIENCES

SERIES C: BIOLOGICAL AND MEDICAL SCIENCES

Articles for these Series cannot be accepted unless formally communicated for publication by one of the members of the Royal Neth. Academy of Sciences.

STRUCTURE AND ZEEMAN EFFECT IN THE SPECTRA OF THE OSMIUM ATOM, Os I AND Os II
IV

BY

TH. A. M. VAN KLEEF

Zeeman-laboratory, University of Amsterdam, the Netherlands

(Communicated by Prof. J. DE BOER at the meeting of January 30, 1960)

TABLE III *(continued)*

Classified lines of Os I

Int.	λ_{air}	$\sigma_{vac.}$	Classification	$\delta\sigma$	Zeeman effect		Notes
30	3789.106	26383.95	4123(3)– 148(4)	+0.02	(0)	1.09	
80	3790.14	26376.76	4122(5)– 148(4)	—0.21	$g_1 = 1.27$	$g_2 = 1.08$	
100	3790.731	26372.64	4122(5)– 149(6)	—0.05	(**0**, 0.13, 0.26, 0.40)	**0.87** ...	
			4258(0)– 162(1)	+0.01	(0)	1.74	9
(4)	3791.061	26370.35					B
			4626(4)– 198(4)	—0.04			
($\frac{1}{2}$)	3791.992	26363.87	4577(3)– 194(2)	—0.02			B
			5032(3)– 239(3)	—0.06			
40	3794.662	26345.33					
			5467(3)–2833(4)	+0.14	(**0**, 0.25)	**0.84** ...	9
	3795.245	26341.31	5475(2)– 284(3)	+0.06			A
40	3795.667	26338.35	5063(6)– 242(5)	+0.06	(0)	1.08	
	3796.179	26334.83	4172(4)– 153(3)	+0.01			A
(8)	3799.563	26311.35	4761(3)– 213(2)	+0.07	$g_1 = 1.12$	$g_2 = 1.25$	B
(1)	3799.896	26309.04	5029(4)– 239(3)	+0.06			B
50	3800.437	26305.29	5467(3)–2837(3)	+0.01	(... **0.20**)	1.78	
(?)	3800.770	26302.99	5540(5) 2909(6)	—0.07			B
20	3801.604	26297.22	4961(2)– 233(2)	—0.02	$g_1 = 1.11$	$g_2 = 1.27$	
5h	3802.612	26290.25	5027(4)– 239(3)	—0.08			
	3803.479	26284.28	6064(4)–3436(5)	+0.12			A
($\frac{1}{2}$)	3804.119	26279.83	4538(4)– 191(4)	+0.01			B
(4)	3809.667	26241.56	5131(2)– 250(2)	+0.03	(**0.04**)	0.89	B
(4)	3810.438	26236.25	4753(2)– 213(2)	+0.03			B
	3811.221	26230.89	5868(3)–3245(2)	+0.13			A
			4953(5)– 234(4)	—0.11			
(df$\frac{1}{2}$)	3814.035	26211.51					B
			5050(4)– 242(5)	—0.05			
			4242(1)– 162(1)	+0.02	$g_1 = 1.87$	$g_2 = 1.74$	9
30	3814.259	26209.97					
			4877(2)– 225(1)	+0.13			
8	3818.641	26179.89	3634(2)– 101(2)	+0.06	(0)	—	2
	3820.814	26165.04	5175(3)– 255(3)	+0.33			A, 1

TABLE III *(continued)*

Classified lines of Os I

Int.	λ_{air}	$\sigma_{vac.}$	Classification	$\delta\sigma$	Zeeman effect		Notes
			(4948(4)– 234(4)	0.00			
8	3821.642	26159.33					
			(5122(3)– 250(2)	+0.41			1
	3821.787	26158.37	5928(3)–3312(3)	0.00			A
(2)	3821.977	26157.04	5175(3)– 256(4)	—0.06	(0)	1.14	B
	3822.808	26151.39	4556(3)– 194(2)	+0.06			A
(½)	3823.304	26147.97	5121(1)– 250(2)	—0.06			B
	3824.878	26137.24	5672(4)–3059(4)	—0.47			A, 1
30	3826.634	26125.21	5113(3)–2501(3)	+0.01	(0.05)	1.72	
50	3827.136	26121.79	4873(4)–2261(4)	+0.04	$g_1 = 1.50$	$g_2 = 1.62$	
	3829.612	26104.93	5922(2)–3312(3)	—0.43			A, 1
(1)	3830.094	26101.61	3887(1)– 127(2)	+0.02			B
(1)	3831.392	26092.80	4550(2)– 194(2)	+0.01			EH
30l	3832.176	26087.43	4229(1)– 162(1)	+0.01	$g_1 = 1.00$	$g_2 = 1.74$	
	3832.672	26084.08	5876(4)–3268(4)	—0.07			A
(½)	3834.228	26073.47	5342(2)– 273(3)	+0.18			B
(1)	3835.925	26061.93	5165(2)– 255(3)	—0.07			B
150	3836.056	26061.04	3480(4)– 87(4)	+0.05	(... 0.23)	1.35	
	3838.290	26045.91	5917(2)–3312(3)	—0.04			A
	3839.894	26035.03	4715(4)– 211(3)	+0.21			A
150	3840.304	26032.22	5513(6)–2909(6)	0.00	(... 0.12)	1.47	
30	3841.292	26025.52	5103(4)–2501(3)	—0.04	$g_1 = 1.59$	$g_2 = 1.73$	
(2)	3841.671	26022.95	4036(4)– 143(5)	+0.02			B
80	3843.665	26009.45	4123(3)– 152(2)	+0.04	$g_1 = 1.08$	$g_2 = 1.62$	
	3843.991	26007.28	5538(3)–2938(3)	+0.06			A
	3844.602	26003.15	5868(3)–3268(4)	—0.44			A, 1
(4)	3844.835	26001.54	5029(4)– 242(5)	—0.05	(0)	—	B
(½)	3845.710	25995.62	4008(4)– 140(3)	—0.02			B
15	3846.411	25990.89	4489(4)– 189(3)	+0.16	(0)	—	
(1)	3846.955	25987.21	5333(3)– 273(3)	—0.05			B
(1)	3847.588	25982.96	5027(4)– 242(5)	+0.02			EH
(2)	3847.852	25981.15	5910(2)–3312(3)	—0.32			B
125	3849.944	25967.04	3874(2)– 127(2)	+0.23	$g_1 = 1.59$	$g_2 = 1.00$	
			(4029(6)– 143(5)	+0.05			
	3852.253	25951.50					A
			(5154(2)– 255(3)	—0.44			1
100	3853.439	25943.49	4361(2)– 176(1)	+0.02	$g_1 = 1.05$	$g_2 = 1.41$	
8	3853.589	25942.48	5622(5)–3027(5)	+0.02			
30	3854.705	25934.97	5503(5)–2909(6)	+0.03	(0)	1.57	
	3854.925	25933.52	4705(3)– 211(3)	—0.11			A
(1)	3856.925	25920.04	5098(2)– 250(2)	—0.02	(0)	—	B, 11
150	3857.089	25918.94	3007(2)– 41(3)	—0.02	(0)	1.44	
(4)	3862.673	25881.47	4577(3)– 198(4)	—0.01	(0)	0.94	B
10	3865.045	25865.58	4575(5)– 198(4)	+0.02			
125	3865.469	25862.75	5113(3)–2527(2)	+0.04	$g_1 = 1.71$	$g_2 = 2.04$	2
10	3866.480	25855.98	3887(1)– 130(1)	+0.08			
			(4840(1)– 225(1)	—0.06			
	3868.034	25845.61					A
			(6064(4)–3480(4)	—0.06			

TABLE III

Classified lines of Os I

Int.	λ_{air}	$\sigma_{vac.}$	Classification	$\delta\sigma$	Zeeman effect		Notes
30	3868.686	25841.24	4123(3)– 153(3)	+0.02	(0.91, 1.37)	—	
(½)	3869.005	25839.09	3861(1)– 127(2)	+0.03			B
	3870.024	25832.31	5895(3)–3312(3)	—0.45			A
(½)	3873.031	25812.23	4492(5)– 191(4)	—0.02	(0)	—	B, 11
20	3873.724	25807.63	5359(2)–2778(1)	—0.12	(0)	0.49	
	3875.509	25795.78	3682(4)– 110(4)	—0.03			A
(1+)	3875.691	25794.57	4911(2)– 233(2)	+0.07			EH
300	3876.768	25787.37	3681(5)– 110(4)	+0.01	$g_1 = 1.29$	$g_2 = 1.16$	
20	3877.307	25783.79	4489(4)– 191(4)	—0.01			
			5890(3)–3312(3)	—0.45			1
(½)	3877.835	25780.27					B
			5313(4)– 273(3)	—0.02			
(2)	3877.967	25779.40	4681(2)– 210(1)	—0.02			B
(8)	3878.527	25775.67	3680(3)– 110(4)	—0.02	$g_1 = 1.48$	$g_2 = 1.16$	B
	3879.390	25769.97	4343(2)– 176(1)	+0.18			A
			4466(2)– 189(3)	—0.24			
10	3880.768	25760.79			(0)	—	2, 12
			4486(3)– 191(4)	—0.05			
			3591(1)– 101(2)	—0.01	$g_1 = 1.29$	$g_2 = 1.45$	9
125	3881.858	25753.56					
			4705(3)– 213(2)	—0.37			1
	3882.699	25748.01	4008(4)– 143(5)	—0.01			A
	3884.528	25735.89	4905(1)– 233(2)	—0.11			A
(1)	3884.596	25735.41	5132(4)– 255(3)	+0.05			B
20	3885.749	25727.77	5132(4)– 256(4)	+0.02			
30	3886.750	25721.14	3874(2)– 130(1)	+0.02	(0)	—	
(1)	3891.585	25689.19	4681(2)– 211(3)	—0.02			B
(?)	3892.823	25681.02	4472(1)– 190(0)	0.00	(0)	—	B
(?)	3893.367	25677.43	5346(1)–2778(1)	+0.22			B, 3
(—)	3894.662	25668.89	4556(3)– 198(4)	—0.03			B
20	3895.177	25665.50	4088(2)– 152(2)	+0.02			
			4677(3)– 211(3)	—0.15			
(1)	3897.158	25652.48					EH
			5406(2)– 284(2)	+0.03			
	3898.406	25644.27	5876(4)–3312(3)	—0.01			A
(1)	3899.03	25640.14	5359(2)–2795(2)	—0.08			EH
	3899.863	25634.69	5122(3)– 255(3)	0.00			A
			2837(3)– 27(2)	—0.02	$g_1 = 1.74$	$g_2 = 1.43$	9
50	3900.394	25631.17					
			5622(5)–3059(4)	+0.21			
	3900.528	25630.32	4961(2)– 239(2)	+0.06			A
10	3901.005	25627.16	5122(3)– 256(4)	+0.08	(0 ...)	—	
	3901.392	25624.64	5975(3)–3412(3)	0.00			A
150	3901.708	25622.54	3436(5)– 87(4)	+0.04	$g_1 = 1.42$	$g_2 = 1.31$	
(1)	3906.143	25593.45	3861(1)– 130(1)	+0.08	(0)	—	B
(4)	3907.651	25583.57	3967(2)– 140(3)	+0.05	(0)	1.33	B, 11
	3910.049	25567.88	5609(2)–3052(1)	+0.34			A, 1
(1)	3911.666	25557.32	4887(3)– 233(2)	—0.01	(0)	—	B
30	3911.812	25556.36	3833(2)– 127(2)	—0.01			

TABLE III *(continued)*

Classified lines of Os I

Int.	λ_{air}	$\sigma_{vac.}$	Classification	$\delta\sigma$	Zeeman effect		Notes
	3912.432	25552.34	4887(3)– 234(4)	+0.07			A
	3912.736	25550.36	5115(5)– 256(4)	0.00			A
(4)	3918.741	25511.17	3887(1)– 133(2)	+0.03	(0)	—	B
30	3918.971	25509.67	4681(2)– 213(2)	+0.16			
			5346(1)–2795(2)	—0.01	(0, 0.66)	—	9
(1)	3919.236	25507.95	5364(2)– 281(3)	+0.20	(0)	1.11	B
20	3920.870	25497.32	4088(2)– 153(3)	+0.03	(0, 0.72	—	9
			4948(4)– 239(3)	—0.09			
(½)	3921.130	25495.63	4538(4)– 198(4)	+0.01	(0)	—	B
30	3922.033	25489.76	3826(3)– 127(2)	—0.02	(0, 0.23, 0.45)	—	
	3923.177	25482.36	4651(1)– 210(1)	+0.36			A, 1
	3924.620	25472.96	4677(3)– 213(2)	+0.03			A
30	3925.103	25469.82	3824(1)– 127(2)	0.00	$g_1 = 1.56$	$g_2 = 1.01$	
30	3926.770	25459.01	4486(3)– 194(2)	—0.04			
			4387(5)– 184(5)	+0.01	(0)	1.12	9
(1)	3927.250	25455.90	4877(2)– 233(2)	+0.01	(... 0.24)	—	B
(1)	3928.163	25449.98	3561(3)– 101(2)	+0.04			B
40	3928.409	25448.39	3682(4)– 113(3)	0.00			
			5104(3)– 255(3)	—0.43			1
50	3928.541	25447.53	3059(4)– 51(5)	0.00	$g_1 = 1.53$	$g_2 = 1.38$	
(1)	3928.853	25445.51	4386(4)– 184(5)	—0.06			B
(½)	3929.506	25441.28	5104(3)– 256(4)	+0.07			B
80	3929.997	25438.10	4029(6)– 149(6)	—0.01	(0.50, 0.60, 0.81, 0.98)	—	
(?)	3930.708	25433.50	4875(4)– 234(4)	+0.06			B
	3931.212	25430.27	5955(3)–3412(3)	—0.37			A, 1
40	3931.525	25428.22	3680(3)– 113(3)	—0.05	$g_1 = 1.50$	$g_2 = 1.27$	
	3933.822	25413.40	5809(4)–3268(4)	—0.18			A
(1)	3935.508	25402.49	3949(2)– 140(3)	+0.06	(0, 0.17, 0.36)	—	B
125	3938.593	25382.58	3412(3)– 87(4)	+0.01	$g_1 = 1.44$	$g_2 = 1.31$	
50	3939.566	25376.32	3874(2)– 133(2)	—0.04	$g_1 = 1.60$	$g_2 = 0.95$	
(1)	3940.011	25373.45	4640(2)– 210(1)	0.00	(0, 0.27)	—	B
	3940.360	25371.21	4793(2)– 255(1)	—0.03			A
	3940.568	25369.90	5782(3)–3245(2)	+0.44			A, 1
	3941.344	25364.90	5271(4)– 273(3)	+0.02			A
(1)	3944.701	25343.29	5093(4)– 255(3)	—0.01	(0, 0.21, 0.41)	—	B
	3945.583	25337.65	4375(4)– 184(5)	+0.13			A
	3945.881	25335.74	5093(4)– 256(4)	+0.05			A
	3947.289	25326.70	5267(3)– 273(3)	+0.08			A
50	3949.784	25310.67	3833(2)– 130(1)	—0.01	$g_1 = 1.41$	$g_2 = 0.31$	9
			5538(3)–3007(2)	+0.08			
	3951.244	25301.35	5090(5)– 256(4)	+0.03			A
	3952.190	25295.29	5467(3)–2938(3)	—0.02			A
40	3952.768	25291.57	3938(3)– 140(3)	—0.01	(0.18, 0.24)	1.18	

TABLE III *(continued)*

Classified lines of Os I

Int.	λ_{air}	$\sigma_{vac.}$	Classification	$\delta\sigma$	Zeeman effect		Notes
	3953.886	25284.44	5342(2)– 281(3)	—0.29	(0)	0.52	A, 1, 11
	3954.081	25283.20	4640(2)– 211(3)	—0.04			A
12	3955.367	25274.95	4049(1)– 152(2)	+0.04	$g_1 = 2.18$	$g_2 = 1.61$	
(df1)	3955.447	25274.44	4873(4)–2346(5)	—0.10			B
(1)	3957.678	25260.19	5032(3)– 250(2)	—0.07	(**0**, 0.33, 0.68)	—	B
(2)	3958.252	25256.52	3663(2)– 113(3)	—0.02			B
(½)	3958.916	25252.29	4466(2)– 194(2)	—0.02			B
			4414(3)– 189(3)	—0.05	(**0**, 0.18)	—	9
50	3960.506	25242.15	4953(5)– 242(5)	—0.16	(**0**, 0.20)	—	9
			5031(2)– 250(2)	+0.15			
			4008(4)– 148(4)	—0.06	$g_1 = 1.36$	$g_2 = 1.08$	9
125	3961.016	25238.90					
			4780(0)– 225(1)	—0.18			
(df6)	3961.538	25235.58	5364(2)– 284(3)	+0.26	(0)	—	B, 1, 11
(2)	3963.333	25224.15	3824(1)– 130(1)	+0.02	(**1.24**)	—	B
500	3963.628	25222.27	2938(3)– 41(3)	—0.06	(0)	1.47	
	3964.461	25217.00	4920(3)– 239(3)	—0.45			A, 1
60	3964.965	25213.76	2795(2)– 27(2)	—0.07	(0.61, 1.21)	—	
(½)	3966.443	25204.37	4632(3)– 211(3)	+0.04			B
(1)	3966.624	25203.22	4852(4)– 234(4)	+0.01	(**0.04**)	—	B
(1)	3968.703	25190.02	4948(4)– 242(5)	0.00			B
100	3969.681	25183.87	4003(7)– 149(6)	—0.07	$g_1 - g_2 = 0.15$		24
(½)	3971.323	25173.40	4407(2)– 189(3)	0.00	(0)	—	B
(+)	3973.855	25157.36	5928(3)–3412(3)	—0.09	(... **0.09**)	—	B
(½)	3974.460	25153.53	4913(3)– 239(3)	0.00	(**0.44**)	—	B
50	3975.441	25147.33	3792(2)– 127(2)	0.00	$g_1 = 1.45$	$g_2 = 1.00$	
	3976.245	25142.27	5782(3)–3268(4)	—0.02			A
	3976.747	25139.10	5541(4)–3027(5)	+0.05			A
			3027(5)– 51(5)	—0.02	$g_1 = 1.47$	$g_2 = 1.38$	9
300	3977.231	25136.01					
			4616(2)– 210(1)	—0.08			
	3978.543	25127.75	4911(2)– 239(3)	+0.23			A
(df4)	3979.368	25122.51	5540(5)–3027(5)	—0.01	(**0.25**)	1.42	B
(df+)	3982.244	25104.37	5922(2)–3412(3)	—0.07	(0)	—	B
(?)	3982.382	25103.50	4640(2)– 213(2)	—0.04			B
	3984.268	25091.64	4840(1)– 233(2)	—0.08			A
(4)	3985.501	25083.85	5015(3)– 250(2)	—0.01	$g_1 = 1.16$	$g_2 = 0.89$	B
50	3988.179	25067.01	3940(5)– 143(5)	+0.02	(... **0.21**)	1.18	
(8)	3988.621	25064.23	4447(1)– 194(2)	+0.01	(0)	0.96	B
			4616(2)– 211(3)	+0.35			1
40	3991.487	25046.23					
			2778(1)– 27(2)	—0.07	(—)	**0.12**	9
	3991.604	25045.53	5917(2)–3412(3)	+0.50			A, 1
	3992.164	25042.02	5345(1)– 284(3)	—0.14			A
	3993.232	25035.32	4414(3)– 191(4)	+0.05			A
(1)	3993.408	25034.19	3780(3)– 127(2)	—0.01			B
	3994.429	25027.82	4492(5)– 198(4)	—0.23			A
30	3994.929	25024.65	4632(3)– 213(2)	+0.02	$g_1 = 1.12$	$g_2 = 1.25$	
	3996.155	25017.01	5914(2)–3412(3)	+0.25			A

TABLE III *(continued)*

Classified lines of Os I

Int.	λ_{air}	$\sigma_{vac.}$	Classification	$\delta\sigma$	Zeeman effect		Notes
50	3996.805	25012.91	2501(3)– 0(4)	—0.02			
80	3998.933	24999.60	4489(4)– 198(4)	0.00	$g_1 = 1.22$	$g_2 = 1.06$	
	4001.031	24986.49	5233(2)– 273(3)	—0.33			A, 1
			4830(3)– 233(2)	—0.28			1
(2)	4001.321	24984.68					B
			4340(5)– 184(5)	—0.02	(0.45)	—	9
	4001.978	24980.61	5910(2)–3412(3)	+0.06			A
($\frac{1}{2}$)	4002.085	24979.91	4830(3)– 234(4)	+0.01			B
	4002.717	24975.99	4753(2)– 225(1)	+0.06			A
	4003.090	24973.67	5809(4)–3312(3)	—0.04			A
50	4003.480	24971.21	4036(4)– 153(3)	+0.05	$g_1 = 1.32$	$g_2 = 1.53$	
50	4004.024	24967.81	3634(2)– 113(3)	0.00	$g_1 = 1.15$	$g_2 = 1.26$	
	4004.293	24966.16	3833(2)– 133(2)	+0.24			A
35	4005.155	24960.76	4386(4)– 189(3)	+0.01	(0)	1.20	
	4006.967	24949.50	5907(3)–3412(3)	—0.07			A
	4007.490	24946.25	5975(3)–3480(4)	+0.03			A
	4009.494	24933.76	5307(2)– 281(3)	+0.04			A
	4010.707	24926.24	5333(3)– 284(3)	—0.04			A
(1)	4010.983	24924.49	3509(2)– 101(2)	—0.03	(0.21)	—	B
(1)	4012.441	24915.44	4258(0)– 176(1)	+0.03	(0)	1.40	B
	4012.763	24913.47	4747(1)– 225(1)	+0.07			A
	4013.394	24909.52	5050(4)– 255(3)	—0.07			A
			3826(3)– 133(2)	0.00	$g_1 = 1.23$	$g_2 = 0.94$	9
20	4015.037	24899.33					
			4620(1)– 213(2)	+0.33			1
(?)	4016.476	24890.41	4887(3)– 239(3)	+0.06			B
60	4018.257	24879.38	3824(1)– 133(2)	+0.01	$g_1 = 1.56$	$g_2 = 0.94$	
(2)	4020.388	24866.19	4616(2)– 213(2)	+0.01	(0.16)	—	B
(?)	4022.738	24851.67	5513(6)–3027(5)	—0.01	(0)	—	B
	4025.956	24831.83	5895(3)–3412(3)	—0.01			A
	4026.627	24827.70	5541(4)–3059(4)	+0.15			A
			5486(2)– 300(2)	—0.13			
(df2)	4029.336	24810.97	5540(5)–3059(4)	—0.05			B
			5216(2)– 273(3)	—0.10			
(df2)	4029.644	24809.07	4813(4)– 234(4)	—0.19	(0)	1.38	B, 11
(4)	4030.659	24802.82	4987(2)– 250(2)	—0.04	(0)	0.88	B
(8)	4032.924	24788.89	4877(2)– 239(3)	—0.02	(0)	0.97	B
($\frac{1}{2}$)	4034.498	24779.23	5958(3)–3480(4)	+0.08			B
(4)	4035.095	24775.56	5037(5)– 256(4)	—0.08	(0)	1.30	B
	4036.145	24769.12	5484(1)–3007(2)	+0.02			A
(4)	4036.458	24767.19	4387(5)– 191(4)	—0.06			B
	4037.841	24758.71	3052(1)– 57(1)	—0.07	(0.09)	—	A
	4038.453	24754.99	4242(1)– 176(1)	—0.03			A
	4038.556	24754.36	5503(5)–3027(5)	—0.04			A
9	4038.640	24753.81	4386(4)– 191(4)	—0.01	(0.33, 0.51, 0.68)	—	
	4040.976	24739.53	4806(5)– 234(4)	—0.03			A
	4041.539	24736.09	5032(3)– 255(3)	+0.06			A

TABLE III *(continued)*

Classified lines of Os I

Int.	λ_{air}	$\sigma_{vac.}$	Classification	$\delta\sigma$	Zeeman effect		Notes
			4414(3)– 194(2)	+0.26	$g_1 = 1.13$	$g_2 = 0.97$	1, 17
100l	4041.917	24733.74					19
			3049(0)– 57(1)	—0.10	(0)	1.46	
(6)	4042.789	24728.41	5032(3)– 256(4)	—0.01	(0)	0.90	B
	4044.477	24718.12	5031(2)– 255(3)	+0.35			A, 1
(½)	4045.994	24708.82	4361(2)– 189(2)	—0.05			B
(1)	4047.046	24702.40	5782(3)–3312(3)	—0.02			B
	4047.504	24699.63	5029(4)– 255(3)	+0.01			A
			4008(4)– 153(3)	0.00	$g_1 = 1.36$	$g_2 = 1.53$	9
20	4048.054	24696.25					
			5475(2)– 300(2)	—0.16			
(2)	4050.556	24680.99	5027(4)– 255(3)	+0.02			B
12	4051.429	24675.67	4088(2)– 162(1)	+0.03	(**0**, 0.93)	—	
(4)	4053.231	24664.70	4407(2)– 194(2)	+0.02	(... **0.34**)	—	B
(1)	4053.796	24661.26	5307(2)– 284(3)	—0.03			B
	4054.046	24659.75	5975(3)–3509(2)	+0.21			A
30	4055.496	24650.93	4577(3)– 211(3)	+0.04	$g_1 = 1.12$	$g_2 = 0.95$	
(4)	4056.346	24645.76	4375(4)– 191(4)	—0.01			B
	4056.751	24643.33	5876(4)–3412(3)	—0.03			A
	4058.554	24632.38	4229(1)– 176(1)	—0.11			A
(4)	4061.614	24613.80	4351(3)– 189(3)	—0.01	(0)	1.20	B
	4064.136	24598.53	5467(3)–3007(2)	—0.15			A
9	4066.313	24585.35	3561(3)– 110(4)	+0.01	$g_1 = 1.51$	$g_2 = 1.16$	
100	4066.693	24583.05	4719(5)–2261(4)	+0.01	(0)	**1.29** ...	
	4070.606	24559.46	5015(3)– 255(3)	—0.17			A
20	4070.855	24557.93	3940(5)– 148(4)	0.00	$g_1 = 1.18$	$g_2 = 1.08$	
12	4071.013	24556.97	3792(2)– 133(2)	+0.09	(0)	1.37	11
20	4071.562	24553.69	3940(5)– 149(6)	+0.04	(0)	1.01	
(4)	4071.826	24552.07	5015(3)– 256(4)	+0.05	(0)	1.08	B
	4073.047	24544.74	4961(2)– 250(2)	—0.39			A, 1
6	4073.604	24541.26	4852(4)– 239(3)	—0.03	(0)	1.07	
			3938(3)– 148(4)	—0.04	$g_1 = 1.18$	$g_2 = 1.08$	9
80	4074.682	24534.86					
			4343(2)– 189(3)	—0.33			
(1)	4075.350	24530.84	4785(4)– 234(4)	—0.03			B
	4076.226	24525.60	5293(3)– 284(3)	—0.05			A
(1)	4076.70	24522.72	5864(2)–3412(3)	+0.43			EH, 1
	4078.542	24511.67	5960(2)–3509(2)	—0.02			A
	4078.755	24510.39	4782(3)– 233(2)	+0.31			A, 1
(1)	4079.653	24504.97	4782(3)– 234(4)	—0.05			B
			5388(3)– 293(4)	—0.32			1
	4081.746	24492.43					A
			5958(3)–3509(2)	—0.04			
100h	4088.442	24452.29	3967(2)– 152(2)	—0.03	$g_1 = 1.90$	$g_2 = 1.61$	
	4089.178	24447.92	5240(3)–2795(2)	+0.43			A, 1
	4089.866	24443.78	3780(3)– 133(2)	+0.03			A
	4090.022	24442.87	5503(5)–3059(4)	—0.03			A
3	4090.769	24438.38	4556(3)– 211(3)	+0.05	(... **0.08**)	—	
100	4091.817	24432.12	3052(1)– 60(0)	—0.01	(**0.42**)	1.56	16

TABLE III *(continued)*

Classified lines of Os I

Int.	λ_{air}	$\sigma_{vac.}$	Classification	$\delta\sigma$	Zeeman effect		Notes
	4092.526	24427.92	5448(1)– 300(2)	+0.44			A, 1
	4095.911	24407.73	5175(3)– 273(3)	+0.04			A
(½)	4096.052	24406.86	4351(3)– 191(4)	—0.02	(0, 0.20)	—	B
9	4098.102	24394.68	3848(3)– 140(3)	+0.04	$g_1 = 1.61$	$g_2 = 1.10$	
60	4100.300	24381.57	3312(3)– 87(4)	—0.08	$g_1 = 1.63$	$g_2 = 1.31$	
20	4103.616	24361.87	5214(2)–2778(1)	—0.03	(0, 0.97)	1.80	
	4105.159	24352.74	4994(3)– 255(3)	—0.38			A, 1
6	4105.442	24351.07	5249(4)– 281(3)	+0.03	$g_1 = 1.11$	$g_2 = 1.24$	
(1)	4106.055	24347.40	5484(1)–3049(0)	0.00	(0.25, 0.32, 0.38)	—	B, 11
	4106.371	24345.56	4994(3)– 256(4)	+0.05			A
(1)	4109.088	24329.46	4274(4)– 184(5)	+0.01			3
	4110.258	24322.53	5484(1)–3052(1)	+0.07			A
6	4111.028	24317.95	4830(3)– 239(3)	—0.03	(... 0.20)	—	
150	4112.018	24312.09	3007(2)– 57(1)	—0.05	(0)	1.51	
	4113.223	24305.00	5165(2)– 273(3)	+0.02			A
	4115.416	24292.05	4761(3)– 234(4)	+0.07			A
5	4116.585	24285.12	4049(1)– 162(1)	+0.05			
	4118.955	24271.18	3949(2)– 152(2)	—0.05			A
			5907(3)–3480(4)	+0.03			
(½)	4120.002	24264.98	4538(4)– 211(3)	—0.05	(0)	—	B
	4123.297	24245.62	5430(1)– 300(2)	—0.04			A
(½)	4124.363	24239.32	3833(2)– 140(3)	—0.06			B
30	4124.599	24237.94	3561(3)– 113(3)	+0.02	$g_1 = 1.51$	$g_2 = 1.25$	
(1)	4125.292	24233.86	4852(4)– 242(5)	—0.04			B
(2)	4127.326	24221.92	4753(2)– 233(2)	—0.06	(... 0.56)	—	B
60	4128.961	24212.33	2837(3)– 41(3)	—0.03	$g_1 = 1.75$	$g_2 = 1.46$	
	4129.421	24209.66	5733(3)–3312(3)	—0.23			A
	4130.189	24205.16	3697(1)– 127(2)	+0.03			A
12	4131.049	24200.09	4361(2)– 194(2)	—0.06	(0.14)	—	12
			4550(2)– 213(2)	0.00			
(1)	4132.041	24194.28	5214(2)–2795(2)	—0.09	(0.50)	—	B
	4132.380	24192.33	5260(3)– 284(3)	+0.15			A
			5928(3)–3509(2)	—0.02			
200	4135.784	24172.42	2833(4)– 41(3)	—0.03	$g_1 = 1.59$	$g_2 = 1.46$	9
			3826(3)– 140(3)	—0.37			1
100	4137.840	24160.41	3938(3)– 152(2)	+0.03	$g_1 = 1.19$	$g_2 = 1.62$	
(½)	4144.602	24120.97	4242(1)– 183(0)	+0.01	(0)	—	B
	4146.557	24109.62	4301(3)– 189(3)	0.00			A
9	4147.331	24105.10	4351(3)– 194(2)	+0.01	$g_1 = 1.20$	$g_2 = 0.97$	
8	4150.699	24085.54	5467(3)–3059(4)	+0.03			
	4151.654	24080.02	5917(2)–3509(2)	+0.09			A
			4511(0)– 210(1)	+0.28			1
9	4153.374	24070.03	5240(3)–2833(4)	—0.01	(0)	—	

TABLE III *(continued)*

Classified lines of Os I

Int.	λ_{air}	σ_{vac}	Classification	$\delta\sigma$	Zeeman effect	Notes
(2)	4153.659	24068.38	4913(3)– 250(2)	—0.02	(**0**, 0.35, 0.69) —	B
	4156.562	24051.59	5914(2)–3509(2)	—0.07		A
50	4158.784	24038.72	3813(4)– 140(3)	0.00	$g_1 = 1.24$ $g_2 = 1.10$	
20	4159.965	24031.89	3680(3)– 127(2)	0.00	$g_1 = 1.48$ $g_2 = 1.00$	
6	4160.268	24030.14	4240(3)–2837(3)	+0.01	(0) —	
(1)	4160.909	24026.44	4343(2)– 194(2)	—0.03	(0) —	B
	4161.561	24022.70	5216(2)– 281(3)	+0.19		A
	4161.876	24020.88	4961(2)– 255(3)	—0.02		A
	4164.121	24007.93	5406(2)– 300(2)	+0.32		A, 1
	4165.755	23998.51	4229(1)– 183(0)	+0.08		A
			5213(3)– 281(3)	—0.08		
	4166.729	23992.90	5404(2)– 300(2)	—0.20		A
	4166.842	23992.25	3938(3)– 153(3)	+0.06		A
	4167.849	23986.45	5960(2)–3561(3)	+0.18		A
	4168.136	23984.80	5907(3)–3509(2)	+0.33		A, 1
	4168.367	23983.47	4905(1)– 250(2)	—0.42		A, 1
	4168.431	23983.10	4387(5)– 198(4)	+0.05		A
	4169.182	23978.79	5132(4)– 273(3)	+0.45		A, 1
	4170.233	23972.74	5809(4)–3412(3)	—0.05		A
(1)	4170.781	23969.58	4386(4)– 198(4)	—0.04		B
	4171.154	23967.45	5958(3)–3561(3)	+0.40		A, 1
	4171.583	23964.98	5876(4)–3480(4)	+0.04		A
($\frac{1}{2}$)	4172.420	23960.16	5131(2)– 273(3)	—0.12		B
	4172.540	23959.49	3697(1)– 130(1)	+0.05	$g_1 = 1.31$ $g_2 = 0.31$	A
60	4172.57	23959.29	3412(3)– 101(2)	—0.13		
100	4173.234	23955.48	2909(6)– 51(5)	—0.01	$g_1 = 1.48$ $g_2 = 1.38$	
	4173.830	23952.08	4651(1)– 225(1)	+0.28		A, 1
	4175.235	23944.02	5333(3)– 293(4)	+0.10		A
100	4175.627	23941.76	3268(4)– 87(4)	—0.02	$g_1 = 1.46$ $g_2 = 1.30$	
	4175.928	23940.05	5955(3)–3561(3)	—0.07		A
6	4182.450	23902.70	4301(3)– 191(4)	+0.01	(0) 0.98	
25	4184.131	23893.10	4231(4)– 184(5)	—0.03	$g_1 = 1.23$ $g_2 = 1.11$	
(1)	4185.021	23888.01	4948(4)– 255(3)	—0.04		B
	4185.719	23884.05	5868(3)–3480(4)	—0.33		A, 1
(1)	4186.352	23880.44	4948(4)– 256(4)	0.00		EH
	4188.318	23869.23	4785(4)– 239(3)	+0.28		A, 1
	4189.673	23861.51	4375(4)– 198(4)	—0.06		A
60	4189.906	23860.16	3663(2)– 127(2)	0.00	$g_1 = 1.36$ $g_2 = 1.00$	
9	4192.637	23844.62	4274(4)– 189(3)	—0.01	(**0**, 0.14, 0.26) —	
			4640(2)– 225(1)	—0.06	(**0**, 0.45) —	9
(2)	4192.888	23843.19	4782(3)– 239(3)	+0.09		B
			6064(4)–3680(3)	—0.03		
(1)	4194.184	23835.83	4715(4)– 234(4)	+0.01		B
100s	4195.144	23830.37	3792(2)– 140(3)	+0.03	$g_1 = 1.44$ $g_2 = 1.09$	9
			5388(3)– 300(2)	+0.11		
	4196.431	23823.08	6064(4)–3682(4)	—0.02		A
	4197.903	23814.73	5890(3)–3509(2)	+0.03		A
(10)	4201.383	23794.98	2795(2)– 41(3)	—0.02	$g_1 = 2.04$ $g_2 = 1.47$	B

TABLE III *(continued)*

Classified lines of Os I

Int.	λ_{air}	$\sigma_{vac.}$	Classification	$\delta\sigma$	Zeeman effect		Notes
100	4202.062	23791.14	3813(4)– 143(5)	+0.04	$g_1 = 1.23$	$g_2 = 1.13$	
12	4204.560	23777.00	5214(2) -2837(3)	—0.01	(0)	1.66	
9	4205.222	23773.26	3480(4)– 110(4)	+0.02			
(½)	4205.972	23769.02	4489(4)– 211(3)	+0.01			B
	4209.967	23746.49	4486(3)– 211(3)	+0.44			A, 1
	4211.146	23739.84	4705(3)– 233(2)	+0.15			A
150	4211.855	23735.83	4719(5)–2346(5)	0.00	(0.10)	1.56	
	4212.358	23733.01	5869(4)–3436(5)	+0.15			A
	4213.656	23725.70	5213(3)– 284(3)	—0.46			A, 1
30	4213.859	23724.54	4873(4)–2501(3)	+0.03	$g_1 = 1.50$	$g_2 = 1.73$	
8	4215.155	23717.24	3780(3)– 140(3)	+0.03	$g_1 = 1.27$	$g_2 = 1.11$	
	4216.066	23712.14	3509(2)– 113(3)	—0.36			A, 1
	4217.943	23701.59	5782(3)–3412(3)	+0.09			A
(4)	4218.840	23696.53	4472(1)– 210(1)	+0.05	$g_1 = 1.01$	$g_2 = 0.87$	B
(½)	4219.673	23691.85	5104(3)– 273(3)	+0.05			B
	4221.296	23682.76	5960(2)–3591(1)	+0.12			A
	4224.116	23666.95	5928(3)–3561(3)	+0.02			A
12	4226.527	23653.43	3887(1)– 152(2)	+0.03	(0 ...)	1.34, 1.61, 1.87	
			4620(1)– 225(1)	+0.06			
	4229.151	23638.77					A
			5098(2)– 273(3)	—0.04			
			3848(3)– 148(4)	—0.25			
(2)	4229.337	23637.71					B
			4274(4)– 191(4)	+0.01			
	4229.825	23635.01	5609(2)–3245(2)	—0.01			A
	4230.831	23629.39	4466(2)– 210(1)	—0.13			A
(1)	4232.027	23622.69	4351(3)– 198(4)	+0.01			B
			3663(2)– 130(1)	+0.22			
12	4233.460	23614.69					
			3697(1)– 133(2)	+0.01	$g_1 = 1.31$	$g_2 = 0.94$	9
	4334.693	23607.84	4920(3)– 255(3)	—0.25			A
			4301(3)– 194(2)	+0.01			
(4)	4235.932	23600.91			(0)	1.21	B, 12
			4920(3)– 256(4)	+0.43			1
	4236.514	23597.69	5868(3)–3509(2)	—0.01			A
	4237.703	23591.07	5364(2)– 300(2)	—0.21			A
9	4241.521	23569.81	3790(4)– 143(5)	+0.03			
(½)	4242.153	23566.30	4486(3)– 213(2)	0.05			B
(½)	4247.514	23536.56	4913(3)– 256(4)	0.00			B
			5165(2)– 281(3)	—0.10			
6	4251.170	23516.32					
			5359(2)–3007(2)	+0.06	(... 0.28)	—	9
9	4252.538	23508.76	4340(5)– 198(4)	+0.02			
			2346(5)– 0(4)	—0.03	$g_1 = 1.55$	$g_2 = 1.44$	9
200	4260.854	23462.87					
			3967(2)– 162(1)	+0.39			1

TABLE III *(continued)*

Classified lines of Os I

Int.	λ_{air}	$\sigma_{vac.}$	Classification	$\delta\sigma$	Zeeman effect		Notes
			4677(3)– 233(2)	—0.07			
	4261.630	23458.62					A
			5907(3)–3561(3)	—0.43			1
			3680(3)– 133(2)	+0.02	$g_1 = 1.48$	$g_2 = 0.94$	9
20	4264.746	23441.46					
			4447(1)– 210(1)	+0.03			
12	4269.364	23416.10	3826(3)– 148(4)	—0.01	(0)	—	
30	4269.610	23414.76	4232(3)– 189(3)	+0.02	$g_1 = 1.08$	$g_2 = 1.20$	
12	4270.788	23408.30	4231(4)– 189(3)	—0.01	(0)	—	
	4272.776	23397.43	5345(1)– 300(2)	+0.11			A
	4273.950	23391.00	3861(1)– 152(2)	+0.13			A
9	4274.905	23385.75	5346(1)–3007(2)	+0.03	$g_1 = 2.71$	$g_2 = 1.49$	
12	4277.147	23373.49	4241(1)– 190(0)	+0.04	(0)	1.85	
	4279.692	23359.62	4466(2)– 213(2)	+0.01			A
(2)	4281.372	23350.43	3874(2)– 153(3)	0.00			B
	4283.006	23341.54	5895(3)–3561(3)	+0.22			A
($\frac{1}{2}$)	4284.250	23334.76	3436(5)– 110(4)	+0.01			B
30	4285.895	23325.79	3634(2)– 130(1)	+0.05	$g_1 = 1.15$	$g_2 = 0.31$	
	4288.713	23310.48	5922(2)–3591(1)	+0.19			A
	4291.631	23294.63	5809(4)–3480(4)	+0.26			A, 1
	4291.935	23292.98	3950(0)– 162(1)	+0.11			A
	4292.672	23288.98	5890(3)–3561(3)	—0.30			A, 1
	4293.718	23283.31	5267(3)– 293(4)	+0.03			A
60	4293.949	23282.04	3813(4)– 148(4)	0.00	$g_1 = 1.24$	$g_2 = 1.09$	
			3949(2)– 162(1)	+0.07			
(8df)	4294.056	23281.46	5333(3)– 300(2)	+0.03			B
			4887(3)– 255(3)	+0.47			1
			3663(2)– 133(2)	+0.03	$g_1 = 1.36$	$g_2 = 0.94$	9
12	4296.218	23269.74					
			3628(0)– 130(1)	—0.04			
(1)	4297.385	23263.42	3848(3)– 152(2)	—0.02	(0)	1.61	B
	4298.694	23256.36	5960(2)–3634(2)	—0.02			A
			4229(1)– 190(0)	—0.03	(0)	—	9
($\frac{1}{2}$)	4299.701	23250.89					B
			5917(2)–3591(1)	+0.01			
(1+)	4300.282	23247.77	4265(2)– 194(2)	+0.07			EH
	4300.976	23244.02	5165(2)– 284(3)	+0.03			A
	4302.994	23233.12	4830(3)– 250(2)	+0.27			A, 1
	4304.945	23222.59	5914(2)– 359(1)	—0.02			A
(1)	4305.287	23220.73	4088(2)– 176(1)	+0.02	$g_1 = 0.82$	$g_2 = 1.40$	B
			5260(3)– 293(4)	+0.39			1
	4307.239	23210.22					A
			5955(3)–3634(2)	—0.01			
($\frac{1}{2}$)	4307.687	23207.79	4232(3)– 191(4)	—0.02			B
18	4308.877	23201.38	4231(4)– 191(4)	0.00	$g_1 = 1.22$	$g_2 = 1.03$	
	4309.554	23197.76	4651(1)– 233(2)	—0.09			A
(8df)	4311.051	23189.68	5132(4)– 281(3)	—0.10			B
150	4311.399	23187.81	2833(4)– 51(5)	—0.04	$g_1 = 1.59$	$g_2 = 1.37$	
	4311.684	23186.30	5910(2)–3591(1)	—0.10			A

TABLE III *(continued)*

Classified lines of Os I

Int.	λ_{air}	$\sigma_{vac.}$	Classification	$\delta\sigma$	Zeeman effect		Notes
(½)	4312.151	23183.76	5113(3)–2795(2)	—0.05			B
	4313.004	23179.20	4877(2)– 255(3)	—0.35			A, 1
	4316.169	23162.20	4875(4)– 255(3)	+0.04			A
(1)	4317.587	23154.57	4875(4)– 256(4)	+0.02	(... 0.15)	—	B
	4317.874	23153.06	5876(4)–3561(3)	+0.22			A
(½)	4317.981	23152.46	5050(4)– 273(3)	—0.11			B
9	4319.339	23145.18	3591(1)– 127(2)	+0.01	(0, 0.29)	—	
	4324.349	23118.39	4301(3)– 198(4)	—0.10			A
30	4326.254	23108.19	3833(2)– 152(2)	+0.01	$g_1 = 1.41$	$g_2 = 1.61$	
			3412(3)– 110(4)	+0.44			1
60	4328.677	23095.26					
			3848(3)– 153(3)	+0.01	$g_1 = 1.62$	$g_2 = 1.54$	9
			4640(2)– 233(2)	+0.25			
	4329.747	23089.55					A
			5122(3)– 281(3)	+0.44			1
(½)	4332.916	23072.66	4705(3)– 239(3)	—0.05			B
	4333.009	23072.19	5868(3)–3561(3)	—0.09			A
	4333.486	23069.65	5359(2)–3052(1)	+0.03			A
			3826(3)– 152(2)	+0.03	$g_1 = 1.23$	$g_2 = 1.62$	9
9	4338.753	23041.62					
			4407(2)– 210(1)	—0.27			1
	4340.642	23031.61	5864(2)–3561(3)	—0.16			A
4	4342.521	23021.63	3824(1)– 152(2)	0.00	(0)	1.67	
			4414(3)– 211(3)	—0.30			1
(?)	4342.795	23020.18					B
			5240(3)–2938(3)	+0.02	(0)	—	9
(½)	4344.654	23010.33	4632(3)– 233(2)	—0.06			B
(?)	4345.599	23005.32	4632(3)– 234(4)	—0.01			B
	4348.837	22988.21	5475(2)– 317(3)	+0.06			A
	4350.198	22981.02	3634(2)– 133(2)	+0.04			A
	4350.576	22979.03	5032(3)– 273(3)	+0.02			A
9	4351.528	22973.98	4187(3)– 189(3)	—0.01	$g_1 = 1.30$	$g_2 = 1.20$	
			5609(2)–3312(3)	—0.02			
	4352.673	22967.96					A
			5960(2)–3663(2)	+0.31			1
(½)	4353.413	22964.03	5346(1)–3049(0)	+0.01			B
			3780(3)– 148(4)	—0.01			
	4354.082	22960.52					A
			5031(2)– 273(3)	—0.23			
9	4354.464	22958.49	3312(3)– 101(2)	—0.01	(0, 0.16, 0.33)	—	
(1+)	4355.755	22951.70	4407(2)– 211(3)	+0.02			EH
	4356.385	22948.38	5958(3)–3663(2)	—0.05			A
	4357.494	22942.54	5029(4)– 273(3)	—0.06			A
(½)	4357.827	22940.77	4626(4)– 234(4)	—0.03			B
			3833(2)– 153(3)	—0.03			
12	4357.980	22939.96					
			4550(2)– 225(1)	+0.16			
9	4358.141	22939.12	5346(1)–3052(1)	+0.04	$g_1 = 2.70$	$g_2 = 1.55$	
	4358.595	22936.75	5928(3)–3634(2)	—0.29			A, 1

TABLE III *(continued)*

Classified lines of Os I

Int.	λ_{air}	$\sigma_{vac.}$	Classification	$\delta\sigma$	Zeeman effect		Notes
	4359.618	22931.37	5538(3)–3245(2)	—0.06			A
			4852(4)– 256(4)	+0.05			
	4360.948	22924.37					A
			5027(4)– 273(3)	+0.42			1
	4361.497	22921.49	5955(3)–3663(2)	—0.01			A
	4364.082	22907.91	4720(5)– 242(5)	—0.37			A, 1
(½)	4364.439	22906.01	4232(3)– 194(2)	—0.01			B
			3591(1)– 130(1)	+0.05	$g_1 = 1.29$	$g_2 = 0.31$	9
60	4365.674	22899.53					
			5131(2)– 284(3)	+0.24			
	4367.704	22888.90	4229(1)– 194(2)	—0.27			A, 1
	4368.500	22884.74	4620(1)– 233(2)	—0.02			A
50	4370.661	22873.41	3826(3)– 153(3)	+0.01	$g_1 = 1.23$	$g_2 = 1.54$	
	4371.949	22866.69	4715(4)– 242(5)	+0.20			A
	4372.234	22865.20	4793(2)– 250(2)	+0.02			A
(½)	4374.470	22853.49	4274(4)– 198(4)	—0.01			B
	4374.812	22851.73	4616(2)– 233(2)	—0.21			A
	4375.032	22850.58	5098(2)– 281(3)	+0.33			A, 1
(½)	4376.761	22841.53	3561(3)– 127(2)	—0.01			B
			4414(3)– 213(2)	0.00	$g_1 = 1.14$	$g_2 = 1.26$	9
6	4376.904	22840.78					
			6064(4)–3780(3)	—0.13			
	4378.925	22830.26	4049(1)– 176(1)	+0.12			A
	4379.232	22828.66	4681(2)– 239(3)	+0.37			A, 1
	4380.193	22823.65	4172(4)– 189(3)	+0.01			A
	4381.598	22816.33	5122(3)– 284(3)	—0.35			A, 1
(1)	4383.223	22807.86	4122(5)– 184(5)	—0.04			B
			5121(1)– 284(3)	+0.36			1
(½)	4383.550	22806.15					B
			5113(3)–2833(4)	—0.21			
	4384.221	22802.68	5015(3)– 273(3)	+0.27			A, 1
			5914(2)–3634(2)	+0.06			
	4385.427	22796.41					A
			5960(2)–3680(3)	+0.49			1
(2)	4386.325	22791.73	4677(3)– 239(3)	+0.02	(0.35, 0.53)	—	B
			4187(3)– 191(4)	—0.01			
15	4391.080	22767.05					
			5214(2)–2938(3)	+0.01	$g_1 = 1.79$	$g_2 = 1.48$	9
	4391.186	22766.52	5113(3)–2837(3)	+0.07			A
(1)	4392.854	22757.87	4782(3)– 250(2)	—0.10			EH
	4393.121	22756.49	5958(3)–3682(4)	—0.09			A
	4394.438	22749.68	5955(3)–3680(3)	—0.09			A
150	4394.858	22747.47	3412(3)– 113(3)	+0.07	$g_1 = 1.44$	$g_2 = 1.26$	
	4396.177	22740.67	6064(4)–3790(4)	—0.05			A
			3813(4)– 153(3)	—0.04			
	4396.444	22739.29					A
			1386(4)– 211(3)	+0.26			1
	4397.008	22736.37	5782(3)–3509(2)	—0.03			A
18	4397.263	22735.03	3682(4)– 140(3)	+0.01	(0, ...)	... 2.35	

TABLE III *(continued)*

Classified lines of Os I

Int.	λ_{air}	$\sigma_{vac.}$	Classification	$\delta\sigma$	Zeeman effect		Notes
(dfl)	4397.390	22734.38	5541(4)–3268(4)	—0.01	(0.03)	1.47	B
	4398.332	22729.53	5955(3)–3682(4)	—0.12			A
	4398.393	22729.21	5907(3)–3634(2)	+0.05			A
	4398.676	22727.75	5864(2)–3591(1)	—0.39			A, 1
18	4400.579	22717.90	5540(5)–3268(4)	+0.04	(0)	1.25	
	4401.158	22714.94	3680(3)– 140(3)	+0.04			A
	4402.438	22708.33	4830(3)– 255(3)	—0.29			A, 1
50	4402.736	22706.77	5103(4) 2833(4)	+0.05			
	4403.231	22704.24	5538(3)–3268(4)	—0.02			A
	4403.846	22701.07	4830(3)– 256(4)	+0.06			A
18	4404.213	22699.16	3792(2)– 152(2)	+0.02	$g_1 = 1.45$	$g_2 = 1.61$	
	4410.495	22666.85	5103(4) 2837(3)	+0.04			A
(4)	4411.135	22663.54	3887(1)– 162(1)	—0.02	(0.15)	—	B
	4414.182	22647.91	5928(3)–3663(2)	—0.40			A, 1
	4417.471	22631.05	4375(4)– 211(3)	+0.07			A
			5104(3)– 284(3)	+0.24			
	4419.156	22622.42	5960(2)–3697(1)	—0.26			A, 1
	4419.401	22621.17	5267(3)– 300(2)	+0.38			A, 1
400R	4420.468	22615.69	2261(4)– 0(4)	0.00			
	4421.314	22611.38	5895(3)–3634(2)	—0.05			A
	4422.347	22606.10	4102(6)– 184(5)	0.00			A
	4424.262	22596.32	4994(3)– 273(3)	+0.22			A
	4424.455	22595.33	5922(2) 3663(2)	0.03			A
(½)	4426.285	22585.97	3780(3)– 152(2)	—0.04			B
(1)	4427.88	22577.83	5098(2) 284(3)	0.01			EH
	4427.983	22577.33	4361(2)– 210(1)	—0.03			A
	4431.514	22559.34	5890(3)–3634(2)	—0.05			A
30	4432.412	22554.75	3591(1)– 133(2)	+0.03	$g_1 = 1.27$	$g_2 = 0.93$	
	4433.866	22547.35	5260(3)– 300(2)	+0.01			A
	4434.746	22542.88	3663(2)– 140(3)	—0.29			A, 1
(?)	4435.720	22537.93	4813(4)– 255(3)	—0.05			B
80	4436.317	22534.89	2527(2)– 27(2)	—0.04	$g_1 = 2.04$	$g_2 = 1.44$	
12	4437.088	22530.98	3792(2)– 153(3)	+0.03			
	4437.177	22530.55	5733(3)–3480(4)	0.00			A
	4437.234	22530.26	4813(4)– 256(4)	—0.11			A
(½)	4437.524	22528.77	3874(2) 162(1)	0.01			B
30	4439.644	22518.03	3790(4)– 153(3)	+0.02	(0)	1.22	
	4441.672	22507.75	5914(2) 3663(2)	0.13			A
9	4445.688	22587.38	3682(4)– 143(5)	—0.02			
			4361(2)– 211(3)	+0.23			
200	4447.354	22478.97	3681(5)– 143(5)	+0.02	$g_1 = 1.28$	$g_2 = 1.13$	
	4449.120	22470.07	4753(2) 250(2)	0.20			A
(1)	4450.059	22465.33	4187(3)– 194(2)	+0.06			EH
	4451.708	22457.01	4577(3)– 233(2)	+0.06			A
3	4451.802	22456.53	5928(3)–3682(4)	+0.07			
	4452.666	22452.17	4577(3)– 234(4)	+0.28			A, 1
	4454.603	22442.39	5512(4)–3268(4)	+0.04			A

TABLE III *(continued)*

Classified lines of Os I

Int.	λ_{air}	$\sigma_{vac.}$	Classification	$\delta\sigma$	Zeeman effect		Notes
	4454.969	22440.57	5907(3)–3663(2)	+0.14			A
	4456.035	22435.20	4574(5)– 234(4)	+0.01			A
3l	4458.331	22423.63	4232(3)– 198(4) 5922(2)–3680(3)	+0.02 +0.06			
	4458.653	22422.03	4640(2)– 239(3)	—0.29			A, 1
15	4459.527	22417.61	3780(3)– 153(3)	—0.21			
(8)	4459.605	22417.22	4231(4)– 198(4)	+0.04	(... **0.70**)	—	B
8	4462.287	22403.75	4343(2)– 210(1)	+0.07			
	4462.808	22401.15	3861(1)– 162(1)	+0.12			A
	4464.595	22392.18	4351(3)– 211(3)	+0.09			A
	4464.967	22390.32	5484(1)–3245(2)	+0.38			A, 1
9	4465.940	22385.42	6064(4)–3826(3)	+0.09			
	4470.206	22364.08	5050(4)– 281(3) 5175(3)– 293(4) 5917(2)–3680(3)	+0.07 —0.27 —0.08			A, 1
	4470.293	22363.62	5672(4)–3436(5)	—0.21			A
3	4473.089	22349.69	5503(5)–3268(4)	—0.05			
	4474.356	22343.34	4632(3)– 239(3)	—0.07			A
	4474.548	22342.38	5868(3)–3634(2)	—0.01			A
2	4474.834	22340.93	4793(2)– 255(3)	—0.02			
	4475.845	22335.90	5914(2)–3680(3)	+0.01			A
	4477.019	22330.03	4123(3)– 189(3)	—0.01			A
	4478.326	22323.51	5240(3)–3007(2)	—0.02			A
	4478.487	22322.73	5895(3)–3663(2)	+0.03			A
	4479.396	22318.16	5237(1)– 300(2)	+0.02			A
l 80	4479.808	22316.12	3509(2)– 127(2)	0.00	(... **1.11**)	... **1.00**, **1.56**, 2.10	
(1+)	4480.331	22313.52	4343(2)– 211(3)	+0.05			EH
	4483.219	22299.14	5406(2)– 317(3)	—0.21			A
	4484.131	22294.61	5541(4)–3312(3)	+0.09			A
100	4484.763	22291.47	3245(2)– 101(2)	+0.01	$g_1 = 1.85$	$g_2 = 1.46$	
	4486.124	22284.70	5404(2)– 317(3)	—0.14			A
	4486.881	22280.94	5233(2)– 300(2)	—0.05			A
	4487.357	22278.60	4626(4)– 239(3)	—0.28			A, 1
60	4488.601	22272.41	2501(3)– 27(2)	—0.03			
(?)	4490.214	22264.41	5538(3)–3312(3)	+0.02			B
	4490.360	22263.71	4961(2)– 273(3)	—0.17			A
	4491.202	22259.51	4785(4)– 255(3)	—0.08			A
(½)	4492.225	22254.44	3634(2)– 140(3)	0.00			B
	4492.723	22251.99	4785(4)– 256(4)	+0.01			A
(1+)	4492.899	22251.12	3561(3)– 133(2)	+0.03			EH
	4493.466	22248.32	5907(3)–3682(4)	—0.26			A, 1
(1)	4495.281	22239.31	4556(3)– 234(4)	—0.02			B
	4496.424	22233.66	4782(3)– 255(3)	—0.08			A
	4497.945	22226.14	4782(3)– 256(4)	+0.01			A
5	4500.729	22212.39	4351(3)– 213(2)	0.00			
4	4504.040	22196.07	4049(1)– 183(0)	—0.01			
	4505.229	22190.23	5032(3)– 281(3)	—0.22			A

TABLE III *(continued)*

Classified lines of Os I

Int.	λ_{air}	$\sigma_{vac.}$	Classification	$\delta\sigma$	Zeeman effect		Notes
(0)	4505.69	22187.94	2795(2)– 57(1)	—0.24			M
	4506.028	22186.27	4550(2)– 233(2)	+0.42			A, 1
(1)	4506.31	22184.88	4616(2)– 239(3)	—0.08			M
2	4510.096	22166.26	4472(1)– 225(1)	—0.02			
	4512.581	22154.05	5029(4)– 281(3)	+0.01			A
	4516.596	22134.38	5027(5)– 281(3)	—0.01			A
(0)	4516.72	22133.75	4343(2)– 213(2)	—0.02			M
	4517.272	22131.05	4948(4)– 273(3)	+0.02			A
(0)	4517.33	22130.76	5895(3)–3682(4)	—0.09			M
15	4518.889	22123.13	4123(3)– 191(4)	+0.02			
	4519.150	22121.87	5388(3)– 317(3)	—0.13			A
10	4519.864	22118.36	3833(2)– 162(1)	+0.02	(0)	1.07 ...	21
20	4520.318	22116.14	4122(5)– 191(4)	—0.01			
	4522.623	22104.88	5216(2)– 300(2)	—0.36			A, 1
	4523.938	22098.44	5890(3)–3680(3)	—0.49			A, 1
80	4524.869	22093.89	3312(3)– 110(4)	—0.01			
	4527.384	22081.64	5213(3)– 300(2)	+0.32			A, 1
80	4529.674	22070.45	3509(2)– 130(1)	+0.02			
			5214(2)–3007(2)	+0.04	(... 0.60)	—	9
(1)	4530.53	22066.29	4538(4)– 234(4)	+0.26			M, 1
50	4537.615	22031.83	3824(1)– 162(1)	+0.04	(0.18)	—	21
100	4539.917	22020.66	4761(3)– 255(3)	—0.04			
			2778(1)– 57(1)	+0.01			
	4541.319	22013.86	5015(3)– 281(3)	—0.19			A
(1)	4541.50	22012.99	4761(3)– 256(4)	—0.10			M
			5864(2)–3663(2)	—0.16			
(1)	4543.67	22002.48	5512(4)–3312(3)	0.00			M
5	4545.800	21992.16	5467(3)–3268(4)	—0.19			
(1+)	4547.049	21986.14	4088(2)– 189(3)	+0.03			EH
100	4548.662	21978.33	3682(4)– 148(4)	—0.01	(0.75, 1.04, 1.37)	—	
(1)	4550.085	21971.45	4626(4)– 242(5)	—0.04			B
150	4550.410	21969.88	3681(5)– 148(4)	—0.01	$g_1 = 1.28$	$g_2 = 1.08$	21
	4551.007	21967.00	5609(2)–3412(3)	—0.06			A
150	4551.298	21965.60	3681(5)– 149(6)	—0.01	(0)	0.40 ...	
(0)	4552.87	21958.01	3680(3)– 148(4)	—0.21			M
(0)	4555.52	21945.24	4753(2)– 255(3)	—0.40			M, 1
(1br)	4555.615	21944.78	4036(4)– 184(5)	—0.02			EH
(1)	4561.19	21917.96	5032(3)– 284(3)	—0.06			M
5	4562.604	21911.17	4447(1)– 225(1)	—0.06			
5	4567.48	21887.78	4301(3)– 211(3)	—0.12			

(To be continued)

STRUCTURE AND ZEEMAN EFFECT IN THE SPECTRA OF THE OSMIUM ATOM, Os I AND Os II
V

BY

TH. A. M. VAN KLEEF

Zeeman-laboratory, University of Amsterdam, the Netherlands

(Communicated by Prof. J. DE BOER at the meeting of January 30, 1960)

TABLE III *(continued)*

Classified lines of Os I

Int.	λ_{air}	$\sigma_{vac.}$	Classification	$\delta\sigma$	Zeeman effect		Notes
			5868(3)–3680(3)	+0.20			
	4568.659	21882.13					A
			5364(2)– 317(3)	—0.09			
2	4570.501	21873.31	4029(6)– 184(5)	—0.01			
	4572.914	21861.77	5868(3)–3682(4)	—0.04			A
(0)	4575.68	21848.55	3059(4)– 87(4)	—0.07			M
			5975(3)–3790(4)	—0.02			
(0)	4577.21	21841.25					M
			5864(2)–3680(3)	—0.17			
(1)	4577.94	21837.77	3950(0)– 176(1)	—0.17			M
	4578.620	21834.52	5122(3)– 293(4)	+0.19			A
15	4579.041	21832.51	4172(4)– 198(4)	0.00			
(1)	4580.32	21826.42	3949(2)– 176(1)	—0.04			M
(1)	4583.70	21810.33	5240(3)–3059(4)	—0.03			M
(1)	4587.25	21793.44	5960(2)–3780(3)	—0.17			M
	4587.985	21789.96	4577(3)– 239(3)	—0.01			A
2	4588.591	21787.07	4913(3)– 273(3)	—0.08			
(1)	4594.08	21761.05	4911(2)– 273(3)	—0.09			M
	4594.806	21757.61	5115(5)– 293(4)	0.00			A
	4594.949	21756.93	3697(1)– 152(2)	—0.01			A
80	4595.040	21756.50	5113(3)–2938(3)	+0.02	(... 0.68)	—	
100	4597.160	21746.47	3312(3)– 113(3)	—0.01	(... 1.08)	—	
8	4597.863	21743.14	4681(2)– 250(2)	—0.02	(... 0.60)	—	21
	4598.258	21741.28	5015(3)– 284(3)	—0.34			A, 1
(1)	4601.59	21725.53	3509(2)– 133(2)	—0.14			M
15	4605.036	21709.28	3792(2)– 162(1)	—0.02			
(1)	4605.58	21706.71	4677(3)– 250(2)	+0.13			M
	4606.663	21701.61	5175(3)– 300(2)	—0.25			A
12	4608.280	21693.99	2778(1)– 60(0)	—0.01			
(1)	4610.81	21682.09	5344(4)– 317(3)	—0.15			M
	4611.116	21680.65	5960(2)–3792(2)	+0.17			A
	4612.432	21674.47	5958(3)–3790(4)	+0.27			A, 1
	4613.487	21669.51	4008(4)– 184(5)	—0.38			A, 1

TABLE III *(continued)*

Classified lines of Os I

Int.	λ_{air}	$\sigma_{vac.}$	Classification	$\delta\sigma$	Zeeman effect		Notes
(0)	4615.26	21661.18	5958(3)–3792(2)	—0.08			M
(1)	4615.66	21659.31	5342(2)– 317(3)	+0.11			M
	4616.213	21656.71	5103(4)–2938(3)	—0.13			A
150	4616.783	21654.04	3268(4)– 110(4)	+0.01	(0.92, 1.22)	1.30	
(0)	4618.00	21648.33	5104(3)– 293(4)	—0.13			M
	4618.199	21647.40	5955(3) 3790(4)	+0.13			A
(1)	4623.03	21624.78	4265(2)– 210(1)	—0.13			M
(1)	4623.27	21623.65	5214(2)–3052(1)	—0.12			M
	4624.048	21620.02	5975(3)–3813(4)	+0.07			A
			4492(5)– 234(4)	+0.24			
10	4628.612	21598.70	4720(5)– 256(4)	0.00			
			5165(2)– 300(2)	—0.45			I
	4629.316	21595.41	5000(1)– 284(2)	0.00			A
100	4631.828	21583.70	3680(3)– 152(2)	0.00	$g_1 = 1.47$	$g_2 = 1.60$	
6	4633.173	21577.43	4556(3)– 239(3)	+0.02			
30	4634.768	21570.01	4489(4)– 234(4)	0.00			
(1)	4637.58	21556.93	4715(4)– 256(4)	0.00			M
	4638.531	21552.51	5467(3)–3312(3)	+0.03			A
25	4638.625	21552.08	4486(3)– 233(2)	—0.03			
	4639.210	21549.36	4258(0)– 210(1)	+0.06			A
(1)	4639.73	21546.94	4486(3)– 234(4)	—0.11			M
(0)	4640.63	21542.77	5093(4)– 293(4)	—0.17			M
30	4641.831	21537.19	3027(5)– 87(4)	+0.07			
			4265(2)– 211(3)	+0.46			I
(1)	4642.27	21535.16					M
			4994(3)– 284(3)	+0.05			
	4644.548	21524.59	3561(3)– 140(3)	+0.04			A
(1)	4644.58	21524.45	4887(3)– 273(3)	+0.48			M, I
(2)	4647.30	21511.85	4407(2)– 225(1)	+0.16			M
(0)	4648.01	21508.56	5090(5)– 293(4)	—0.01			M
	4652.291	21488.77	5154(2)– 300(2)	—0.32			A, I
(1)	4652.86	21486.14	5975(3)–3826(3)	+0.26			M, I
	4653.976	21480.99	5782(3)–3634(2)	—0.10			A
(3)	4655.202	21475.33	4961(2)– 281(3)	+0.01			
	4655.395	21474.44	5928(3)–3780(3)	+0.17			A
6	4657.251	21465.88	4574(5)– 242(5)	0.00			
(1)	4657.81	21463.31	4705(3)– 255(3)	—0.04			M
	4658.508	21460.09	4036(4)– 189(3)	+0.11			A
(1)	4659.48	21455.64	4705(3)– 256(4)	—0.10			M
(1)	4661.02	21448.53	4049(1)– 190(0)	—0.04			M
(1)	4661.63	21445.72	4651(1)– 250(2)	—0.02			M
100	4663.822	21435.64	3682(4)– 153(3)	+0.01	(0)	1.04	21
	4665.928	21425.97	5955(3)–3813(4)	+0.02			A
	4666.623	21422.78	4877(2)– 273(3)	+0.25			A
5	4667.542	21418.56	5622(5)–3480(4)	—0.03			
(1)	4668.20	21415.54	3680(3)– 153(3)	+0.03			M
			3663(2)– 152(2)	+0.02			
(1)	4668.93	21412.19					M
			4472(1)– 233(2)	—0.14			

TABLE III *(continued)*

Classified lines of Os I

Int.	λ_{air}	$\sigma_{vac.}$	Classification	$\delta\sigma$	Zeeman effect	Notes
6	4670.686	21404.14	4538(4)– 239(3)	+0.03		
3	4674.014	21388.90	4242(1)– 210(1)	—0.01		
	4677.300	21373.87	5928(3)–3790(4)	—0.21		A
	4679.048	21365.89	5313(4)– 317(3)	—0.31		A, 1
	4679.846	21362.24	5917(2)–3780(3)	+0.39		A, 1
	4680.116	21361.01	5928(3)–3792(2)	—0.13		A
2	4681.428	21355.02	4265(2)– 213(2)	+0.02		
18	4682.312	21350.99	3412(3)– 127(2)	—0.03		
(0)	4684.16	21342.48	4948(4)– 281(3)	+0.01		M
(1)	4684.96	21338.83	4123(3)– 198(4)	—0.08		M
(2)	4686.491	21331.95	4122(5)– 198(4)	0.00		M
	4689.474	21318.39	5958(3)–3826(3)	—0.42		A, 1
			5922(2)–3792(2)	—0.13		
(2)	4691.76	21308.00				M
			5307(2)– 317(3)	—0.19		
80	4692.062	21306.63	3268(4)– 113(3)	+0.02	$g_1 = 1.47$ $g_2 = 1.26$	21
	4694.997	21293.31	5541(4)–3412(3)	—0.29		A, 1
			5809(4)–3682(4)	—0.28		1
	4699.807	21271.52				A
			5960(2)–3833(2)	+0.08		
(2)	4702.73	21258.30	4632(3)– 250(2)	+0.02		M
(1)	4703.59	21254.41	5131(2)– 300(2)	—0.04		M
(—)	4704.05	21252.33	5958(3)–3833(2)	+0.11		M
(2)	4704.85	21248.72	5917(2)–3792(2)	0.00		M
			3663(2)– 153(3)	+0.03		
15	4705.936	21243.81				
			6064(4)–3940(5)	+0.30		1
2	4710.018	21225.40	5955(3)–3833(2)	+0.11		
	4711.415	21219.11	4681(2)– 255(3)	+0.18		A
	4713.840	21208.19	3887(1)– 176(1)	—0.44		A, 1
(2)	4715.02	21202.88	4961(2)– 284(2)	—0.01		M
(1)	4717.21	21193.04	4232(3)– 211(3)	+0.02		M
	4717.370	21192.32	5782(3)–3663(3)	—0.04		A
	4718.560	21186.98	4231(4)– 211(3)	+0.39		A, 1
6	4718.989	21185.05	4008(4)– 189(3)	—0.02		
(2)	4719.60	21182.31	4677(3)– 255(3)	—0.04		M
			4677(3)– 256(4)	+0.01		
12	4721.284	21174.75				
			4852(4)– 273(3)	—0.16		
(1)	4724.37	21160.92	5121(1)– 300(2)	—0.03		M
	4727.047	21148.94	5895(3)–3780(3)	+0.28		A, 1
	4729.750	21136.85	5359(2)–3245(2)	—0.25		A
15	4732.800	21123.23	3634(2)– 152(2)	—0.01	(... 0.92) —	21
(2)	4733.74	21119.04	4242(1)– 213(2)	+0.04		M
	4734.360	21116.27	5960(2)–3848(3)	+0.09		A
3	4734.410	21116.05	2527(2)– 41(3)	—0.05		
(1)	4735.03	21113.28	5672(4)–3561(3)	+0.04		M
(1)	4735.92	21109.32	5050(4)– 293(4)	+0.09		M
12	4738.040	21099.87	4616(2)– 250(2)	+0.04		

TABLE III *(continued)*

Classified lines of Os I

Int.	λ_{air}	$\sigma_{vac.}$	Classification	$\delta\sigma$	Zeeman effect	Notes
	4741.053	21086.46	4049(1)– 194(2)	—0.36		A, 1
2	4742.626	21079.47	3245(2)– 113(3)	+0.03		
60	4743.890	21073.86	3874(2)– 176(1)	+0.01	$g_1 = 1.60$ $g_2 = 1.40$	21
(1)	4744.67	21070.39	5955(3)–3843(3)	+0.36		M, 1
	4747.104	21059.58	5113(3)–3007(2)	—0.27		A, 1
(2)	4748.46	21053.57	5541(4)–3436(5)	—0.10		M
30	4752.158	21037.19	5540(5) 3436(5)	+0.05	(0) —	
	4752.594	21035.26	5895(3)–3792(2)	—0.27		A, 1
10	4755.155	21023.93	4531(6)– 242(5)	+0.02		
	4756.299	21018.87	5928(3)–3826(3)	+0.18		A
(2)	4757.55	21013.35	4232(3)– 213(2)	+0.03		M
			5512(4)–3412(3)	+0.35		I
(2)	4760.14	21001.91				M
			5609(2)–3509(2)	—0.05		
5	4760.770	20999.13	3509(2)– 140(3)	0.00		
			5733(3)–3634(2)	+0.30		I
18	4763.099	20988.86	5960(2)–3861(1)	+0.11		
			3940(5)– 184(5)	—0.01		
	4764.465	20982.85	5037(5)– 293(4)	—0.04		A
(0)	4765.51	20978.25	4008(4)– 191(4)	+0.11		M
	4770.768	20955.13	3634(2)– 153(3)	+0.08		A
(1)	4771.77	20950.72	5271(4)– 317(3)	—0.07		M
(1)	4772.83	20946.07	3861(1)– 176(1)	—0.03		M
(1)	4775.21	20935.63	5032(3)– 293(4)	—0.04		M
(1)	4775.83	20932.91	5098(2)– 300(2)	—0.07		M
(2)	4781.51	20908.05	4489(4)– 239(3)	—0.04		M
	4781.945	20906.15	5917(2) 3826(3)	—0.12		A
			5029(4)– 293(4)	—0.04		
(2)	4783.53	20899.22				M
			5922(2)–3833(2)	+0.13		
	4783.764	20898.20	5914(2) 3824(1)	+0.24		A
	4787.830	20880.45	5027(4)– 293(4)	—0.16		A
300	4793.994	20853.60	2501(3)– 41(3)	—0.01	$g_1 = 1.73$ $g_2 = 1.46$	
(0)	4797.21	20839.62	5917(2)–3833(2)	—0.06		M
(1)	4800.24	20826.47	4414(3)– 233(2)	—0.07		M
6	4807.091	20796.79	5928(3) 3848(3)	—0.05		
(1)	4810.74	20781.01	4813(4)– 273(3)	+0.05		M
2	4812.620	20772.90	3967(2)– 189(3)	—0.05		
18	4813.798	20767.81	3561(3)– 148(4)	—0.06		
			3697(1)– 162(1)	—0.33		I
(1)	4814.04	20766.77	5513(6)–3436(5)	+0.47		M, 1
			5868(3) 3792(2)	0.28		I
	4815.120	20762.11	3512(4)–3436(5)	+0.48		A, 1
18	4815.495	20760.49	3412(3)– 133(2)	—0.08		
60	4815.957	20758.50	5103(4)–3027(5)	—0.04		
(0)	4817.39	20752.33	4187(3)– 211(3)	+0.06		M
(1)	4821.65	20733.99	4632(3)– 255(3)	—0.06		M

TABLE III *(continued)*

Classified lines of Os I

Int.	λ_{air}	$\sigma_{vac.}$	Classification	$\delta\sigma$	Zeeman effect		Notes
			4632(3)– 256(4)	—0.10			
8h	4823.43	20726.34	4913(3)– 284(3)	+0.18			
			5960(2)–3887(1)	+0.12			
			5864(2)–3792(2)	+0.36			1
18	4826.656	20712.49	3480(4)– 140(3)	+0.04	(0)	0.49 ...	11
3	4828.441	20704.83	4577(3)– 250(2)	—0.01			3
	4831.129	20693.31	5895(3)–3826(3)	+0.23			A
(2)	4834.61	20678.41	4466(2)– 239(3)	+0.02			M
			4626(4)– 255(3)	—0.05			
	4836.703	20669.47					A
			5503(5)–3436(5)	+0.45			1
2	4838.122	20663.40	3833(2)– 176(1)	—0.01			
			2938(3)– 87(4)	+0.07	(0)	—	9
25	4843.868	20638.89					
			5876(4)–3813(4)	+0.22			
(0)	4845.00	20634.07	4877(2)– 281(3)	+0.10			M
	4846.125	20629.28	4492(5)– 242(5)	+0.13			A
	4848.386	20619.66	5910(2)–3848(3)	—0.28			A, 1
			4875(4)– 281(3)	—0.07			
	4849.126	20616.51					A
			5922(2)–3861(1)	+0.11			
	4849.435	20615.20	5541(4)–3480(4)	+0.02			A
(2)	4852.57	20601.88	4172(4)– 211(3)	—0.04			M
3	4854.940	20591.82	3949(2)– 189(3)	—0.04			
2	4858.470	20576.86	3824(1)– 176(1)	0.00			
(1)	4858.78	20575.55	4616(2)– 255(3)	—0.05			M
			4187(3)– 213(2)	+0.05			
3	4859.471	20572.62					
			5233(2)– 317(3)	—0.11			
	4863.214	20556.79	5917(2)–3861(1)	—0.20			A
6	4864.009	20553.43	4387(5)– 234(4)	—0.03			
			4483(6)– 242(5)	—0.40			1
80	4865.598	20546.72					
			5113(3)–3059(4)	+0.04	$g_1 = 1.73$	$g_2 = 1.55$	9, 22
8	4867.177	20540.05	4386(4)– 234(4)	+0.02			
(1)	4868.83	20533.08	5058(1)– 300(2)	—0.02			M
	4875.520	20504.90	5876(4)–3826(3)	+0.30			A, 1
(1)	4876.09	20502.51	4785(4)– 273(3)	—0.06			M
			4556(3)– 250(2)	+0.02	(0)	1.18	9
18	4878.518	20492.30					
			5910(2)–3861(1)	—0.21			
			5609(2)–3561(3)	—0.05			
12	4882.285	20476.49					
			4782(3)– 273(3)	—0.23	(0.21)	1.11	9
(1)	4883.82	20470.06	5359(2)–3312(3)	0.00			M
	4884.098	20468.89	4036(4)– 198(4)	+0.04			A
(1)	4885.07	20464.82	3480(4)– 143(5)	—0.01			M
(2)	4889.32	20447.03	5103(4)–3059(4)	—0.01			M
(1)	4892.50	20433.74	4550(2)– 250(2)	0.00			M

TABLE III *(continued)*

Classified lines of Os I

Int.	λ_{air}	$\sigma_{vac.}$	Classification	$\delta\sigma$	Zeeman effect		Notes
(0)	4892.93	20431.96	4375(4)– 234(4)	—0.02			M
	4894.867	20423.86	5868(3)–3826(3)	—0.18			A
8	4895.268	20422.18	3663(2)– 162(1)	+0.05	(0)	0.96 ...	
(2)	4895.96	20419.30	5890(3)–3848(3)	+0.11			M
60	4899.215	20405.73	4873(4)–2833(4)	+0.06	(... 0.35)	1.54	
	4899.762	20403.46	5864(2)–3824(1)	—0.03			A
2	4902.180	20393.39	3561(3)– 152(2)	+0.04			
(0)	4908.83	20365.77	4873(4)–2837(3)	+0.01			M
(1)	4909.84	20361.58	4877(2)– 284(3)	+0.04			M
8	4910.463	20358.99	3052(1)– 101(2)	+0.05			
80	4912.605	20350.11	3312(3)– 127(2)	+0.01	$g_1 = 1.63$	$g_2 = 1.02$	
6	4921.804	20312.08	3861(1)– 183(0)	+0.04			
(2)	4925.43	20297.13	3940(5)– 191(4)	+0.02			M
3	4926.385	20293.19	4361(1)– 233(2)	—0.02			
(0)	4928.96	20282.59	5876(4)–3848(3)	—0.16			M
(1)	4931.26	20273.13	5032(3)– 300(2)	—0.05			M
(1)	4933.45	20264.13	3967(2)– 194(2)	—0.10			M
			4761(3)– 273(3)	+0.45			1
12	4935.813	20254.43	3792(2)– 176(1)	+0.06			
			5031(2)– 300(2)	—0.49			1
(0)	4941.76	20230.06	5503(5)–3480(4)	—0.47			1
			5910(2)–3887(1)	+0.08			M
18	4942.940	20225.23	3561(3)– 153(3)	+0.07	(0)	1.53	
(0)	4949.56	20198.17	4351(3)– 233(2)	+0.02			M
3	4950.590	20193.97	4008(4)– 198(4)	+0.03			
(1)	4951.90	20188.63	4753(2)– 273(3)	+0.01			M
(1)	4953.86	20180.64	4577(3)– 255(3)	+0.03			M
(2)	4955.73	20173.03	4577(3)– 256(4)	+0.03			M
			5609(2)–3591(1)	+0.12			
			5955(3)–3938(3)	—0.06			
(2)	4958.17	20163.10	4830(3)– 281(3)	+0.06			M
2	4959.034	20159.59	4414(3)– 239(3)	+0.03			
(0)	4963.86	20139.99	4953(5)– 293(4)	+0.01			M
(1)	4965.47	20133.46	3634(2)– 162(1)	+0.06			M
(3)	4968.91	20119.52	4343(2)– 233(2)	—0.01			M
(1)	4971.67	20108.35	4123(3)– 211(3)	+0.03			M
			5960(2)–3949(2)	—0.04			
(1)	4975.04	20094.73	4265(2)– 225(1)	+0.02			M
(1)	4976.02	20090.77	4407(2)– 239(3)	+0.01			M
(0)	4976.43	20089.12	5958(3)–3949(2)	—0.05			M
(0)	4976.78	20087.71	4948(4)– 293(4)	+0.02			M
(1)	4977.91	20083.15	3949(2)– 194(2)	+0.01			M
(1)	4978.90	20079.15	4340(5)– 234(4)	—0.01			M, 3
18	4979.318	20077.47	3628(0)– 162(1)	+0.03			

TABLE III *(continued)*

Classified lines of Os I

Int.	λ_{air}	$\sigma_{vac.}$	Classification	$\delta\sigma$	Zeeman effect	Notes
			3412(3)– 140(3)	+0.04		
6	4990.103	20034.07				
			5864(2)–3861(1)	—0.18		
(0)	4992.02	20026.38	3436(5)– 143(5)	+0.04		M
(0)	4993.84	20019.08	4258(0)– 225(1)	—0.02		M
(0)	4999.27	19997.34	4840(1)– 284(3)	—0.03		M
(1)	5000.50	19992.42	4813(4)– 281(3)	+0.02		M
			4556(3)– 255(3)	+0.01		
(1)	5006.60	19968.06				M
			5809(4)–3813(4)	—0.04		
(1)	5009.68	19955.78	3480(4)– 148(4)	+0.01		M
(0)	5011.01	19950.49	5000(1)– 300(2)	—0.08		M
12	5012.525	19944.46	5240(3)–3245(2)	+0.09		
(0)	5016.50	19928.66	4123(3)– 213(2)	+0.04		M
(0)	5016.88	19927.14	5960(2)–3967(2)	—0.16		M
(1)	5017.97	19922.82	5672(4)–3680(3)	—0.07		M
(1)	5020.64	19912.22	3007(2)– 101(2)	—0.08		M
7	5020.892	19911.22	5672(4)–3681(5)	0.00		
(1)	5021.32	19909.53	4550(2)– 255(3)	+0.02		M
(1)	5021.70	19908.02	5958(3)–3967(2)	—0.06		M
(2)	5023.04	19902.71	3672(4)–3682(4)	—0.06		M
(1)	5023.77	19899.81	5928(3)–3938(3)	—0.09		M
			4830(3)– 284(3)	+0.18		
(1)	5026.05	19890.79				M
			5165(2)– 317(3)	—0.10		
8	5029.247	19878.14	4386(4)– 239(3)	+0.03		
20	5031.831	19867.94	3509(2)– 152(2)	+0.01		
12	5034.172	19858.69	4242(1)– 225(1)	—0.02	(0.25) —	
50	5039.122	19839.19	3874(2)– 189(3)	—0.06		
(3)	5042.19	19827.12	3887(1)– 190(0)	+0.06		M
(0)	5045.09	19815.73	4987(2)– 300(2)	—0.05		M
			4920(3)– 293(4)	—0.11		
3	5047.154	19807.62				
			4715(4)– 273(3)	+0.10		
(1)	5048.33	19803.01	5541(4)–3561(3)	—0.07		M
(1)	5049.10	19799.99	4486(3)– 250(2)	—0.01		M
5	5050.417	19794.82	4538(4)– 255(3)	+0.07		
			4538(4)– 256(4)	+0.07		
(1)	5052.36	19787.21				M
			5917(2)–3938(3)	—0.27		1
(1)	5053.99	19780.83	5154(2)– 317(3)	0.00		M
3h	5056.01	19772.93	5538(3)–3561(3)	—0.02		
(1)	5056.73	19770.11	4375(4)– 239(3)	+0.05		M
			3312(3)– 133(2)	+0.03		
(1)	5059.40	19759.68				M
			5914(2)–3938(3)	+0.47		1
(1)	5063.46	19743.83	4913(3)– 293(4)	+0.02		M

TABLE III *(continued)*

Classified lines of Os I

Int.	λ_{air}	$\sigma_{vac.}$	Classification	$\delta\sigma$	Zeeman effect		Notes
			4229(1)– 225(1)	—0.03			
(0)	5065.43	19736.15					M
			5922(2)–3949(2)	+0.11			
(1)	5071.11	19714.05	4785(4)– 281(3)	+0.04			M
12	5072.884	19707.15	3591(1)– 162(1)	+0.01			
12	5074.769	19699.83	3509(2)– 153(3)	+0.09	(0)	1.51	
8	5076.223	19694.19	4301(3)– 233(2)	+0.23			
			5214(3)–3245(2)	+0.29			l
5	5076.906	19691.54					
			5907(3)–3938(3)	—0.48			l
3	5077.59	19688.89	4301(3)– 234(4)	—0.01			
15	5079.088	19683.08	3245(2)– 127(2)	+0.02			
(0)	5080.75	19676.64	5917(2)–3949(2)	+0.01			M
5	5093.092	19628.96	2837(3)– 87(4)	+0.11			
(0)	5093.78	19626.31	4361(2)– 239(3)	+0.08			M
30	5103.495	19588.95	2833(4)– 87(4)	+0.01			
			3848(3)– 189(3)	+0.11			
8	5104.740	19584.18					
			4387(5)– 242(5)	+0.03			
(1)	5107.35	19574.17	5895(3)-3938(3)	—0.12			M
3	5108.264	19570.67	4386(4)– 242(5)	—0.05			
			3861(1)– 190(0)	—0.02			
(2)	5109.87	19564.51					M
			5132(4)– 317(3)	+0.26			l
(5)	5110.82	19560.88	3059(4)– 110(4)	+0.01			M
(0)	5111.51	19558.24	4961(2)– 300(2)	+0.19			M
(1)	5118.59	19531.19	4351(3)– 239(3)	+0.02			M
(1)	5119.95	19526.00	5733(3)–3780(3)	+0.21			M
(1)	5120.75	19522.95	4793(2)– 284(3)	+0.01			M
25	5122.229	19517.31	3436(5)– 148(4)	+0.03			
			3436(5)– 149(6)	—0.08			
8	5123.381	19512.92					
			3940(5)– 198(4)	+0.01			
12	5124.349	19509.23	2527(2)– 57(1)	—0.05			
			5917(2)–3967(2)	+0.03			
(1)	5127.94	19495.57					M
			5958(3)–4008(4)	—0.39			l
(1)	5128.98	19491.62	3790(4)– 184(5)	—0.03			M
(1)	5129.44	19489.87	3938(3)– 198(4)	—0.01			M
(1)	5131.92	19480.45	4887(3)– 293(4)	—0.18			M
			5359(2)–3412(3)	+0.01			
7	5134.898	19469.15					
			5955(3)–4008(4)	+0.12			
5	5135.898	19465.36	3887(1)– 194(2)	+0.05			
(1)	5136.61	19462.67	4375(4)– 242(5)	0.00			M
(1)	5137.88	19457.85	5609(2)–3663(2)	—0.07			M
7	5143.285	19437.41	3245(2)– 130(1)	+0.04			
15	5145.543	19428.88	3833(2)– 189(3)	+0.07			

TABLE III *(continued)*

Classified lines of Os I

Int.	λ_{air}	$\sigma_{vac.}$	Classification	$\delta\sigma$	Zeeman effect		Notes
			5733(3)–3790(4)	—0.30			1
(2)	5146.49	19425.30					M
			4677(3)– 273(3)	—0.03			
5	5146.86	19423.90	4274(4)– 234(4)	—0.01			
			3480(4)– 153(3)	0.00	$g_1 = 1.35$	$g_2 = 1.52$	9
80	5149.736	19413.06					
			5733(3)–3792(2)	+0.40			1
7	5152.013	19404.48	5622(5)–3681(5)	+0.01	(... **0.38**)	—	
(0)	5154.28	19395.94	5622(5)–3682(4)	—0.08			M
(2)	5156.41	19387.93	5975(3)–4036(4)	—0.19			M
(1)	5159.29	19377.11	3848(3)– 191(4)	—0.03			M
			3826(3)– 198(3)	—0.01			
(2)	5163.26	19362.21					M
			4875(4)– 293(4)	+0.41			1
(1)	5164.97	19355.80	4873(4)–2938(3)	+0.01			M
			4265(2)– 233(2)	+0.05	(... **0.30**)	1.42	9
8	5168.975	19340.81					
			5782(3)–3848(3)	—0.08			
8	5171.72	19330.54	3874(2)– 194(2)	+0.01			
(1)	5174.65	19319.59	4492(5)– 256(4)	+0.02			M
(0)	5176.62	19312.24	3697(1)– 176(1)	+0.07			M
(1)	5180.24	19298.75	4489(4)– 255(3)	+0.02			M
5	5182.282	19291.14	4489(4)– 256(4)	+0.02			
			3412(3)– 148(4)	0.00			
(0)	5185.99	19277.35	5240(3) -3312(3)	+0.02			M
			5104(3)– 317(3)	—0.36			1
(1)	5186.42	19275.75	4486(3)– 255(3)	—0.02			M
(1)	5188.41	19268.36	4486(3)– 256(4)	+0.20			M
30	5193.525	19249.38	3027(5)– 110(4)	+0.01			
(1)	5199.27	19228.11	3813(4)– 189(3)	—0.04			M
30h	5202.634	19215.68	2938(3)– 101(2)	+0.01	(0)	1.52	
12	5203.232	19213.47	3059(4)– 113(3)	+0.02			
3	5226.57	19127.67	4753(2)– 284(3)	+0.04			
(1)	5231.43	19109.91	4340(5)– 242(5)	+0.06			M
			4242(1)– 233(2)	—0.19			
5	5232.89	19104.57					
			5960(2)–4049(1)	—0.14			
(1)	5236.16	19092.64	3245(2)– 133(2)	+0.03			M
(1)	5240.91	19075.34	3848(3)– 194(2)	—0.01			M
5	5241.20	19074.29	4414(3)– 250(2)	—0.14			
(1)	5244.85	19061.01	5467(3)–3561(3)	—0.03			M
(0)	5246.24	19055.96	4640(2)– 273(3)	+0.02			M
(1)	5249.68	19043.48	5538(3)–3634(2)	+0.42			M, 1
(1)	5252.53	19033.14	3312(3)– 140(3)	+0.03			M
(1)	5254.17	19027.20	4301(3)– 239(3)	+0.22			M
(2)	5254.99	19024.23	5214(2)–3312(3)	+0.02			M
20	5255.823	19021.22	3813(4)– 191(4)	0.00			
(1)	5256.22	19019.78	3792(2)– 189(3)	+0.01			M
15	5259.797	19006.85	3790(4)– 189(3)	+0.02			

TABLE III *(continued)*

Classified lines of Os I

Int.	λ_{air}	$\sigma_{vac.}$	Classification	$\delta\sigma$	Zeeman effect	Notes
(1)	5260.12	19005.68	4407(2)– 250(2)	+0.05		M
(1)	5260.63	19003.84	5733(3)–3833(2)	+0.22		M
(1)	5261.94	18999.10	4232(3)– 233(2)	+0.02		M
			4231(4)– 234(4)	—0.07	(... 0.55) —	9
30	5265.150	18987.52				
			5907(3)–4008(4)	—0.44		1
8w	5271.84	18963.43	4008(4)– 211(3)	+0.08		
			3833(2)– 194(2)	+0.09		
8	5283.889	18920.18				
			5672(4)–3780(3)	—0.40		1
(0)	5286.03	18912.52	4626(4)– 273(3)	+0.02		M
10	5287.70	18906.55	3780(3)– 189(3)	—0.09		
(1)	5288.73	18902.87	3412(3)– 152(2)	+0.04		M
20	5295.65	18878.16	3509(2)– 162(1)	+0.07		
20	5298.781	18867.01	4719(5)–2833(4)	+0.05		
15	5302.58	18853.50	3826(3)– 194(2)	0.00		
(1)	5308.18	18833.61	3824(1)– 194(2)	+0.07		M
			5890(3)–4008(4)	+0.46		1
(1)	5312.40	18818.65				M
			4616(2)– 273(3)	+0.07		
(1)	5335.36	18737.67	4813(4)– 293(4)	+0.05		M
20	5336.23	18734.62	3412(3)– 153(3)	—0.02		
(1)	5339.59	18722.83	5570(0)–3697(1)	—0.15		M
(1)	5341.32	18716.76	4877(2)– 300(2)	+0.06		M
(0)	5342.30	18713.33	5907(3)–4036(4)	+0.28		M, 1
8	5346.03	18700.27	3007(2)– 113(3)	—0.01		
(1)	5348.32	18692.27	5809(4)–3940(5)	+0.06		M
			3634(2)– 176(1)	+0.07		
20	5352.25	18678.54				
			3697(1)– 183(0)	+0.43		1
			4265(2)– 239(3)	—0.05		
(1)	5353.63	18673.73				M
			4681(2)– 281(3)	+0.38		1
			4806(5)– 293(4)	+0.02		
(1)	5355.29	18667.94				M
			5955(3)–4088(2)	—0.05		
(1)	5361.64	18645.83	4705(3)– 284(3)	+0.49		M, 1
8	5362.893	18641.47	3967(2)– 210(1)	+0.03		
(1)	5364.23	18636.83	4677(3)– 281(3)	+0.06		M
			5541(4)–3681(5)	+0.01		
(1)	5374.54	18601.07				M
			5868(3)–4008(4)	—0.12		
(2)	5375.12	18599.07	5672(4)–3813(4)	0.00		M
			3268(4)– 140(3)	+0.04	$g_1 = 1.10$ $g_2 = 1.37$	9
50	5376.792	18593.28	3848(3)– 198(4)	+0.34		1
			5733(3)–3874(2)	+0.10		
7	5379.308	18584.59	5540(5)–3681(5)	+0.06		
(0)	5381.72	18576.26	5540(5)–3682(4)	+0.18		M
8h	5385.72	18562.46	5538(3)–3682(4)	—0.02		

TABLE III *(continued)*

Classified lines of Os I

Int.	λ_{air}	$\sigma_{vac.}$	Classification	$\delta\sigma$	Zeeman effect		Notes
4	5386.926	18558.31	4187(3)– 233(2)	—0.02			
(2)	5387.14	18557.57	5484(1)–3628(0)	+0.04			M
(1)	5389.27	18550.24	4414(3)– 255(3)	+0.04			M
3	5391.48	18542.63	4414(3)– 256(4)	+0.04			
(2)	5391.92	18541.12	4361(2)– 250(2)	+0.02			M
(0)	5395.57	18528.58	5029(4)– 317(3)	+0.07			M
(1)	5400.66	18511.11	3792(2)– 194(2)	+0.06			M
(1)	5402.71	18504.09	5359(2)–3509(2)	+0.05			M
8	5403.432	18501.62	5484(1)–3634(2)	+0.05			
(1)	5409.33	18481.44	4407(2)– 255(3)	+0.04			M
15	5412.14	18471.85	3950(0)– 210(1)	+0.02			
80	5416.345	18457.51	4873(4)–3027(5)	+0.02	(0)	1.51	
50	5416.693	18456.32	2261(4)– 41(3)	—0.05			
(1)	5417.17	18454.70	4274(4)– 242(5)	+0.10			M
40	5417.507	18453.55	5113(3)–3268(4)	+0.03	$g_1 = 1.73$	$g_2 = 1.46$	
8	5419.73	18445.98	4351(3)– 250(2)	—0.06			
(1)	5432.40	18402.96	4172(4)– 234(4)	+0.04			M
			4681(2)– 284(3)	—0.03			
(1)	5433.01	18400.89					M
			3681(5)– 184(5)	+0.07			
(0)	5433.87	18397.98	3780(3)– 194(2)	+0.06			M
(1)	5436.82	18388.00	5015(3)– 317(3)	—0.32			M, 1
(2)	5441.10	18373.53	5346(1)–3509(2)	+0.03			M
			3826(3)– 198(4)	+0.01			
12	5441.821	18371.10					
			3967(2)– 213(2)	—0.43			1
			3949(2)– 211(3)	+0.08			
(2)	5442.08	18370.22					M
			5960(2)–4123(3)	+0.01			
(1)	5442.92	18367.39	4343(2)– 250(2)	—0.03			M
50	5443.310	18366.07	3245(2)– 140(3)	0.00	$g_1 = 1.84$	$g_2 = 1.09$	
(1)	5443.79	18364.45	4677(3)– 284(3)	+0.11			M
(4)	5446.93	18353.87	5103(4)–3268(4)	—0.01			M
			2938(3)– 110(4)	0.00			
3	5447.76	18351.07					
			5958(3)–4123(3)	+0.08			
20	5449.37	18345.65	3268(4)– 143(5)	+0.03			
18	5453.395	18332.11	4232(3)– 239(3)	+0.01	(0)	1.09	
(1)	5455.29	18325.71	4231(4)– 239(3)	+0.04			M
25	5457.298	18318.99	2346(5)– 51(5)	+0.01			
			5513(6)–3681(5)	0.00			
(1)	5458.88	18313.69					M
			5622(5)–3790(4)	+0.05			
(1)	5462.76	18300.68	5512(4)–3682(4)	+0.11			M
(1)	5467.76	18283.95	5609(2)–3780(3)	+0.07			M
			3312(3)– 148(4)	+0.04			
30	5469.998	18276.47					
			5240(3)–3412(3)	+0.06	(... 0.13)	—	9
2	5474.58	18261.17	4386(4)– 256(4)	+0.03			

TABLE III *(continued)*

Classified lines of Os I

Int.	λ_{air}	σ_{vac}	Classification	$\delta\sigma$	Zeeman effect		Notes
15	5475.13	18259.34	3938(3)– 211(3)	+0.05			
30	5477.268	18252.21	3591(1)– 176(1)	0.00			
(1)	5479.18	18245.84	4830(3)– 300(2)	+0.07			M
(1)	5479.99	18243.15	5672(4)–3848(3)	0.00			M
15	5481.852	18236.95	3813(4)– 198(4)	—0.07			
(0)	5489.10	18212.87	5484(1)–3663(3)	+0.03			M
(1)	5489.63	18211.11	4556(3)– 273(3)	+0.08			M
8	5492.28	18205.64	2837(3)– 101(2)	—0.06			
(1)	5504.86	18160.72	4375(4)– 255(3)	+0.02			M
(1)	5507.15	18153.17	4375(4)– 256(4)	+0.08			M
(1)	5507.33	18152.58	4550(2)– 273(3)	+0.09			M
15	5509.330	18145.99	4873(4)–3059(4)	0.00			
7	5516.011	18124.01	4626(4)– 281(3)	+0.07			
100	5523.531	18099.34	4719(5)–2909(6)	+0.02	(0)	0.97 ...	
(1)	5525.66	18092.36	5622(5)–3813(4)	+0.04			M
(2)	5529.55	19079.63	3938(3)– 213(2)	+0.04			M
(1)	5542.39	18037.75	4538(4)– 273(3)	+0.02			M
8	5546.819	18023.35	5214(2)–3412(3)	+0.06			
3	5548.76	18017.04	4361(2)– 255(3)	+0.17			
			5890(3)–4088(2)	—0.11			
(1)	5549.17	18015.71	3790(4)– 198(4)	+0.01			M
(4)	5549.79	18013.70	5113(3)–3312(3)	+0.05			M
12	5552.883	18003.67	2938(3)– 113(3)	+0.02			
7	5560.622	17978.61	5359(2)–3561(3)	—0.01			
(0)	5569.05	17951.40	5733(3)–3938(3)	—0.02			M
(3)	5572.01	17941.87	4301(3)– 250(2)	+0.02			M
(1)	5573.05	17938.52	5917(2)–4123(3)	+0.07			M
(1)	5574.48	17933.92	4049(1)– 225(1)	+0.09			M
(2)	5580.20	17915.53	3780(3)– 198(4)	+0.02			M
8	5580.659	17914.06	4123(3)– 233(2)	—0.32			I
			4351(3)– 256(4)	—0.14			
			5103(4)–3312(3)	+0.05	(0)	1.57	9
(0)	5582.10	17909.44	4123(3)– 234(4)	+0.12			M
(2)	5583.69	17904.34	3680(3)– 189(3)	+0.01			M
50	5584.444	17901.92	3312(3)– 152(2)	+0.01	(0)	1.62	9
			4122(5)– 234(4)	—0.44			I
(2)	5587.73	17891.39	4187(3)– 239(3)	+0.04			M
(1)	5591.87	17878.14	4793(2)– 300(2)	+0.04			M
(1)	5594.18	17870.76	5467(3)–3680(3)	+0.07			M
(1)	5595.07	17867.92	5484(1)–3697(1)	+0.05			M
(3)	5600.50	17850.60	5467(3)–3682(4)	+0.03			M
(0)	5601.22	17848.30	5609(2)–3824(1)	+0.04			M
(0)	5604.89	17836.61	3268(4)– 148(4)	+0.05			M
(1)	5614.53	17805.99	4720(5)– 293(4)	+0.04			M
(0)	5619.42	17790.49	4620(1)– 284(3)	+0.08			M
30	5620.085	17788.39	2795(2)– 101(2)	+0.05	(... 1.19)	—	
(1)	5629.82	17757.63	4616(2)– 284(3)	+0.04			M

TABLE III *(continued)*

Classified lines of Os I

Int.	λ_{air}	$\sigma_{vac.}$	Classification	$\delta\sigma$	Zeeman effect	Notes
(2)	5632.06	17750.57	3052(1)– 127(2)	+0.03		M
(1)	5635.08	17741.05	4172(4)– 239(3)	+0.05		M
(3)	5637.41	17733.72	3312(3)– 153(3)	0.00		M
(2)	5637.76	17732.62	3663(2)– 189(3)	+0.02		M
4	5642.558	17717.55	3682(4)– 191(4)	+0.03		
5	5645.253	17709.09	3681(5)– 191(4)	+0.02		
(1)	5645.66	17707.81	3874(2)– 210(1)	+0.07		M
(2)	5648.98	17697.40	3680(3)– 191(4)	0.00		M
(1)	5656.12	17675.06	5359(2)–3591(1)	+0.07		M
(3)	5674.38	17618.18	3591(1)– 183(0)	+0.03		M
(1)	5676.88	17610.43	5541(4)–3780(3)	+0.01		M
(1)	5678.16	17606.46	5609(2)–3848(3)	+0.01		M
20	5680.884	17598.01	5240(3)–3480(4)	+0.02		
(1)	5683.91	17588.64	4265(2)– 250(2)	—0.01		M
(1)	5686.61	17580.29	3861(1)– 210(1)	+0.30		I
			5538(3)–3780(3)	0.00		M
(1)	5689.09	17572.63	3887(1)– 213(2)	+0.02		M
(1)	5698.25	17544.38	5346(1)–3591(1)	—0.07		M
4	5709.370	17510.21	5541(4)–3790(4)	—0.02		
(1)	5711.10	17504.91	3052(1)– 130(1)	+0.06		M
(2)	5714.75	17493.73	5540(3)–3790(4)	+0.03		M
(1)	5718.32	17482.80	4753(2)– 300(2)	+0.01		M
(2)	5719.21	17480.08	3049(0)– 130(1)	+0.17		M
			5538(3)–3790(4)	—0.02		
80	5721.931	17471.77	2261(4)– 51(5)	0.00	(0, 0.24 ...) —	
(0)	5726.19	17458.77	5570(0)–3824(1)	+0.48		M, I
2	5731.076	17443.90	3634(2)– 189(3)	+0.03		
(0)	5733.05	17437.89	3874(2)– 213(2)	+0.06		M
3	5737.888	17423.19	3509(2)– 176(1)	+0.03		
(1)	5738.08	17422.60	4556(3)– 281(3)	+0.13		M
(0)	5738.84	17420.30	4747(1)– 300(2)	+0.04		M
3	5739.717	17417.63	4301(3)– 255(3)	+0.01		
(1)	5742.23	17410.01	4301(3)– 256(4)	0.00		M
(1)	5746.97	17395.65	3680(3)– 194(2)	+0.06		M
5	5751.492	17381.98	4677(3)– 293(4)	—0.01		
(1)	5757.46	17363.96	4550(2)– 281(3)	+0.03		M
(1)	5757.94	17362.51	3848(3)– 211(3)	+0.16		M
			4577(3)– 284(3)	—0.09		
(1)	5761.21	17352.65	4242(1)– 250(2)	0.00		M
15	5765.047	17341.10	2837(3)– 110(4)	0.00		
(0)	5771.03	17323.13	5672(4)–3940(5)	—0.05		M
(2)	5774.98	17311.28	5240(3)–3509(2)	—0.03		M
(0)	5775.35	17310.17	3861(1)– 213(2)	+0.09		M
(1)	5777.40	17304.03	3007(2)– 127(2)	+0.13		M
(1)	5778.33	17301.24	2833(4)– 110(4)	+0.05		M
(1)	5779.64	17297.32	3833(2)– 210(1)	+0.02		M

TABLE III *(continued)*

Classified lines of Os I

Int.	λ_{air}	$\sigma_{vac.}$	Classification	$\delta\sigma$	Zeeman effect	Notes
50	5780.815	17293.80	3268(4)– 153(3)	—0.05	(0) 1.30	
(2)	5782.44	17288.94	5541(4)–3813(4)	+0.03		M
(0)	5792.54	17258.80	5538(3)–3813(4)	+0.02		M
			4538(4)– 281(3)	—0.44		I
(2)	5795.92	17248.73				M
			5359(2)–3634(2)	0.00		
			4123(3)– 239(3)	+0.02		
			4232(3)– 250(2)	+0.45		I
(2)	5796.36	17247.42				M
			5733(3)–4008(4)	+0.06		
			6064(4)–4340(5)	—0.25		
(1)	5796.97	17245.61	5955(3)–4231(4)	—0.18		M
50	5800.603	17234.81	3245(2)– 152(2)	—0.06	$g_1 = 1.86$ $g_2 = 1.62$	
			4229(1)– 250(2)	+0.03		
(1)	5802.17	17230.15				M
			5910(2)–4187(3)	+0.13		
(1)	5804.27	17223.92	3663(2)– 194(2)	+0.04		M
(2)	5808.70	17210.79	3824(1)– 210(1)	+0.04		M
(1)	5809.94	17207.11	3833(2)– 211(3)	+0.02		M
			4049(1)– 233(2)	+0.09		
(0)	5819.12	17179.97	5890(3)–4172(4)	+0.35		M, I
			5960(2)–4242(1)	+0.14		
(1)	5821.08	17174.18	5346(1)–3628(0)	+0.03		M
3	5830.986	17145.01	4274(4)– 256(4)	—0.01		
5	5842.49	17111.25	3967(2)– 225(1)	+0.01		
			4550(2)– 284(3)	0.00		
(1)	5849.24	17091.50				M
			5975(3)–4265(2)	—0.18		
(1)	5849.98	17089.34	5570(0)–3861(1)	+0.29		M, I
80	5857.760	17066.64	3245(2)– 153(3)	—0.04		
			3007(2)– 130(1)	+0.04		
8	5860.641	17058.25	5214(2)–3509(2)	+0.06		
			5538(3)–3833(2)	+0.13		
(2)	5871.25	17027.43	3833(2)– 213(2)	+0.04		M
(1)	5876.31	17012.77	5113(3)–3412(3)	+0.04		M
(1)	5878.48	17006.49	3813(4)– 211(3)	+0.06		M
7	5882.916	16993.66	2837(3)– 113(3)	—0.02		
(0)	5883.81	16991.08	4875(4)– 317(3)	+0.03		M
(2)	5894.29	16960.87	3826(3)– 213(2)	+0.07		M
(3)	5894.59	16960.01	5359(2)–3663(2)	+0.01		M
(1)	5896.75	16953.80	2833(4)– 113(3)	+0.03		M
(2)	5900.99	16941.61	3950(0)– 225(1)	—0.02		M
(3)	5903.23	16935.19	3634(2)– 194(2)	+0.04		M
			3682(4)– 198(4)	—0.29		I
3	5903.982	16933.03	4122(5)– 242(5)	—0.02		
			5541(4)–3848(3)	+0.04		
			3681(5)– 198(4)	—0.03		
3	5906.84	16924.84				
			5958(3)–4265(2)	—0.23		

TABLE III *(continued)*

Classified lines of Os I

Int.	λ_{air}	$\sigma_{vac.}$	Classification	$\delta\sigma$	Zeeman effect	Notes
(4)	5908.95	16918.79	4719(5)–3027(5)	+0.01		M
(1)	5914.28	16903.54	4088(2)– 239(3)	+0.07		M
(1)	5919.61	16888.33	3792(2)– 210(1)	+0.07		M
(0)	5925.82	16870.63	3591(1)– 190(0)	—0.01		M
			5917(2)–4229(1)	+0.03		
(0)	5926.59	16868.43	5467(3)–3780(3)	+0.05		M
(1)	5927.30	16866.42	5809(4)–4123(3)	+0.21		M
(0)	5931.75	16853.76	5917(2)–4231(3)	+0.01		M
(3)	5940.31	16829.48	5346(1)–3663(2)	+0.02		M
(1)	5948.53	16806.22	4187(3)– 250(2)	0.00		M
			5910(2)–4229(1)	+0.10		
(1)	5951.41	16798.09	3792(2)– 211(3)	+0.04		M
(2)	5954.86	16788.36	5359(2)–3680(3)	+0.09		M
(2)	5955.74	16785.88	5240(3)–3561(3)	—0.01		M
(2)	5962.01	16768.22	5467(3)–3790(4)	+0.03		M
(2)	5964.81	16760.35	4852(4)– 317(3)	—0.47		M, 1
(2)	5967.38	16753.13	4489(4)– 281(3)	—0.02		M
(0)	5975.17	16731.29	4102(6)– 242(5)	+0.04		M
(2)	5978.25	16722.67	4232(3)– 255(3)	—0.07		M
(0)	5979.39	16719.48	4677(3)– 300(2)	—0.02		M
			5914(2)–4242(1)	—0.32		1
(2)	5981.36	16713.98	3561(3)– 189(3)	0.00		M
(3)	5983.22	16708.78	4231(4)– 256(4)	+0.08		M
(2)	5991.76	16684.97	3780(3)– 211(3)	+0.05		M
50	5995.998	16673.17	5103(4)–3436(5)	+0.01	(0) **0.75** ...	
(2)	6007.19	16642.11	5672(4)–4008(4)	—0.04		M
8	6015.973	16618.31	3792(2)– 213(2)	—0.04		
(1)	6016.97	16615.06	5359(2)–3697(1)	+0.03		M
(3)	6019.81	16607.22	2938(3)– 127(2)	—0.05		M
			4719(5)–3059(4)	—0.06		
(1)	6031.03	16576.32	2795(2)– 113(3)	0.00		M
(1)	6045.35	16537.06	4830(3)– 317(3)	—0.45		M, 1
(1)	6052.89	16516.46	5484(1)–3833(2)	—0.17		M
(3)	6054.63	16511.72	5917(2) 4265(2)	—0.35		1
			4386(4)– 273(3)	—0.01		M
(1)	6056.32	16507.11	3561(3)– 191(4)	+0.06		M
(1)	6057.02	16505.20	3780(3)– 213(2)	—0.02		M
			6064(4)–4414(3)	—0.15		
(1)	6058.90	16500.08	3059(4)– 140(3)	0.00		M
(0)	6064.67	16484.38	5346(1)–3697(1)	—0.11		M
(2)	6074.13	16458.71	4651(1)– 300(2)	+0.05		M
			5876(4)–4231(4)	+0.20		

TABLE III *(continued)*

Classified lines of Os I

Int.	λ_{air}	$\sigma_{vac.}$	Classification	$\delta\sigma$	Zeeman effect		Notes
(1)	6074.49	16457.73	4486(3)– 284(3)	—0.03			M
(1)	6089.40	16417.43	5609(2)–3967(2)	—0.14			M
(2)	6091.15	16412.72	5467(3)–3826(3)	—0.08			M
(1)	6100.83	16386.68	3480(4)– 184(5)	—0.02			M
(2)	6103.24	16380.21	4577(3)– 293(4)	—0.04			M
(2)	6104.32	16377.31	4036(4)– 239(3)	—0.03			M
(2)	6115.94	16346.19	5467(3)–3833(2)	—0.02			M
(3)	6120.38	16334.33	5113(3)–3480(4)	+0.02			M
(0)	6126.52	16317.96	4472(1)– 284(3)	—0.02			M
(2)	6140.05	16282.00	4187(3)– 255(3)	+0.01			M
(1)	6143.07	16274.00	4187(3)– 256(4)	—0.38			M, 1
8	6144.526	16270.14	2501(3)– 87(4)	+0.04			
(2)	6151.19	16252.52	3059(4)– 143(5)	+0.06			M
2h	6154.019	16245.05	3245(2)– 162(1)	+0.02			
4h	6158.03	16234.47	5103(4)–3480(4)	—0.20			
			5975(3)–4351(3)	+0.18			
(1)	6160.04	16229.17	5214(2)–3591(1)	+0.03			M
(2)	6166.92	16211.06	5895(3)–4274(3)	+0.39			M, 1
(1)	6174.52	16191.11	5467(3)–3848(3)	+0.16			M
(1)	6195.81	16135.47	5622(5)–4008(4)	+0.07			M
(0)	6204.55	16112.75	4616(2)– 300(2)	0.00			M
(2)	6215.93	16083.25	3940(5)– 234(4)	—0.07			M
(0)	6220.99	16070.16	4036(4)– 242(5)	+0.21			M
(0)	6222.05	16067.43	5958(3)–4351(3)	+0.21			M
(0)	6222.85	16065.36	3938(3)– 233(2)	+0.01			M
(0)	6224.81	16060.30	3938(3)– 234(4)	+0.01			M
(3)	6226.50	16055.94	5240(3)–3634(2)	—0.06			M
30	6227.701	16052.85	4873(4)–3268(4)	+0.02	(0)	1.51	
(2)	6228.91	16049.73	3861(1)– 225(1)	—0.06			M
4	6241.704	16016.84	2938(3)– 133(2)	+0.02			
(2)	6248.87	15998.46	4029(6)– 242(5)	—0.01			M
(1)	6250.47	15994.37	4538(4)– 293(4)	—0.02			M
8	6269.414	15946.04	3697(1)– 210(1)	—0.02			
			5895(3)–4301(3)	+0.36			1
(2)	6271.42	15940.94	3027(5)– 143(5)	—0.02			M
0	6273.45	15935.78	4407(2)– 281(3)	—0.04			
			5467(3)–3874(2)	+0.01			
3	6274.937	15932.01	5622(5)–4029(6)	+0.04			
5	6286.831	15901.87	3480(4)– 189(3)	—0.01			
(2)	6303.25	15860.45	5622(5)–4036(4)	—0.04			M
(1)	6320.05	15818.28	4088(2)– 250(2)	—0.06			M
(1)	6326.76	15801.51	5955(3)–4375(4)	+0.11			M

(To be continued)

STRUCTURE AND ZEEMAN EFFECT IN THE SPECTRA OF THE OSMIUM ATOM, Os I AND Os II
VI

BY

TH. A. M. VAN KLEEF

Zeeman-laboratory, University of Amsterdam, the Netherlands

(Communicated by Prof. J. DE BOER at the meeting of January 30, 1960)

TABLE III *(continued)*

Classified lines of Os I

Int.	λ_{air}	$\sigma_{vac.}$	Classification	$\delta\sigma$	Zeeman effect	Notes
(3)	6333.01	15785.91	5359(2)–3780(3)	—0.05		M
(0)	6335.59	15779.48	6064(4)–4486(3)	—0.30		M, 1
(0)	6337.63	15774.41	4753(2)– 317(3)	—0.12		M
(2)	6340.51	15767.24	3833(2)– 225(1)	+0.14		M
			5240(3)–3663(2)	—0.03		
			5928(3)–4351(3)	+0.14		
(3)	6350.12	15743.38	3059(4)– 148(4)	—0.02		M
(0)	6354.64	15732.18	4414(3)– 284(3)	—0.01		M
(2)	6358.39	15722.90	3561(3)– 198(4)	+0.05		M
			4386(4)– 281(3)	—0.27		1
(2)	6366.55	15702.75	3682(4)– 211(3)	+0.02		M
(2)	6375.57	15680.53	3824(1)– 225(1)	—0.02		M
(3)	6375.82	15679.92	3509(2)– 194(2)	+0.08		M
(2)	6378.72	15672.79	5359(2)–3792(2)	—0.04		M
(2)	6382.58	15663.31	4407(2)– 284(2)	—0.08		M
(2)	6383.72	15660.52	4301(3)– 273(3)	—0.08		M
(1)	6392.91	15638.00	4123(3)– 255(3)	—0.04		M
			5907(3)–4343(2)	+0.16		
2)	6393.73	15636.00	5864(2)–4301(3)	—0.13		M
3	6398.857	15623.47	4122(5)– 256(4)	0.00		
15	6403.150	15613.00	4873(4)–3312(3)	+0.04		
(3)	6409.60	15597.29	2837(3)– 127(2)	—0.01		M
(1)	6410.32	15595.53	5240(3)–3680(3)	—0.01		M
(2)	6418.60	15575.42	4486(3)– 293(4)	+0.01		M
			5240(3)–3682(4)	0.00		
(2)	6425.67	15558.28	3887(1)– 233(2)	—0.09		M
(1)	6440.61	15522.19	5113(3)–3561(3)	—0.02		M
(1)	6443.96	15514.12	5214(2)–3663(2)	—0.03		M
(1)	6445.31	15510.87	3663(2)– 211(3)	—0.01		M
(1)	6446.00	15509.21	3949(2)– 239(3)	—0.01		M

TABLE III *(continued)*

Classified lines of Os I

Int.	λ_{air}	$\sigma_{vac.}$	Classification	$\delta\sigma$	Zeeman effect	Notes
(3)	6447.68	15505.17	4556(3)– 300(2)	—0.03		M
3	6448.126	15504.10	5672(4)–4122(5)	—0.04		
(0)	6450.50	15498.39	4489(4)– 293(4)	+0.02		M
(0)	6461.73	15471.46	4361(2)– 281(3)	+0.17		M
(3)	6478.30	15431.88	3027(5)– 148(4)	—0.02		M
(3)	6480.09	15427.62	3027(5)– 149(6)	0.00		M
			4049(1)– 250(2)	—0.15		
(1)	6481.80	15423.55	3874(2)– 233(2)	—0.04		M
(0)	6482.21	15422.57	5103(4)–3561(3)	0.00		M
(1)	6493.57	15395.59	4274(4)– 273(3)	—0.02		M
(2)	6509.46	15358.01	3792(2)– 225(1)	—0.05		M
(2)	6511.34	15353.58	5484(1)–3942(2)	0.00		M
(1)	6512.73	15350.30	5359(2)–3824(1)	—0.04		M
(3)	6516.07	15342.43	5214(2)–3680(3)	+0.01		M
			5484(1)–3950(0)	+0.33		l
2	6520.855	15331.17	3663(2)– 213(2)	—0.01		
(1)	6521.20	15330.36	5359(2)–3826(3)	—0.02		M
2	6528.871	15312.36	3634(2)– 210(1)	0.00		
3h	6533.139	15302.35	3052(1)– 152(2)	0.00		
			5538(3)–4008(4)	+0.49		l
10	6538.295	15290.28	2938(3)– 140(3)	0.00		
(2)	6549.65	15263.77	5359(2)–3833(2)	—0.02		M
(2)	6552.80	15256.44	3436(5)– 191(4)	—0.02		M
			3628(0)– 210(1)	+0.04		
(2)	6568.59	15219.76	5346(1)–3824(1)	—0.04		M
3	6576.828	15200.70	3059(4)– 153(3)	+0.01		
(1)	6577.51	15199.12	4361(2)– 284(2)	+0.26		l
			5622(5)–4102(6)	—0.07		M
(2)	6584.49	15183.01	5467(3)–3949(2)	—0.15		M
(0)	6589.05	15172.50	5484(1)–3967(2)	+0.01		M
			5868(3)–4351(3)	+0.05		
(3)	6590.50	15169.16	5214(2)–3697(1)	—0.02		M
(0)	6606.13	15133.27	5346(1)–3833(2)	+0.02		M
3	6614.56	15113.99	3940(5)– 242(5)	—0.02		
(3)	6615.43	15112.00	5540(5)–4029(6)	—0.03		M
(4)	6616.56	15109.42	2527(2)– 101(2)	—0.02		M
(2)	6619.03	15103.78	4351(3)– 284(2)	—0.02		M
(0)	6622.79	15095.20	5917(2)–4407(2)	+0.11		M
			5513(6)–4003(7)	—0.16		
(2)	6639.58	15057.03	5541(4)–4036(4)	—0.05		M
(0)	6643.64	15047.83	4681(2)– 317(3)	+0.01		M
(2)	6653.65	15025.19	4343(2)– 284(2)	+0.01		M

TABLE III *(continued)*

Classified lines of Os I

Int.	λ_{air}	$\sigma_{vac.}$	Classification	$\delta\sigma$	Zeeman effect	Notes
(2)	6659.01	15013.10	3833(2)– 233(2)	—0.05		M
2	6661.81	15006.79	2837(3)– 133(2)	—0.06		
(1)	6663.94	15001.99	5467(3)–3967(2)	—0.08		M
(3)	6665.99	14997.37	5622(5)–4122(5)	—0.02		M
(1)	6673.12	14981.35	5359(2)–3861(1)	+0.25		M
(3)	6688.68	14946.51	3826(3)– 233(2)	—0.05		M
(1)	6694.16	14934.27	2795(2)– 130(1)	+0.02		M
(2)	6697.62	14926.55	3824(1)– 233(2)	—0.05		M
(1)	6706.90	14905.90	5876(4)–4386(4)	—0.17		M
(1)	6715.83	14886.08	3591(1)– 210(1)	—0.02		M
30	6729.556	14855.72	3007(2)– 152(2)	+0.01		
(1)	6730.70	14853.19	5359(2)–3874(2)	—0.16		M
			5672(4)–4187(3)	—0.04		
(2)	6751.52	14807.39	3813(4)– 234(4)	—0.04		M
(0)	6758.33	14792.47	5113(3)–3634(2)	+0.15		M
(1)	6759.42	14790.08	3245(2)– 176(1)	—0.02		M
(2)	6770.09	14766.77	2778(1)– 130(1)	+0.05		M
(2)	6773.00	14760.43	2909(6)– 143(5)	+0.01		M
			4036(4)– 256(4)	+0.06		
(0)	6774.74	14756.64	3874(2)– 239(3)	+0.03		M
(0)	6777.86	14749.84	4414(3)– 293(4)	0.00		M
(1)	6780.65	14743.78	5503(5)–4029(6)	—0.13		M
(2)	6790.30	14722.82	5346(1)–3874(2)	+0.01		M
10	6791.60	14720.01	2346(5)– 87(4)	—0.06		
8	6806.61	14687.54	3007(2)– 153(3)	+0.02		
(2)	6839.85	14616.17	3591(1)– 213(2)	—0.02		M
(2)	6841.79	14612.03	4873(4)–3412(3)	—0.01		M
(1)	6847.62	14599.58	4301(3)– 284(2)	—0.03		M
(1)	6850.60	14593.23	5240(3)–3780(3)	0.00		M
(1)	6852.17	14589.89	2795(2)– 133(2)	+0.40		1
			5467(3)–4008(4)	—0.06		M
3	6878.74	14533.53	2938(3)– 148(4)	—0.07		
(1)	6882.82	14524.92	4187(3)– 273(3)	—0.05		M
(2)	6887.98	14514.04	4719(5)–3268(4)	—0.08		M
(1)	6893.98	14501.39	3848(3)– 239(3)	—0.04		M
(1)	6895.42	14498.38	4626(4)– 317(3)	—0.03		M
(3)	6898.73	14491.42	3780(3)– 233(2)	+0.44		M, 1
3	6901.58	14485.44	3780(3)– 234(4)	—0.48		1
			4008(4)– 256(4)	—0.02		
(1)	6903.31	14481.81	4387(5)– 293(4)	—0.01		M
(1)	6904.14	14480.07	5240(3)–3792(2)	—0.03		M
(3)	6907.86	14472.27	3436(5)– 198(4)	+0.01		M
(1)	6909.71	14468.39	4386(4)– 293(4)	0.00		M
(1)	6930.90	14424.16	3949(2)– 250(2)	+0.07		M
(1)	6931.94	14421.99	2778(1)– 133(2)	+0.03		M

TABLE III *(continued)*

Classified lines of Os I

Int.	λ_{air}	$\sigma_{vac.}$	Classification	$\delta\sigma$	Zeeman effect	Notes
(1)	6933.42	14418.92	5672(4)–4231(4)	+0.01		M
(1)	6952.52	14379.30	5540(5)–4102(6)	+0.05		M
(1)	6954.82	14374.55	4172(4)– 273(3)	—0.07		M
3	6956.02	14372.07	4873(4)–3436(5)	—0.04		
(1)	6966.82	14349.79	5484(1)–4049(1)	—0.11		M
(2)	6971.49	14340.16	5214(2)–3780(3)	+0.06		M
(1)	6975.53	14331.87	5113(3)–3680(3)	+0.01		M
(0)	6983.78	14314.94	5467(3)–4036(4)	—0.10		M
10	6984.95	14312.54	3052(1)– 162(1)	+0.03		
			3561(3)– 213(2)	—0.02		
(1)	6997.19	14287.51	3049(0)– 162(1)	—0.06		M
(0)	7004.94	14271.70	5240(3)–3813(4)	—0.02		M
3	7007.04	14267.42	3268(4)– 184(5)	—0.07		
(2)	7017.37	14246.42	4265(2)– 284(2)	+0.01		M
			5975(3)–4550(2)	—0.17		
(1)	7020.43	14240.21	2833(4)– 140(3)	—0.19		M
/1)	7024.34	14232.28	3412(3)– 198(4)	—0.05		M
			5103(4)–3680(3)	+0.06		
3	7029.20	14222.45	3312(3)– 189(3)	—0.09		
			5809(4)–4387(5)	+0.38		1
(0)	7030.11	14220.60	5103(4)–3681(5)	+0.05		M
4	7034.31	14212.11	5103(4)–3682(4)	+0.01		
(1)	7043.22	14194.13	5541(4)–4122(5)	+0.15		M
			5958(3)–4538(4)	—0.15		
(1)	7051.48	14177.51	4232(3)– 281(3)	+0.35		1 M
			5540(5)–4122(5)	+0.06		
8	7054.86	14170.71	4231(4)– 281(3)	—0.02		
15	7060.67	14159.05	2938(3)– 152(2)	—0.03		
(1)	7067.45	14145.47	3813(4)– 239(3)	—0.04		M
(0)	7071.35	14137.67	5240(3)–3826(3)	+0.02		M
(1)	7089.86	14100.76	5359(2) 3949(2)	+0.02		M
(1)	7096.59	14087.38	4414(3)– 300(2)	+0.03		M
			5895(3)–4486(3)	—0.15		
3	7104.86	14070.99	3663(2)– 225(1)	+0.10		
			5240(3)–3833(2)	—0.07		
(1)	7111.90	14057.06	3509(2)– 210(1)	+0.01		M
30	7145.54	13990.88	2938(3)– 153(3)	—0.01		
15	7148.91	13984.28	5864(2)–4466(2)	—0.44		1
3h	7157.86	13966.80	3509(2)– 211(3)	—0.04		
10	7184.10	13915.79	5240(3)–3848(3)	—0.01		

TABLE III *(continued)*

Classified lines of Os I

Int.	λ_{air}	$\sigma_{vac.}$	Classification	$\delta\sigma$	Zeeman effect	Notes
			4232(3)– 284(2)	—0.02		
(1)	7189.82	13904.71				M
			5214(2)–3824(1)	+0.22		
(2)	7202.10	13881.01	4123(3)– 273(3)	—0.01		M
			2261(4)– 87(4)	0.00		
15	7206.33	13872.86				
			6064(4)–4677(3)	—0.34		1
8	7209.96	13865.88	3007(2)– 162(1)	+0.01		
(1)	7211.48	13862.96	2795(2)– 140(3)	+0.01		M
3	7224.43	13838.10	3813(4)– 242(5)	—0.02		
(1)	7242.06	13804.42	3940(5)– 256(4)	—0.01		M
(1)	7245.98	13796.94	4556(3)– 317(3)	0.00		M
			3938(3)– 255(3)	+0.08		
(1)	7250.11	13789.09	5346(1)–3967(2)	—0.02		M
			5467(3)–4088(2)	+0.18		
10	7251.16	13787.09	3509(2)– 213(2)	—0.05		
15	7253.49	13782.67	3268(4)– 189(3)	0.00		
(1)	7287.85	13717.69	5672(4)–4301(3)	+0.09		M
(0)	7300.70	13693.54	5541(4)–4172(4)	+0.12		M
(0)	7312.51	13671.42	3874(2)– 250(2)	—0.06		M
			3797(1)– 233(2)	+0.41		1
(1)	7317.38	13662.32				M
			5214(2)–3848(3)	—0.36		1
(1)	7338.16	13623.64	4538(4)– 317(3)	0.00		M
10	7364.05	13575.74	3268(4)– 191(4)	0.00		
(3)	7375.07	13555.45	3245(2)– 189(3)	—0.05		M
(2)	7403.34	13503.69	3682(4)– 234(4)	—0.04		M
10	7407.95	13495.29	3681(5)– 234(4)	+0.01		
(0)	7418.67	13475.79	5622(5)–4274(4)	—0.05		M
(0)	7425.20	13463.94	4187(3)– 284(2)	—0.04		M
(0)	7451.60	13416.24	3848(3)– 250(2)	—0.06		M
(1)	7456.46	13407.49	5214(2)–3874(2)	—0.01		M
(2)	7485.28	13355.87	3591(1)– 225(1)	—0.03		M
(2)	7500.05	13329.57	5113(3)–3780(3)	+0.02		M
(0)	7507.20	13316.87	3663(2)– 233(2)	—0.07		M
(1)	7555.68	13231.43	3312(3)– 198(4)	+0.02		M
(0?)	7565.98	13213.41	5672(4)–4351(3)	0.00		M
			2837(3)– 152(2)	+0.05		
20	7602.95	13149.16				
			5955(3)–4640(2)	+0.02		
2	7618.97	13121.52	4873(4)–3561(3)	0.00		
(1)	7673.57	13028.15	3634(2)– 233(2)	—0.06		M
2	7701.46	12980.97	2837(3)– 153(3)	+0.05		
(0)	7769.94	12866.56	5672(4)–4386(4)	+0.09		M
(0)	7778.82	12851.88	3792(2)– 250(2)	—0.12		M
3	7789.96	12833.50	4719(5)–3436(5)	+0.10		
			3412(3)– 213(2)	0.00		
(0)	7796.92	12822.04	3680(3)– 239(3)	+0.35		M, 1
			6064(4)–4782(3)	+0.23		

TABLE III *(concluded)*

Classified lines of Os I

Int.	λ_{air}	$\sigma_{vac.}$	Classification	$\delta\sigma$	Zeeman effect	Notes
(0)	7797.82	12820.57	5622(5)–4340(5)	—0.02		M
(1)	7815.53	12791.51	3268(4)– 198(4)	—0.03		M
(0)	7847.80	12738.92	3780(3)– 250(2)	+0.05		M
			5890(3)–4616(2)	+0.34		1
(0)	7849.60	12736.00				M
			4008(4)– 273(3)	—0.05		
3	7852.17	12731.83	2795(2)– 152(2)	+0.08		
(0)	7890.34	12670.23	3826(3)– 255(3)	+0.01		M
2	7901.57	12652.23	5113(3)–3848(3)	+0.11		
2	7957.31	12563.60	2795(2)– 153(3)	+0.04		
(0)	7964.35	12552.49	5103(4)–3848(3)	+0.01		M
			3813(4)– 255(3)	+0.02		
2	7974.72	12536.17				
			5809(4)–4556(3)	—0.03		
			3681(5)– 242(5)	+0.02		
2	7981.20	12525.99				
			5958(3)–4705(3)	+0.31		1
(0)	7997.12	12501.06	2527(2)– 127(2)	+0.02		M
(1)	8014.59	12473.81	5214(2) 3967(2)	+0.01		M
2	8041.29	12432.39	2346(5)– 110(4)	—0.07		
(0)	8055.15	12411.00	3007(2)– 176(1)	+0.06		M
			3790(4)– 255(3)	—0.02		
(0)	8118.07	12314.81				M
			5240(3)–4008(4)	+0.01		
			3561(3)– 233(2)	+0.01		
(0)	8128.95	12298.33				M
			5907(3)–4677(3)	—0.35		1
			3561(3)– 234(4)	—0.03		
(0)	8132.32	12293.23				M
			5910(2)–4681(2)	+0.15		
(2)	8157.40	12255.43	2527(2)– 130(1)	+0.08		M
(0)	8178.77	12223.41	3052(1)– 183(0)	—0.11		M
(1)	8211.76	12174.32	3059(4)– 184(5)	—0.01		M
(0)	8263.74	12097.74	4386(4)– 317(3)	+0.10		M
(1)	8303.41	12039.94	5240(3)–4036(4)	+0.05		M
			4122(5)– 293(4)	+0.04		
(1)	8450.22	11830.76				M
			5733(3)–4550(2)	—0.16		
(0)	8457.05	11821.21	3312(3)– 213(2)	+0.09		M
(1)	8514.20	11741.86	2795(2)– 162(1)	—0.05		M
(0)	8644.8	11564.47	3663(2)– 250(2)	—0.36		M, 1

NOTES TO TABLE III

1. Tentative classification; $\delta\sigma$ is too large.
2. The spark intensity is higher than the arc intensity.
3. This line has also been classified as a transition between two Os II levels.
4. When two or more classifications have been given, they are all possible.

5. This line has already been measured by KAYSER [2] but it was not given in the M.I.T. Wavelength Tables [7].
6. The two classifications—with nearly complementary values of $\delta\sigma$—, prove this probably to be a double line. Obviously the two lines are about equally strong.
7. When the type of Zeeman pattern cannot be determined, the values given refer to the centers of gravity of the π- and σ-pattern respectively.
7a. Zeeman data in clarendon refer to the strongest components.
8. The spark intensity is 1.
9. Observed Zeeman effect not in agreement with the other classification.
10. When the g-factors are given, g_1 always corresponds to the level mentioned first in the column headed „Classification".
11. Observed Zeeman effect is not in agreement with the given classification.
12. Observed Zeeman effect is in agreement with both classifications.
13. The σ-pattern was very difficult to measure.
14. A Zeeman pattern has been observed that has not yet been interpreted.
15. The Zeeman pattern observed here belongs to an Os II-transition. See table IX.
16. The π-component is somewhat shifted from its zero field position.
17. $\delta\sigma$ is too large, but the Zeeman effect is in accordance with the classification.
18. The Zeeman pattern of this transition could not be determined because of disturbance by the adjacent pattern.
19. The two classifications—with nearly complementary values of $\delta\sigma$—, prove this to be a double line as reported in the M.I.T. Wave-length Tables. Of each of the lines a Zeeman effect has been measured.
20. The two measured σ-components are equally strong; at both sides weaker components are present, but they could not be measured.
21. Observed Zeeman effect has been measured by HOOYKAAS and SURINGAR [13].
22. This and all following Zeeman patterns have been determined by HOOYKAAS and SURINGAR.
23. The σ-pattern observed here belongs to an Os II-transition. See table IX. The π-pattern is in agreement with the Os I-transition given.
24. 13 π-components have been measured; the outer σ-component is the strongest.

5. *Ground configurations*

In table IV the low even configurations and terms expected from the vector model are displayed. The binding energies of the configurations d^n, $d^{n-1}s$ and $d^{n-2}s^2$ in the arc spectra of the elements in this part

TABLE IV

Predicted low even levels of Os I

Configuration	Terms	Number of levels
$5d^66s^2$	^5D, $^3(HGFDP)$, $^1(IGFDS)$, $^3(FP)$, $^1(GDS)$	34
$5d^76s$	$^{5,3}(FP)$, $^{3,1}(HGFDP)$, $^{3,1}(D)$	38
$5d^8$	$^3(FP)$, $^1(GDS)$	9

of the periodic system are very much alike, so that a considerable overlapping of the configurations can be expected with strong mutual perturbations. In view of this, the assignment of the levels to certain configurations cannot always be made unambiguously. However, the J- and g-values of the lowest levels prove unequivocally that a ^5D is the

lowest multiplet in the spectrum. This can arise only from the configuration $5d^6 6s^2$. In this respect the structure is similar to that in Fe I [18]. The level $^5D_2$ is perturbed by other levels with $J=2$. The following multiplet, a ^5F (recognized by the $^5F_5$ level), can unambiguously be ascribed to the $5d^7 6s$ configuration. On account of the observed Zeeman effect the interpretation of the levels $^5F_4$, $^5F_3$, $^5F_2$ and $^5F_1$ is certain. The level which we now identify as $5d^7(a^4F)6s\ ^5F_2$ was interpreted by Albertson [1] and Van den Bosch [12] as $5d^7(a^4F)6s\ ^3F_2$, while they located the $5d^7(a^4F)6s\ ^5F_2$ level at 10165.98, a level now identified as $5d^6 6s^2\ ^3P_2$, in agreement with the g-values. This level cannot belong to $5d^7(a^4P)6s\ ^3P$ because that term should be higher than $5d^7(a^4P)6s\ ^5P$ according to Hund's rules; the latter term is unambiguous because of the very characteristic g-values. Moreover in the Fe I spectrum $d^6s^2\ ^3P$ is found to be considerably lower than $d^7s\ ^3P$. In addition the two corresponding levels $d^6s^2\ ^3P_1$ and $^3P_0$ are found in such a position as to establish a ^3P term very similar to $d^6s^2\ ^3P$ in Fe I, the distance between $^3P_2$ and $^3P_1$ being one of the biggest intervals in the spectrum. These similarities would be destroyed by interchanging the d^7s and $d^6s^2\ ^3P$-levels. The remaining low levels constitute the anticipated $5d^7(a^4F)6s\ ^3F$.

Though in Os I the $5d^7 6s$ configuration is shifted downwards relative to $5d^6 6s^2$ in comparison with the corresponding configurations in Fe I, it was as yet impossible to establish the $^3H_6$ level generated by adding a $6s$-electron to $5d^7(a^2H)$ in the region below 20000 K. We identified the levels 143 and 148 as $5d^6 6s^2\ ^3G_5$ and $^3G_4$ respectively, in contradistinction to the interpretation of Albertson and Van den Bosch, who labelled these levels as $5d^6 6s^2\ ^3H_5$ and $^3H_4$. This interpretation is untenable in view of the higher position of $5d^6 6s^2\ ^3H_6$ because it is the only $J=6$ level that can be expected low in the term system. The newly detected level 184 and the level 191 are $5d^6 6s^2\ ^3H_5$ and $^3H_4$ respectively. The assignment of the levels $5d^6 6s^2\ ^3G_5$ and $5d^6 6s^2\ ^3H_5$ is also suggested by the g-values. It cannot be expected that the observed g-value of the $^3G_5$ level becomes smaller than the g-value of the $^3H_5$ level. A similar argument applies to the $^3G_4$ and $^3H_4$ levels, with theoretical g-values of 1.04 and 0.80 respectively. However, it is obvious that those levels perturb each other as a result of which the g-values share and the ^3G multiplet is rather irregular, the $^3G_5$ and $^3G_4$ being very close and $^3G_3$, which cannot be perturbed by ^3H, at a considerable distance. Consequently the multiplet width is larger than could be expected.

The multiplet $5d^7(a^2D)6s\ ^3D$ is unexpectedly low, while $5d^7(a^4P)6s\ ^3P$ shows normal instead of inverted order. The peculiar position of the $5d^6 6s^2\ ^3P_2$ is probably caused by the repulsion by $5d^7(a^4P)6s\ ^3P_2$. The distinction between $5d^7(a^2D)6s\ ^3D_2$ and $5d^7(a^4P)6s\ ^3P_2$ was made on account of the g-values only. The multiplets $5d^6 6s^2\ ^3F$ and $5d^7(a^2G)6s\ ^3G$ which affect each other very strongly, and the level $5d^7(a^2G)6s\ ^3G_4$ have been identified practically unambiguously. The level 28411.95, having

$g = 1.35$ or 1.41 as determined from a measurement of the π-pattern, could be interpreted as $5d^7(a^2P)6s\ ^3P_2$, because in this region the other expected terms with $J = 2$ should have lower g-values. No terms of the $5d^8$ configuration could be located. In order to discover terms of this configuration it will be necessary to explore the region above 8000 Å. Such an investigation is on the programme.

The strong interaction between various levels can be demonstrated by comparing the experimental g-values with the theoretical g-values in Russell–Saunders coupling. It is not possible to make up complete g-sums as yet, because for each J-value several levels are missing. However, as a rule the incomplete g-sums, extended to both configurations $5d^66s^2$ and $5d^76s$ do not differ too much from the theoretical ones, which shows that the missing levels do not very much influence the established system. This is demonstrated by table V, in which "g-sums" for the levels with $J = 1$, 2 and 4 have been displayed. The uncertain g-value of $5d^7(a^2P)6s\ ^3P_2$ has been omitted. The perturbations of the g-values of the $J = 1$ levels are

TABLE V

"g-sums" of the levels of the groundsystem

$J = 1$				$J = 2$				$J = 4$			
level		$g_{obs.}$	g_{LS}	level		$g_{obs.}$	g_{LS}	level		$g_{obs.}$	g_{LS}
$5d^66s^2$	^5D	1.47	1.50	$5d^66s^2$	^5D	1.44	1.50	$5d^66s^2$	^5D	1.44	1.50
$5d^7(a^4F)6s$	^5F	0.31	0.00	$5d^66s^2$	^3P	1.45	1.50	$5d^7(a^4F)6s$	^5F	1.31	1.35
$5d^7(a^4P)6s$	^5P	1.74	2.50	$5d^7(a^4F)6s$	^5F	1.00	1.00	$5d^7(a^4F)6s$	^3F	1.16	1.25
$5d^66s^2$	^3P	1.40	1.50	$5d^7(a^4F)6s$	^3F	0.94	0.67	$5d^66s^2$	^3G	1.08	1.05
$5d^7(a^2D)6s$	^3D	0.88	0.50	$5d^7(a^4P)6s$	^5P	1.61	1.83	$5d^66s^2$	^3H	1.03	0.80
$5d^7(a^4P)6s$	^3P	1.61	1.50	$5d^7(a^2D)6s$	^1D	0.97	1.00	$5d^66s^2$	^1G	1.06	1.00
				$5d^7(a^2D)6s$	^3D	1.26	1.17	$5d^7(a^2G)6s$	^3G	1.04	1.05
				$5d^7(a^4P)6s$	^3P	1.27	1.50	$5d^66s^2$	^3F	1.14	1.25
				$5d^66s^2$	^3F	0.89	0.67				
"g-sum"		7.41	7.50	"g-sum"		10.83	10.84	"g-sum"		9.26	9.25

particularly strong, (with one departure of 0.76) although the "g-sum" shows a discrepancy of only 0.09. The designations of the levels with $J = 2$ are at variance with those given recently by Van den Bosch [19]. It is certainly not allowed to apply the g-sum rule within one configuration in this case.

It should be possible to predict fairly accurately the levels which thus far escaped detection by means of a quantitative treatment taking into account configuration interaction and spin orbit interaction according to the method of Racah [20], because most of the interpretations in the ground system are certain. The influence of the unknown configuration $5d^8$ cannot be accounted for of course, but since this configuration has only 9 levels in total, the calculation may be reasonably reliable. This computation is being set up with the aid of the electronic computer of the Amsterdam Mathematical Centre. The results will be published later.

6. *Odd levels*

In table VI the theoretical terms associated with the $6p$-electron have been collected. In connection with various other spectra it is to be expected that the configuration $5d^76p$ is appreciably higher than $5d^66s6p$. About the relative positions of the configurations $5d^56s^26p$ and $5d^66s6p$ no theoretical prediction could be made. However, only d^6sp produces a ^7F and a ^7D, so that the detection of the $^7F_6$ level at 29099 K and the $^7D_5$ level at 23462 K made it certain that d^6sp is the lowest odd configuration.

TABLE VI

Predicted odd levels of Os I

Configuration	Terms	Number of levels
$5d^56s^26p$	$^{7,5}(P)$, $^{5,3}(HGF, FDP)$, $^{3,1}(KIH, HGF, GFD, FDP, P)$, $^{5,3}(GFD, DPS)$, $^{3,1}(IHG, HGF, GFD, FDP, DPS)$, $^{3,1}(FDP)$	214
$5d^66s6p$	$^{7,5,5,3}(FDP)$, $^{5,3,3,1}(IHG, HGF, GFD, FDP, DPS)$, $^{3,1}(KIH, HGF, GFD, FDP, P)$, $^{5,3,3,1}(GFD, DPS)$, $^{3,1}(HGF, FDP, P)$	360
$5d^76p$	$^{5,3}(GFD, DPS)$, $^{3,1}(IHG, HGF, GFD, FDP, DPS)$, $^{3,1}(FDP)$	110

It is not difficult to recognize most of the other ^7F- and ^7D-states among the known numerical levels. The newly detected levels at 27786 (with $J=1$ and $g=2.77$) and 30499 (with $J=0$) complete these multiplets. The remaining 6 low levels, with characteristic g-values, belong to the only two ^7P multiplets, which could be expected in the entire system. The lowest of these, we assigned to the $5d^56s^26p$; the other one to the $5d^66s6p$. The levels which we now identify as $5d^56s^2(a^2S)6p\ ^7P_4$ and $^7P_3$ were interpreted by Albertson [1] and Van den Bosch [12] as $5d^66s(a^6D)6p\ ^7P_4$ and $^7P_3$; they did not identify the other levels belonging to these terms. The transition $d^6sp - d^6s^2$ is a one electron-jump and the $d^5s^2p - d^6s^2$ is a two electron-jump. Consequently the levels of d^6sp should combine more strongly with those of d^6s^2 than the levels of d^5s^2p. As will be proved in section 8, the configuration $5d^56s^2$ in the Os II-spectrum is situated low in the term system, while the term $5d^56s(a^7S)6p\ ^8P$ is the lowest in the odd system, analogous to the situation in Re I [21]. In addition the corresponding term $d^5s^2p\ ^7P$ in Os I is found in a position which is in agreement with the recognized $d^5sp\ ^8P$ term in Os II. The third reason why the designations of the ^7P-terms are probably correct is the fact that in no other spectra of neutral atoms which contain d^4sp and d^6sp configurations [18, 22, 23, 24, 25], the ^7P term has been located between the ^7D and ^7F terms.

Since the width of $5d^56s^2(a^6S)6p\ ^7P$ is very small it can be expected that the corresponding $d^5s^2p\ ^5P$ also is narrow. The levels 38486, 38741 and 38875 could be identified with these ^5P levels. The $5d^66s(a^6D)6p\ ^5P_1$ level

was found to be higher in the system than could be expected. Of the 50 levels, arising from the $5d^6 6s\ ^{6,4}(D)$ by addition of a p-electron, 49 have been found. Only $5d^6 6s(a^4D)6p\ ^3D_1$ has not been found. The terms are partly regular, partly inverted and sometimes partially inverted.

Some of the higher levels (as recognized by the newly detected $^5H_7$ level) can unambiguously be ascribed to the $5d^6 6s(a^4H)6p$ multiplet. The $d^6sp\ ^5I$ and ^3I terms, which also can be expected in this region could not be located. All the levels belonging to the ^5H, ^5G, ^3H and ^3G terms of the $d^6s(a^4H)p$ triads have been identified.

Most remaining levels in this region must be ascribed to the $5d^7 6p$ configuration. It can be expected—since it is the only odd configuration whose lowest terms are quintets—that fairly strong combinations with the low even terms will be present. This is indeed the case, although the combinations of the low lying septets in the other odd configurations with the ground system are still much stronger. From comparison of the transitions $d^3s\ ^5F_5 - d^3p\ ^5G_6$ in Ti I [26], Zr I [27] and Hf I [28], and $d^7s\ ^5F_5 - d^7p\ ^5G_6$ in Fe I [18] and Ru I [24] it could be inferred that the corresponding transition in the Os I spectrum should have a wave-number of about 39000 K. In agreement herewith $d^7p\ ^5G_6$ has been located in Os I at 45315.88 K and the line in question at 40171.96 K. The g-value of this level is nearly in agreement with the theoretical value in LS-coupling. The remaining expected levels, arising from $5d^7\ ^4F$ by addition of a p-electron, could also be located.

A brief discussion of the Os I levels 4574(5) and 4575(5), which both are typically $^3G_5$-levels, seems justified because an analogous case of extremely close-lying levels with the same J-value was found in the Re I spectrum [21] with the levels 273′ and 273″. The conclusion in that case was that both levels were hyperfine structure sublevels of one electronic level with $J = \frac{1}{2}$. In our case such an explanation does not apply, because the two odd Os-isotopes (^{187}Os and ^{189}Os) contain only 17.7 % of the total mass. Furthermore the wave-lengths 3234.654 Å and 3234.731 Å give definitely independent Zeeman patterns (see table III). Because the strongest combinations of 4575(5) are with d^7s levels, we ascribed it to the $5d^7 6p$ configuration. The combinations with d^6s^2 levels are due to two-electron jumps. The striking similarity of the levels is doubtlessly connected with a configuration interaction between d^7p and d^6sp.

The uninterpreted levels belong to the configurations mentioned above. It is impossible to make more assignments. It should be mentioned, however, that the g-sums for the interpreted levels are all in reasonable agreement with the expected g-sums in Russell–Saunders coupling.

7. *High even levels and ionization potential*

The even configurations containing a $7s$- or a $6d$-electron and the resulting terms which can be expected from the Hund theory are shown in table VII.

The total number of levels is 1294. The total number found experimentally is 39 (6 of which are new), and most of these belong to the configurations d^5s^2s, d^6ss and d^6sd. Though some terms of the other configurations may lie rather low, no level can be attributed to them with

TABLE VII

Predicted high even levels of Os I

Configuration	Terms	Number of levels
$5d^56s^27s$	$^{7,5}(S)$, $^{5,3}(GD)$, $^{3,1}(IGFDS)$, $^{5,3}(FP)$, $^{3,1}(HGFDP)$, $^{3,1}(D)$	74
$5d^66s7s$	$^{7,5,5,3}(D)$, $^{5,3,3,1}(HGFDP)$, $^{3,1}(IGFDS)$, $^{5,3,3,1}(FP)$ $^{3,1}(GDS)$	126
$5d^77s$	$^{5,3}(FP)$, $^{3,1}(HGFDP)$, $^{3,1}(D)$	38
$5d^56s^26d$	$^{7,5}(D)$, $^{5,3}(IHGFD, GFDPS)$, $^{3,1}(LKIHG, IHGFD, HGFDP, GFDPS, D)$, $^{5,3}(HGFDP, FDP)$, $^{3,1}(KIHGF, IHGFD, HGFDP, GFDPS, FDP)$, $^{3,1}(GFDPS)$	334
$5d^66s6d$	$^{7,5,5,3}(GFDPS)$, $^{5,3,3,1}(KIHGF, IHGFD, HGFDP, GFDPS, FDP)$, $^{3,1}(LKIHG, IHGFD, HGFDP, GFDPS, D)$, $^{5,3,3,1}(HGFDP, FDP)$, $^{3,1}(IHGFD, GFDPS, D)$	554
$5d^76d$	$^{5,3}(HGFDP, FDP)$, $^{3,1}(KIHGF, IHGFD, HGFDP, GFDPS, FDP)$, $^{3,1}(GFDPS)$	168

certainty. The lowest high even level has been correctly interpreted as $5d^66s(a^6D)7s\ ^7D_5$ by Albertson [1]. We interchanged the interpretation of the next two levels (both with $J=4$), because the g-factors then are in better agreement with the Landé values. The levels 5113(3), 5214(2) and the newly detected level 5346(1) complete the ^7D multiplet. The level $5d^66s(a^6D)7s\ ^5D_2$ was identified with 5359(2) instead of 5214(2) [12], in view of the g-values. The state 54847 was recognized as $^5D_1$ after the uncertainty in the J-value was eliminated by finding three combinations with newly detected levels with $J=0$ (30499, 36289 and 39505), although the g-value is unknown; it is the only possible $J=1$ level to be expected in this region except $^7D_1$, which was located at 53464 K on account of the very characteristic g-value. The newly detected level 5570 (0) and the level 5240(3) complete $5d^66s(a^6D)7s\ ^5D$.

In the neighbourhood two states (54676 and 55388) with $J=3$ and high g-values (1.82 and 1.78 respectively) suggested the presence of the $^7P_3$ and $^7D_3$ of the $5d^66s6d$ configuration, which is to be expected low. However, this configuration also contains ^7G, ^7F and ^7S levels. Thus the states $^7G_7$, $^7G_6$, $^7G_5$, $^7F_6$, $^7F_5$, $^7F_4$, $^7D_5$, $^7D_4$ and $^7P_4$ can be expected. Indeed, we could locate $^7G_5$, $^7F_6$, $^7F_5$, $^7F_4$, $^7D_5$, $^7D_4$ and $^7D_3$ after detection of 5503(5), 5512(4) and 5513(6). $^7D_2$ is tentative because the g-value is uncertain.

The remaining low level (at 54676 K) was first interpreted as $5d^66s(a^6D)6d\ ^7P_3$ but this interpretation had to be abandoned because $^7P_4$ and $^7P_2$ could not be found, and because the ^7P term cannot be

expected to be the lowest term of the pentad formed from $5d^6 6s\, a^6D$ by addition of a d-electron. Finally we interpreted this level definitely as $5d^5 6s^2(a^6S)7s\, {}^7S_3$. The reasons were the following. First this state has its strongest combinations with the levels $5d^5 6s^2(a^6S)6p\, {}^7P_4$, ${}^7P_3$ and ${}^7P_2$. Secondly the configuration $d^5 s^2 s$ must be expected low in this term-system, analogous to the low situation of $d^5 s^2 p$ configuration in the odd system and in agreement with the low positions of $d^5 s$ and $d^5 p$ in the Os II spectrum.

The configurations $5d^7 7s$ and $5d^7 6d$ are expected to lie somewhat higher in view of the position of the corresponding odd configuration $5d^7 6p$ with respect to $5d^6 6s 6p$. Although some of the levels may be present among the high even group it is yet impossible to make identifications with reasonable certainty. In section 3 it was already mentioned why some of the levels in this group have been called in question.

The level 4873(4) has been interpreted as $5d^6 6s 7s\, {}^5D_4$, which is the second member of a series beginning with $5d^6 6s^2\, {}^5D_4$. In computing the approximate ionization potential it has been assumed, in analogy to Ta I [6], Re I [21] and Ir I [14], that the quantum defect undergoes a change of 0.10 and the result is I.P. $= (8.5 \pm 0.1)$ V, instead of Albertson's value 8.7 V, based on the wrong interpretation of the $5d^6 6s 7s\, {}^5D_4$ level. Our calculation has been made for each ${}^5D$-level separately (except ${}^5D_2$) and for the centroids.

8. *The* Os II *spectrum; terms, transitions and identifications*

A preliminary list of 22 low even and 17 odd levels and g-values for Os II was included in Atomic Energy Levels, Vol. III [12]. These results were mentioned already at the Rydberg Centennial Conference on Atomic Spectroscopy [10] (Lund, 1954), where Van den Bosch announced the detection of 250 observed lines between 2280 Å and 4550 Å, 73 of which were classiffied.

We extended the odd system with 4 odd levels. In table VIII all levels of Os II and their properties have been displayed. The successive columns have the same meaning as the corresponding ones in table II. (Os I levels). In each group the order is according to decreasing binding energy. The identifications will be discussed below.

TABLE VIII

Relative levels in Os II

Symbol	Value	J	g	Interpretation		Notes
			low even group			
0	0.00	9/2	1.52	$5d^6({}^5D)6s$	${}^6D_{9/2}$	
35	3593.15	7/2	1.57	$5d^6({}^5D)6s$	${}^6D_{7/2}$	
39	3928.94	5/2	1.62	$5d^6({}^5D)6s$	${}^6D_{5/2}$	
55	5592.05	3/2	1.79	$5d^6({}^5D)6s$	${}^6D_{3/2}$	
66	6636.57	1/2	3.17	$5d^6({}^5D)6s$	${}^6D_{1/2}$	

TABLE VIII *(concluded)*

Relative levels in Os II

Symbol	Value	J	g	Interpretation				Notes
				low even group *(continued)*				
78	7891.93	5/2	1.70	$5d^5 6s^2$		$^6S_{5/2}$		1
114	11459.90	7/2	1.27	$5d^6(^5D)6s$	$^4D_{7/2}$			
116	11654.08	5/2	1.55	$5d^6(^5D)6s$	$^4D_{5/2}$			
131	13136.61	3/2	1.40	$5d^6(^5D)6s$	$^4D_{3/2}$			
132	13203.88	7/2	1.25	$5d^7$			$^4F_{7/2}$	
134	13414.80	5/2	1.34	$5d^7$			$^4F_{5/2}$	
156	15605.58	9/2	1.14	$5d^7$			$^2G_{9/2}$	
172	17242.26	7/2	0.99	$5d^7$			$^2G_{7/2}$	
174	17424.39	3/2	0.97	$5d^7$			$^2P_{3/2}$	
175	17569.40	5/2	1.35	$5d^7$			$^4P_{5/2}$	
176	17688.64	11/2	1.20	$5d^7$			$^2H_{11/2}$	
195	19590.91	5/2	0.81					
199	19985.93	7/2	1.10					
215	21590.81	9/2	1.11	$5d^6(^3G)6s$	$^4G_{9/2}$?			
244	24465.66	5/2	1.27					
249	24980.73	7/2	1.18					
254	25452.13	5/2	1.09					
				odd group				
3732	37321.53	5/2	2.22	$5d^5 6s(a^7S)6p$	$^8P_{5/2}$			2
3938	39389.49	7/2	1.85	$5d^5 6s(a^7S)6p$	$^8P_{7/2}$			2
4128	41282.95	9/2	1.82	$5d^5 6s(a^7S)6p$	$^8P_{9/2}$			2, 3
4380	43802.36	7/2	1.56	$5d^6(^5D)6p$		$^6D_{7/2}$		
4431	44315.40	9/2	1.44	$5d^6(^5D)6p$		$^6D_{9/2}$		
4615	46157.19	3/2	1.78	$5d^6(^5D)6p$		$^6D_{3/2}$		
4637	46373.51	5/2	1.61	$5d^6(^5D)6p$		$^6D_{5/2}$		
8172	48128.08	1/2	2.96	$5d^6(^5D)6p$		$^6D_{1/2}$		
4919	48798.70	5/2	1.39	$5d^6(^5D)6p$		$^6F_{5/2}$		1
4484	49149.39	7/2	1.51	$5d^5 6s(a^7S)6p$	$^6P_{7/2}$			
5177	51770.38	5/2	1.69	$5d^5 6s(a^7S)6p$	$^6P_{5/2}$			3
5195	51951.61	9/2	1.40	$5d^6(^5D)6p$		$^6F_{9/2}$		
5220	52206.48	7/2	1.42	$5d^6(^5D)6p$		$^6F_{7/2}$		
5437	54379.27	7/2	1.34	$5d^6(^5D)6p$		$^4F_{7/2}$		
5444	54445.19	5/2	1.45	$5d^6(^5D)6p$		$^4D_{5/2}$		
5553	55538.65	5/2	1.09	$5d^6(^5D)6p$		$^4F_{5/2}$		
5563	55635.92	3/2	0.70					
5638	56384.14	9/2	1.39					3
5679	56791.35	7/2	1.28					
5740	57402.59	7/2	1.29					
6297	62974.25	5/2						3

NOTES TO TABLE VIII

1. This and the following levels of this group have not been interpreted previously.
2. First interpretation.
3. New level.

In table IX the classified lines of Os II have been collected in the order of increasing wave-length. The symbol in the first column denotes the author, whose wave-length has been quoted. In the intensity-column the numbers and symbols refer to arc and spark respectively. For the general structure of the table the reader is referred to table III (see section 4). The total number of classified Os II-lines is now 162 corresponding to 163 transitions between 22 ground levels and 21 odd levels. Of 94 lines the splitting is given; of these 57 show resolved patterns.

TABLE IX

Classified lines of Os II

Int.		λ_{air}	$\sigma_{vac.}$	Classification	$\delta\sigma$	Zeeman effect		Notes
4	8	2005.87	49837.56	6297(5/2)–131(3/2)	—0.08			
2	7	2017.13	49559.39	6297(5/2)–134(5/2)	—0.06			
3	5	2044.36	48899.37	5679(7/2)– 78(5/2)	—0.05			
3	10	2046.28	48853.49	5444(5/2)– 55(3/2)	+0.35			
10	40	2067.21	48358.93	5195(9/2)– 35(7/2)	+0.47			1
25	50	2164.85	46178.08	5177(5/2)– 55(3/2)	—0.25			
40	100	2194.39	45556.52	4914(7/2)– 35(7/2)	+0.28			
	1	2194.70	45550.08	6297(5/2)–174(5/2)	+0.22			
	1	2211.42	45205.72	4879(5/2)– 35(7/2)	+0.17			
5	30	2214.76	45137.55	5679(7/2)–116(5/2)	+0.28			
8	20	2225.27	44924.39	5638(9/2)–114(7/2)	+0.15			
30	30	2227.98	44869.75	4879(5/2)– 39(5/2)	—0.01			
2	125	2255.847	44315.53	4431(9/2)– 0(9/2)	+0.13			
100	125	2282.26	43802.70	4380(7/2)– 0(9/2)	+0.34			
20	25	2293.54	43587.29	5679(7/2)–132(7/2)	—0.18			2
10	—	2304.69	43376.44	5679(7/2)–134(5/2)	—0.11			
15	30	2313.75	43206.59	4879(5/2)– 55(3/2)	—0.06			
10	25	2315.16	43180.28	5638(9/2)–132(7/2)	+0.02			
	1	2325.50	42988.31	6297(5/2)–199(7/2)	—0.02			2
6	15	2325.65	42985.53	5444(5/2)–114(7/2)	+0.24			
50	80	2336.803	42780.40	4637(5/2)– 35(7/2)	+0.04	(0)	1.49	3
7	—	2339.819	42725.26	5437(7/2)–116(5/2)	+0.07			
30	50	2350.242	42535.80	4812(1/2)– 55(3/2)	—0.23	(0.59)	1.20 ...	4
15	25	2355.284	42444.74	4637(5/2)– 39(5/2)	+0.17	(0)	1.62	
15	4	2357.654	42402.08	5553(5/2)–131(3/2)	+0.04			
		2361.402	42334.78	5553(5/2)–132(7/2)	+0.01			
50	80	2367.354	42228.36	4615(3/2)– 39(5/2)	+0.11	(0)	1.36 ...	
		2373.218	42124.01	5553(5/2)–134(5/2)	+0.16			
5l	20	2391.770	41797.30	5740(7/2)–156(9/2)	+0.29	(0)	0.80	1, 5
	1	2409.391	41491.64	4812(1/2)– 66(1/2)	+0.13	$g_1 = 2.96$	$g_2 = 3.16$	6
	1	2420.062	41308.71	5444(5/2)–131(3/2)	+0.13	(0)	1.48	
	1	2421.59	41282.65	4128(9/2)– 0(9/2)	—0.30			2
25	80	2423.071	41257.42	4914(7/2)– 78(5/2)	—0.04	$g_1 = 1.52$	$g_2 = 1.72$	
8	10	2424.024	41241.20	5444(5/2)–132(7/2)	—0.11	$g_1 = 1.44$	$g_2 = 1.25$	
?		2427.287	41185.75	5679(7/2)–156(9/2)	—0.02	(0)	—	
8	40	2427.900	41175.36	5437(7/2)–132(7/2)	—0.03	(... 0.27)	1.31	
		2443.837	40906.86	4879(5/2)– 78(5/2)	+0.09	$g_1 = 1.39$	$g_2 = 1.70$	
1/2		2451.369	40781.18	4637(5/2)– 55(3/2)	—0.28	(0.08, 0.26 ...)	1.40	1, 5

TABLE IX *(continued)*

Classified lines of Os II

Auth.	Int.		λ_{air}	$\sigma_{vac.}$	Classification	$\delta\sigma$	Zeeman effect	
EH		1	2451.55	40778.17	5638(9/2)–156(9/2)	—0.39		
B			2453.440	40746.76	5220(7/2)–114(7/2)	+0.18	(... 0.46)	—
B	2		2454.912	40722.33	4431(9/2)– 35(7/2)	+0.08	(0)	0.99 ...
EH		1	2464.42	40565.23	4615(3/2)– 55(3/2)	+0.09		
H	10	30	2468.898	40491.66	5195(9/2)–114(7/2)	—0.05	(0)	... 1.94
A			2480.002	40310.37	5177(5/2)–114(7/2)	—0.11		
H	8h	15h	2486.244	40209.18	4380(7/2)– 35(7/2)	—0.03	(0)	1.55
H	10	10h	2489.280	40160.14	5740(7/2)–172(7/2)	—0.19	$g_1 = 1.29$	$g_2 = 1.00$
EH		1	2492.01	40116.15	5177(5/2)–116(5/2)	—0.15		
B	?		2507.185	39873.36	4380(7/2)– 39(5/2)	—0.06	(0)	1.47
H	8	20	2509.708	39833.28	5740(7/2)–175(5/2)	+0.09	(0)	1.15
H	3	10h	2527.756	39548.89	5679(7/2)–172(7/2)	—0.20		
B	?		2529.563	39520.64	4615(3/2)– 66(1/2)	+0.02	$g_1 = 1.74$	$g_2 = 3.17$
H	—	15	2537.997	39389.32	3938(7/2)– 0(9/2)	—0.17	$g_1 = 1.85$	$g_2 = 1.52$
H	3	15	2548.832	39221.88	5679(7/2)–175(5/2)	—0.07	(0)	1.20
A			2554.035	39141.99	5638(9/2)–172(7/2)	+0.11		
H	8	25	2563.164	39002.59	5220(7/2)–132(7/2)	—0.01	$g_1 = 1.42$	$g_2 = 1.26$
EH		1	2577.13	38791.24	5220(7/2)–134(5/2)	—0.44		
H	10	10	2578.321	38773.32	5437(7/2)–156(9/2)	—0.37	$g_1 = 1.35$	$g_2 = 1.15$
H	15	100w	2580.026	38747.70	5195(9/2)–132(7/2)	—0.03	$g_1 = 1.40$	$g_2 = 1.25$
EH		1	2583.574	38695.49	5638(9/2)–176(11/2)	—0.01		
EH		1	2592.18	38566.03	5177(5/2)–132(7/2)	—0.47		
H	12	3	2596.005	38509.21	6297(5/2)–244(5/2)	—0.18		
EH		1	2597.851	38481.86	4637(5/2)– 78(5/2)	+0.28	(... 0.19)	1.65
A			2610.446	38296.19	5553(5/2)–172(7/2)	—0.20		
B	1/2		2631.211	37993.99	6297(5/2)–249(7/2)	—0.03		
H	5	2	2632.892	37969.73	5553(5/2)–175(5/2)	+0.48		
EH		1	2652.45	37689.78	4128(9/2)– 35(7/2) 4914(7/2)–114(7/2)	—0.02 +0.29	(... 0.62, 0.86)	—
B	1/2		2664.281	37522.41	6297(5/2)–254(5/2)	+0.15		
H	5	1	2666.211	37495.25	4914(7/2)–116(5/2)	—0.06	—	1.41
EH		1	2671.803	37416.79	5740(7/2)–199(7/2)	+0.13	$g_1 = 1.28$	$g_2 = 1.09$
EH		1	2677.372	37338.96	4879(5/2)–114(7/2)	+0.16	(0)	0.92 ...
B	?		2687.169	37202.84	5444(5/2)–172(7/2)	—0.09	$g_1 = 1.44$	$g_2 = 0.99$
B	1/2		2691.378	37144.66	4879(5/2)–116(5/2)	+0.04	$g_1 = 1.37$	$g_2 = 1.54$
EH		1	2691.907	37137.36	5437(7/2)–172(7/2)	+0.35	$g_1 = 1.35$	$g_2 = 1.00$
B	?		2711.005	36875.75	5444(5/2)–175(5/2)	—0.04	(... 0.20)	1.38
B	?		2715.865	36809.77	5437(7/2)–175(5/2)	—0.10	(0)	1.31
B	?		2716.184	36805.45	5679(7/2)–199(7/2)	—0.03	(... 0.51, 0.72)	
B	2		2731.358	36600.99	5220(7/2)–156(9/2)	+0.09	$g_1 = 1.39$	$g_2 = 1.14$
B	?		2750.516	36346.07	5195(9/2)–156(9/2)	+0.04	$g_1 = 1.40$	$g_2 = 1.15$
B	?		2773.487	36045.05	5563(3/2)–195(5/2)	+0.04	(0)	0.91
B			2780.995	35947.73	5553(5/2)–195(5/2)	—0.01	$g_1 = 1.10$	$g_2 = 0.81$
A			2781.161	35945.60	4914(7/2)–132(7/2)	+0.09		
B	2		2783.874	35910.57	4380(7/2)– 78(5/2)	+0.14	(0)	1.17 ...
B	?		2797.616	35734.19	4914(7/2)–134(5/2)	—0.40		
B	?		2803.277	35662.09	4879(5/2)–131(3/2)	0.00	(0)	1.43
B	1		2819.209	35460.50	3938(7/2)– 39(5/2)	—0.05	$g_1 = 1.85$	$g_2 = 1.62$

TABLE IX *(continued)*

Classified lines of Os II

Int.		λ_{air}	$\sigma_{vac.}$	Classification	$\delta\sigma$	Zeeman effect		Notes
1/2		2825.316	35383.86	4879(5/2)–134(5/2)	—0.04	(0.12)	1.37	
2		2839.992	35201.02	5679(7/2)–215(9/2)	+0.48			1
?		2856.999	34991.49	4812(1/2)–131(3/2)	+0.02	(**0.78**)	—	
1		2863.374	34913.58	4637(5/2)–114(7/2)	—0.03	$g_1 = 1.61$	$g_2 = 1.27$	
1		2879.379	34719.52	4637(5/2)–116(5/2)	+0.09	(... **0.12**)	1.58	
1/2		2880.222	34709.36	5195(9/2)–172(7/2)	+0.01	$g_1 = 1.40$	$g_2 = 0.99$	
	1	2886.231	34637.11	5220(7/2)–175(5/2)	+0.03	(0)	1.50	
1/2		2901.125	34459.29	5444(5/2)–199(7/2)	+0.03	$g_1 = 1.46$	$g_2 = 1.11$	
2		2910.676	34346.23	5177(5/2)–174(3/2)	+0.24	$g_1 = 1.68$	$g_2 = 0.97$	
2		2917.751	34262.94	5195(9/2)–176(11/2)	—0.03	$g_1 = 1.41$	$g_2 = 1.20$	
2		2980.319	33543.66	4914(7/2)–156(9/2)	—0.15	$g_1 = 1.51$	$g_2 = 1.14$	
4		3013.936	33169.57	4637(5/2)–132(7/2)	—0.06	$g_1 = 1.60$	$g_2 = 1.24$	
		3027.533	33020.57	4615(3/2)–131(3/2)	—0.01	$g_1 = 1.74$	$g_2 = 1.40$	
1		3033.205	32958.83	4637(5/2)–134(5/2)	+0.12	$g_1 = 1.62$	$g_2 = 1.33$	
?		3035.224	32936.90	5740(7/2)–244(5/2)	+0.03	(0)	1.29	
20	50	3042.739	32855.57	4431(9/2)–114(7/2)	+0.07	$g_1 = 1.45$	$g_2 = 1.27$	
4		3048.965	32788.48	5437(7/2)–215(9/2)	+0.02	$g_1 = 1.32$	$g_2 = 1.10$	
1		3053.256	32742.40	4615(3/2)–134(5/2)	+0.01	$g_1 = 1.76$	$g_2 = 1.35$	
1/2		3065.100	32615.88	5220(7/2)–195(5/2)	+0.31			1
?		3083.430	32421.99	5740(7/2)–249(7/2)	+0.13	(... **0.32**)	1.23	
20	8	3102.716	32220.48	5220(7/2)–199(7/2)	—0.07	(0)	1.56	2, 7
2		3106.643	32179.75	5177(5/2)–195(5/2)	+0.28			1
20	20	3109.679	32148.34	4380(7/2)–116(5/2)	+0.06	$g_1 = 1.57$	$g_2 = 1.54$	2
1/2		3127.497	31965.19	5195(9/2)–199(7/2)	—0.49			1
20	20	3165.659	31579.86	4914(7/2)–175(5/2)	—0.13	$g_1 = 1.51$	$g_2 = 1.35$	
		3168.021	31556.33	4879(5/2)–172(7/2)	—0.11	(**0.19**, 0.58, 1.00)	—	
80	30	3173.926	31497.61	3938(7/2)– 78(5/2)	+0.05	$g_1 = 1.84$	$g_2 = 1.68$	
		3183.445	31403.43	5638(9/2)–249(7/2)	+0.02	$g_1 = 1.39$	$g_2 = 1.18$	
15	30	3186.402	31374.29	4879(5/2)–174(3/2)	—0.02	$g_1 = 1.39$	$g_2 = 0.97$	2
		3189.973	31339.14	5679(7/2)–254(5/2)	—0.08	$g_1 = 1.28$	$g_2 = 1.08$	
1/2		3201.196	31229.30	4879(5/2)–175(5/2)	0.00	(... **0.09**)	1.37	
?		3207.261	31170.24	5563(3/2)–244(5/2)	—0.02	$g_1 = 0.70$	$g_2 = 1.27$	
50	40	3213.312	31111.55	4431(9/2)–132(7/2)	+0.03	$g_1 = 1.44$	$g_2 = 1.25$	
2		3217.301	31072.98	5553(5/2)–244(5/2)	—0.01	$g_1 = 1.09$	$g_2 = 1.27$	
?		3255.999	30703.69	4812(1/2)–174(1/2)	0.00	$g_1 = 2.95$	$g_2 = 0.98$	2
4		3265.356	30615.71	5220(7/2)–215(9/2)	+0.04	$g_1 = 1.41$	$g_2 = 1.12$	
20	15	3267.200	30598.43	4380(7/2)–132(7/2)	—0.05	$g_1 = 1.56$	$g_2 = 1.24$	
1		3289.870	30387.59	4380(7/2)–134(5/2)	+0.03			
1		3292.763	30360.89	5195(9/2)–215(9/2)	+0.09	$g_1 = 1.41$	$g_2 = 1.11$	
		3312.105	30183.59	5563(3/2)–254(5/2)	—0.20			
1/2		3334.642	29979.60	5444(5/2)–244(5/2)	+0.07	(... **0.42**)	—	
4		3392.961	29464.32	5444(5/2)–249(7/2)	—0.14	$g_1 = 1.44$	$g_2 = 1.18$	2
8		3396.961	29429.63	3732(5/2)– 78(5/2)	+0.03	$g_1 = 2.22$	$g_2 = 1.70$	
?		3400.555	29398.53	5437(7/2)–249(7/2)	—0.01	$g_1 = 1.33$	$g_2 = 1.17$	
		3431.751	29131.32	4637(5/2)–172(7/2)	+0.07			
?		3448.108	28993.10	5444(5/2)–254(5/2)	+0.04	$g_1 = 1.44$	$g_2 = 1.09$	
2		3470.741	28804.03	4637(5/2)–175(5/2)	—0.08	$g_1 = 1.62$	$g_2 = 1.36$	
4		3479.352	28732.76	4615(3/2)–174(3/2)	—0.04	$g_1 = 1.74$	$g_2 = 0.98$	

TABLE IX *(concluded)*

Classified lines of Os II

Auth.	Int.		λ_{air}	$\sigma_{vac.}$	Classification	$\delta\sigma$	Zeeman effect		
H	40	15	3482.112	28709.98	4413(9/2)–156(9/2)	+0.16			2
B	4		3497.000	28587.76	4615(3/2)–175(5/2)	—0.03	$g_1 = 1.72$	$g_2 = 1.34$	
A			3545.449	28197.14	4380(7/2)–156(9/2)	+0.36			1
B	?		3560.410	28078.63	4128(9/2)–132(7/2)	—0.44			1
A			3579.418	27929.56	3938(7/2)–114(7/2)	—0.03			
B	?		3603.776	27740.76	5220(7/2)–244(5/2)	—0.06	$g_1 = 1.41$	$g_2 = 1.27$	
H	15	100	3604.475	27735.38	3938(7/2)–116(5/2)	—0.03	$g_1 = 1.85$	$g_2 = 1.56$	
A			3661.363	27304.49	5177(5/2)–244(5/2)	—0.23			
EH		1+	3671.95	27225.73	5220(7/2)–249(7/2)	—0.02	$g_1 = 1.41$	$g_2 = 1.18$	
B	6		3692.642	27073.18	4431(9/2)–172(7/2)	+0.04	$g_1 = 1.44$	$g_2 = 0.98$	
B	1		3706.644	26970.91	5195(9/2)–249(7/2)	+0.03			
B	1/2		3754.544	26626.82	4431(9/2)–176(11/2)	+0.06	$g_1 = 1.44$	$g_2 = 1.20$	2
B	1		3810.922	26232.92	4380(7/2)–175(5/2)	—0.04			
B	1		3817.835	26185.42	3938(7/2)–132(7/2)	—0.19			
B	1		3848.805	25974.72	3938(7/2)–134(5/2)	+0.03	$g_1 = 1.86$	$g_2 = 1.35$	
B	?		3893.367	25677.43	4128(9/2)–156(9/2)	+0.06			2
B	2		3894.891	25667.38	3732(5/2)–116(5/2)	—0.07	$g_1 = 2.22$	$g_2 = 1.56$	
B	1		4050.140	24683.53	4914(7/2)–244(5/2)	—0.20	(0.12, 0.36, 0.60)		
A			4108.398	24333.54	4879(5/2)–244(5/2)	+0.50			1
EH	1		4109.088	24329.46	4431(9/2)–199(7/2)	—0.01			2
A			4133.717	24184.50	3732(5/2)–131(3/2)	—0.42			1
A			4197.769	23816.00	4380(7/2)–199(7/2)	—0.43			1
EH	1		4237.15	23594.13	4128(9/2)–176(11/2)	—0.18			
A			4399.274	22724.66	4431(9/2)–215(9/2)	+0.07			
A			4581.747	21819.62	3938(7/2)–175(5/2)	—0.47			1
A			4608.769	21691.69	4615(3/2)–244(5/2)	+0.16			
H	3		4828.441	20704.83	4615(3/2)–254(5/2)	—0.23			2
M	1		4978.90	20079.15	3732(5/2)–172(7/2)	—0.12			2
M	1		5311.54	18821.70	4380(7/2)–249(7/2)	+0.07			

NOTES TO TABLE IX

1. Tentative classification; $\delta\sigma$ is too large.
2. Also classified as a transition between two Os I levels.
3. When the type of Zeeman pattern cannot be determined, the values refer to the centers of gravity of the π- and σ-pattern respectively.
4. Zeeman data in clarendon refer to the strongest components.
5. $\delta\sigma$ is too large, but the Zeeman effect is in accordance with the classification.
6. When the g-factors are given, g_1 always corresponds to the level mentioned first in the column headed „Classification".
7. Of the Os I-transition a Zeeman pattern has also been measured.
8. The Zeeman pattern observed here belongs to an Os I-transition. See table III.
9. Observed Zeeman effect not in agreement with the other classification.
10. When two classifications have been given both are possible.
11. The π-pattern belongs to the Os I-transition 4852(4)–110(4). See table III. The σ-pattern belongs to the given classification.
12. A Zeeman pattern has been observed that has not yet been interpreted.

The ground configurations in the Os II system which could be expected belong to $5d^56s^2$, $5d^66s$ and $5d^7$. The multiplets of these configurations, which in all probability will lie low in the term system, are ^6S and $^4(GD)$ of d^5s^2, $^{6,4}(D)$ and $^{4,2}(HGFDP)$ of d^6s and $^4(FP)$ and $^2(HGFDP)$ of d^7. The lowest six levels were interpreted by VAN DEN BOSCH [12] as $5d^6(^5D)6s\ ^6D$ levels. It is the only sextet (except ^6S) in the whole system, so the interpretation is unambiguously correct. The next level we assigned to $5d^56s^2\ ^6S_{5/2}$. Of the detected levels with $J=5/2$ it is the level which possesses the highest g-value (1.70). In LS-coupling all other expected levels with $J=5/2$ should have a g-factor which is considerably smaller than 1.70. The g_{LS}-value of $^6S_{5/2}$ is 2.00. A different interpretation of this level is unacceptable. The next three levels belong to the $5d^6(a^5D)6s\ ^4D$ term. The level $5d^6(a^5D)6s\ ^4D_{1/2}$ could not be detected. The subsequent seven levels were ascribed to the $5d^7$ configuration. The analogy with the Fe II [29] spectrum is not pronounced, because in that spectrum the $3d^7$ configuration is low in the system. The expected level $5d^7\ ^4F_{9/2}$ could not be located. However, the g-values of the interpreted levels are in passable agreement with the theoretical g-values in LS-coupling. The interpretation of 215(9/2) is tentative only.

The odd configurations which could be expected, are $5d^46s^26p$, $5d^56s6p$ and $5d^66p$. The lowest expected terms of these are $^{6,4}(FDP)$, $^{8,6,6,4}(P)$ and $^{6,4}(FDP)$ respectively.

The two lowest levels, which were not interpreted by previous authors and the newly detected level 4128 constitute the $5d^56s(^7S)6p\ ^8P$. This term is expected to be low in the system, since $5d^56s^2\ ^6S$ also lies low in the even system of Os II. The g-values of the levels belonging to that term are very characteristic and in good agreement with the g-values in LS-coupling. As a result of its low position these levels are practically not perturbed by the higher ones in the system. Of the associated $5d^56s(^7S)6p\ ^6P$ term we identified only the $^6P_{7/2}$ and $^6P_{5/2}$ levels. The g-values of the levels are also very characteristic. The distance $^8P-{}^6P$ ($\approx$ 10000 K) is in agreement with the distance $^7P-{}^5P$ in the $5d^56s^2(^6S)6p$ configuration in the Os I-system.

The $d^5s(^5S)p\ ^6P$ and ^4P have not been detected and other terms of this configuration are expected higher. Hence the remaining observed terms should be ascribed to either d^6p or d^4s^2p. These configurations produce the same multiplets but with different signs of spin-orbit interaction. The detected ^6D and ^6F multiplets are rather irregular, but they show preponderantly inverted order, so that we conclude that the configuration d^6p is the lowest. VAN DEN BOSCH already identified the ^6D term [12]. It must be mentioned that fairly strong combinations with the low even terms are present. From comparison of the transitions $d^4s\ ^6D_{9/2}-d^4p\ ^6F_{11/2}$ in Cr II [30], Mo II [31] and W II [32] and $d^6s\ ^6D_{9/2}-d^6p\ ^6F_{11/2}$ in Fe II [29] and Ru [12] it could be inferred, that the corresponding transition in the Os II-spectrum should have a wave-

number of about 51000 K. This is just beyond our region of observation so that we could not locate the expected $^6F_{11/2}$ level. In the accessible region of observation, this level has at most three combinations. There were several pairs of lines showing one of the three expected intervals but there is no additional information to prove which is the real one. It will be very useful to make observations in the vacuum region not only for locating the $d^6p\ ^6F_{11/2}$ but also for detecting the d^4s^2p configuration and for verifying some of the classifications given.

For finding the high even levels the long wave-length region should be more fully explored, preferably with light sources containing pure osmium metal.

Acknowledgements

The author wishes to express his indebtedness to Dr. P. F. A. KLINKENBERG for devoting many hours to helpful discussions on the interpretation of energy levels and for giving valuable hints with regard to the detection of new levels, to Dr. J. C. VAN DEN BOSCH for putting unpublished measurements at his disposal which helped in locating new levels and in determining the missing g-values, to Dr. W. ALBERTSON for surrendering his wave-length data to the Zeeman laboratory, to H. HOOYKAAS and W. J. SURINGAR for making Zeeman spectrograms on the osmium spectrum, to Dr. G. J. VAN DEN BERG for valuable help with the experiments, to Mr. P. VAN DER ROEST for his readiness in giving all technical assistance requested, to Mr. C. DRIJVER for computational work on wave-length measurements and for statistical work on wave numbers and to Mr. A. COMPANJEN for similar arithmetical help. Finally the author should like to express his appreciation to Miss L. LÖHNING for the great care bestowed on typing the list of classified Os I-lines.

REFERENCES

1. ALBERTSON, W., Phys. Rev. **45**, 304 (1934).
2. KAYSER, H., Astrophys. J. **7**, 181 (1898).
3. EXNER, F. and E. HASCHEK, Die Spektren der Elemente bei nomalem Druck. (Deuticke, Leipzig und Wien 1911/1912).
4. MEGGERS, W. F., Sci. Papers Nat. Bur. Stand. **20**, 35 (1924).
5. ALBERTSON, W., Phys. Rev. **53**, 940(A) (1938).
6. KLINKENBERG, P. F. A., G. J. VAN DEN BERG and J. C. VAN DEN BOSCH, Physica **16**, 861 (1950).
7. HARRISON, G. R., *et al.*, M.I.T.Wave-length Tables, Technology Press., Mass. Inst. Techn., Cambridge 1939.
8. BOSCH, J. C. VAN DEN, Unpublished material 1949.
9. KLEEF, TH. A. M. VAN, Master's thesis; unpublished 1952.
10. BOSCH, J. C. VAN DEN, Lunds Univ. Årsskr., Proc. Rydberg Cent. Conf., on Atomic Spectroscopy 1955, p. 80.
11. ALBERTSON, W., Unpublished material 1938.
12. MOORE, CH. E., Atomic Energy Levels, Vol. III, Circular of the Nat. Bur. Stand. **467**, 171 (1958).

13. Hooykaas, H. and W. J. Suringar, Master's thesis; unpublished 1954.
14. Kleef, Th. A. M. van, Physica 23, 843 (1957).
15. ————, Thesis for the doctorate, Amsterdam 1957.
16. Klinkenberg, P. F. A., Physica 13, 581 (1947).
17. Edlén, B., J.O.S.A. 43, 339 (1953).
18. Russell, H. N., Ch. E. Moore and D. W. Weeks, Trans. Am. Phil. Soc. 34, Part 2, 111 (1944).
19. Bosch, J. C. van den, Handbuch der Physik, Band XXVIII, Spektroskopie II, 317. Springer-Verlag, Berlin, Göttingen, Heidelberg.
20. Racah, G., Phys. Rev. 61, 186 (1942); 62, 438 (1942); 63, 367 (1943).
21. Klinkenberg, P. F. A., W. F. Meggers, R. Velasco and M. A. Catalán, J. Research Nat. Bur. Stand. 59, 319 (1957).
22. Catalán, M. A. and P. M. Sancho, An. Soc. Esp. Fisica y Quimica (Madrid) 29, 327 (1931).
23. Trees, R. E. and M. M. Harvey, J. Research Nat. Bur. Stand. 49, 397 (1953).
24. Kessler, K. G. and W. F. Meggers, J. Research Nat. Bur. Stand. 55, 97 (1955).
25. Laporte, O. and J. E. Mack, Phys. Rev. 63, 246 (1943).
26. Russell, H. N., Astroph. J. 66, 347 (1927).
27. Kiess, C. C. and H. K. Kiess, J. Research. Nat. Bur. Stand. 6, 621 (1931).
28. Moore, Ch. E., Atomic Energy Levels, Vol. III, etc. (see reference 12) p. 143.
29. Dobbie, J. C., Phys. Rev. 45, 76 (1934).
30. Kiess, C. C., J. Research Nat. Bur. Stand. 47, 385 (1951).
31. ————, J. Research Nat. Bur. Stand. 60, 375 (1958).
32. Laun, D. D., J. Research Nat. Bur. Stand. 21, 207 (1938).

NOTE ADDED IN PROOF

Recently the level $5d^7(a^2H)6s\ ^3H_6$ in Os I has been found at 24222.97 K ($g = 1.15$) on 18 combinations. Herewith the identifications given in table II have been substantially confirmed. Only the ^3D and ^1D configuration assignments should be changed (cf a subsequent article in "Physica"). Three odd levels have also been added whereby the total number of classified lines was raised to 3008.

DAMPED TIDES IN A NAVIGATION CANAL

BY

J. TH. THIJSSE

(Communicated at the meeting of June 25, 1960)

The port of Rotterdam is in open connection with the sea. Amsterdam, on the contrary, can only be reached by ships after passing a lock (fig. 1).

Halfway the nineteenth century plans were made for both Rotterdam and Amsterdam to substitute new and capacious waterways for the old ones, which had become insufficient and which both included locks. In both cases the string of sandhills along the coast (dunes) had to be pierced, thus providing a direct access from the North Sea.

There was no doubt that the road leading to Rotterdam should be open: it is part of a river system. For Amsterdam it was not so evident. There was a project for an open canal, between the North Sea and the southwestern corner of the Zuyderzee, but the other solution was preferred: a canal (Noordzeekanaal), separated at both ends from the sea, in which neither the tides nor the storm surges could penetrate. One of the reasons for this decision was the fear of strong tidal currents in an open canal, hampering or even preventing navigation.

At the time, a century ago, it was not possible to predict the strength of the tidal currents: mere guesswork had to be done.

Sixty years later a similar problem had to be solved by a committee, headed by H. A. LORENTZ. A prediction had to be made for the tides and the storm surges in the Wadden Sea, the part of the Zuyderzee outside the planned enclosure dam. In a region like this the motion of the water may not be determined without taking the acceleration into account (oceanography) nor by leaving the friction out (river hydraulics).

Lorentz developed a method by which, with a reasonable amount of labour, an approximate solution can be obtained [1]. He linearized both the equations of continuity and of acceleration (motion). The most radical of the approximations is the substitution of a frictional resistance proportional with the velocity of the fluid for the real resistance, which is, roughly speaking, proportional with the square of the velocity.

The result is two simple linear differential equations:

$$\text{(a)} \qquad \frac{\partial v}{\partial t} + g\frac{\partial z}{\partial s} + \omega \operatorname{tg} 2\vartheta \cdot v = 0 \qquad \frac{\partial z}{\partial t} + h\frac{\partial v}{\partial s} = 0$$

t time; s coordinate along the axis of the channel; h the depth of the channel, supposed to be a constant; g the acceleration of gravity; v the

Fig. 1.

mean value in a cross section of the velocity of the fluid; z the level of the surface, compared with its mean position.

The phenomenon is supposed to be harmonic with a frequency ω, z and v containing a factor $e^{i\omega t}$. The dimensionless factor tg 2ϑ (between 0 and $+\infty$) represents the relative importance of friction, compared with acceleration. The value of this factor is chosen in such a way that the energy taken out of the system during the period $2\pi/\omega$ by the last term of the equation of motion is equal to the real loss of energy in that period. This leads to:

(b) $$\text{tg } 2\vartheta = \frac{8}{3\pi} \cdot \frac{g}{C^2} \cdot \frac{v_m}{\omega h}.$$

In this equation v_m is an average value for the module of the velocity, taken over the whole length of the channel. C is the Chezy coefficient of uniform flow:

$$\frac{dz}{ds} = v^2/C^2h.$$

The value of C depends on the roughness of the canal walls. A formula by COLEBROOK–WHITE [3] has been modified in the Netherlands to:

(c) $$C = 18 \log [6\, h/(a + {}^1/_7\, \delta)].$$

The size of the elements of which the "roughness" of the perimeter of the canal consists, is denoted by a. The thickness of a laminar sub-layer, if any, along the walls is δ.

In a perfectly smooth channel ($a = 0$) the frictional resistance is concentrated in this very thin sub-layer.

A group of students in civil-engineering, shortly before graduating, has applied the Lorentz formulae on the Noordzeekanaal supposed to be in open connection with the sea. No exact solution can be obtained, of course, but experience with these formulae guarantees that the result is a very good approximation. Starting from a sinusoidal motion and the equations being linear, z and v for any point of the channel must be

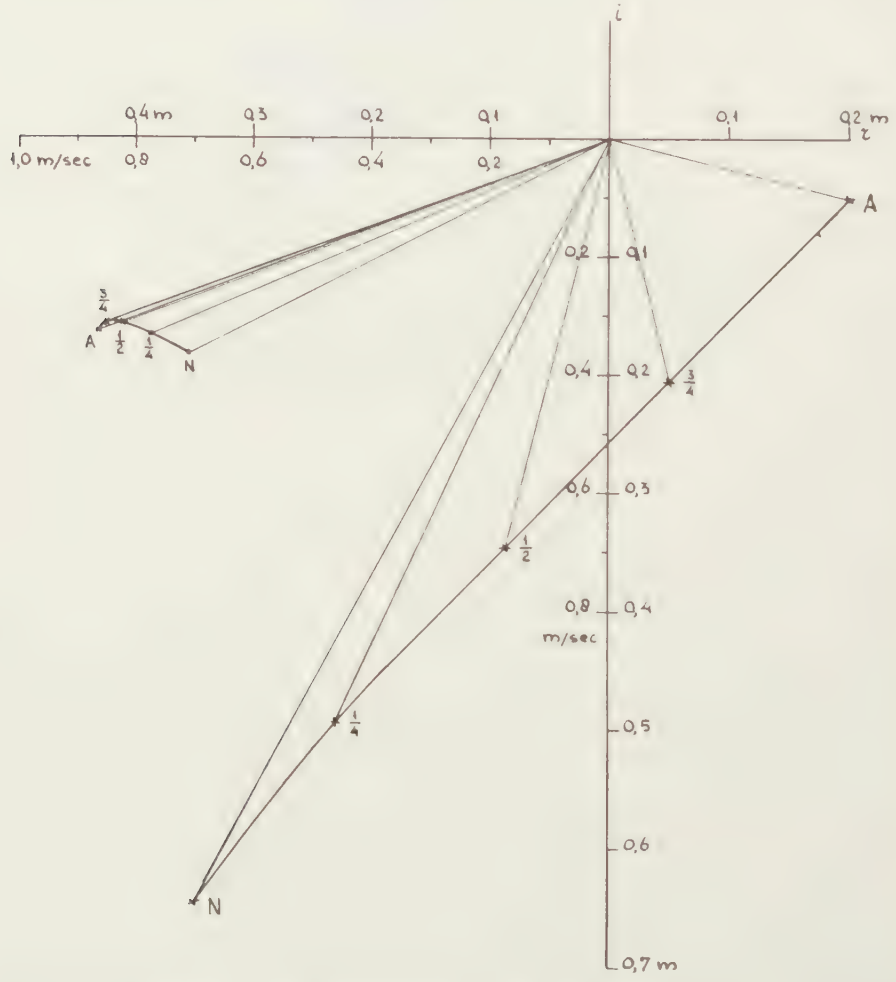

Fig. 2. Hodographs of the vertical tide (z) and the current (v) for $\operatorname{tg} \vartheta = 2{,}1$.

harmonic functions of time. The sinusoids which represent $z(t)$ and $v(t)$ are equal to the first harmonics of the Fourier series describing the real motion. This means that the damping of the tidal waves is correctly calculated, but that their deformation is not.

The canal is schematized: uniform cross section on the whole length of $L = 28 \times 10^3$ m between the North Sea (N) and Amsterdam (A). The depth is assumed to be 9 m.

The main harmonic component of the North Sea tide (principal lunar semi-diurnal tide $M\,2$, having an angular frequency $\omega = 1{,}405 \times 10^{-4}$ radians per second) has a module of about $^3/_4$ meters and a maximum (high tide) about four hours after $t = 0$. This means that:

$$z_N = {}^3/_4\, e^{-i(4 \text{ hours})}\, e^{i\omega t} = (-0{,}35 - 0{,}65\, i)\, e^{i\omega t}.$$

At the other end the tide, before the enclosure of the Zuiderzee, was

$$z_A = 0{,}2\, e^{-i(1 \text{ hour})}\, e^{i\omega t} = (+0{,}20 - 0{,}05\, i)\, e^{i\omega t}.$$

The problem is to calculate v_N and v_A, satisfying the fundamental equations and the boundary conditions z_N and z_A.

This leads to the following equations:

$$z_A = z_N\{(1) + (2)\, i\} + \frac{h}{c \cos \vartheta}\, v_N\{(3) + (4)\, i\},$$

$$\frac{h}{c \cos \vartheta}\, v_A = z_N\{(5) + (6)\, i\} + \frac{h}{c \cos \vartheta}\, v_N\{(1) + (2)\, i\},$$

in which the velocity of propagation of the tidal waves is $c = \sqrt{gh(1 - \operatorname{tg}^2 \vartheta)}$.

The coefficients (1)...(6) are functions of ϑ, of the length of the canal $\omega L/c = \alpha$ and of a roughness parameter $\omega L \operatorname{tg} \vartheta / c = \beta$, viz:

$$(1) = +\cos\,\alpha \cdot \cosh\,\beta$$
$$(2) = +\sin\,\alpha \cdot \sinh\,\beta$$
$$(3) = -\cos\,\vartheta \cdot \cos\,\alpha \cdot \sinh\,\beta - \sin\,\vartheta \cdot \sin\,\alpha \cdot \cosh\,\beta$$
$$(4) = +\sin\,\vartheta \cdot \cos\,\alpha \cdot \sinh\,\beta - \cos\,\vartheta \cdot \sin\,\alpha \cdot \cosh\,\beta$$
$$(5) = -\cos\,\vartheta \cdot \cos\,\alpha \cdot \sinh\,\beta + \sin\,\vartheta \cdot \sin\,\alpha \cdot \cosh\,\beta$$
$$(6) = -\sin\,\vartheta \cdot \cos\,\alpha \cdot \sinh\,\beta - \cos\,\vartheta \cdot \sin\,\alpha \cdot \cosh\,\beta$$

The result of the calculation may be represented by points for z_N, v_N, z_A and v_A in the complex plane. It is easy to complete the study by calculating z and v in intermediate points, taking other values of L. In this way a hodograph is constructed, connecting z_N and z_A, and another hodograph which runs from v_N to v_A. We shall not elaborate upon the interesting properties of these hodographs, but only give an example: figure 2, representing the result for $\operatorname{tg} 2\vartheta = 2{,}1$.

Now the value of v_m can be read from the diagram and then formula (b) enables us to calculate C and by applying formula (c) the value of $(a + {}^1/_7\, \delta)$ is found. So, starting from a given value of $\operatorname{tg} 2\vartheta$, we find the full strength of the flood current and of the ebb current (that is v_m) and

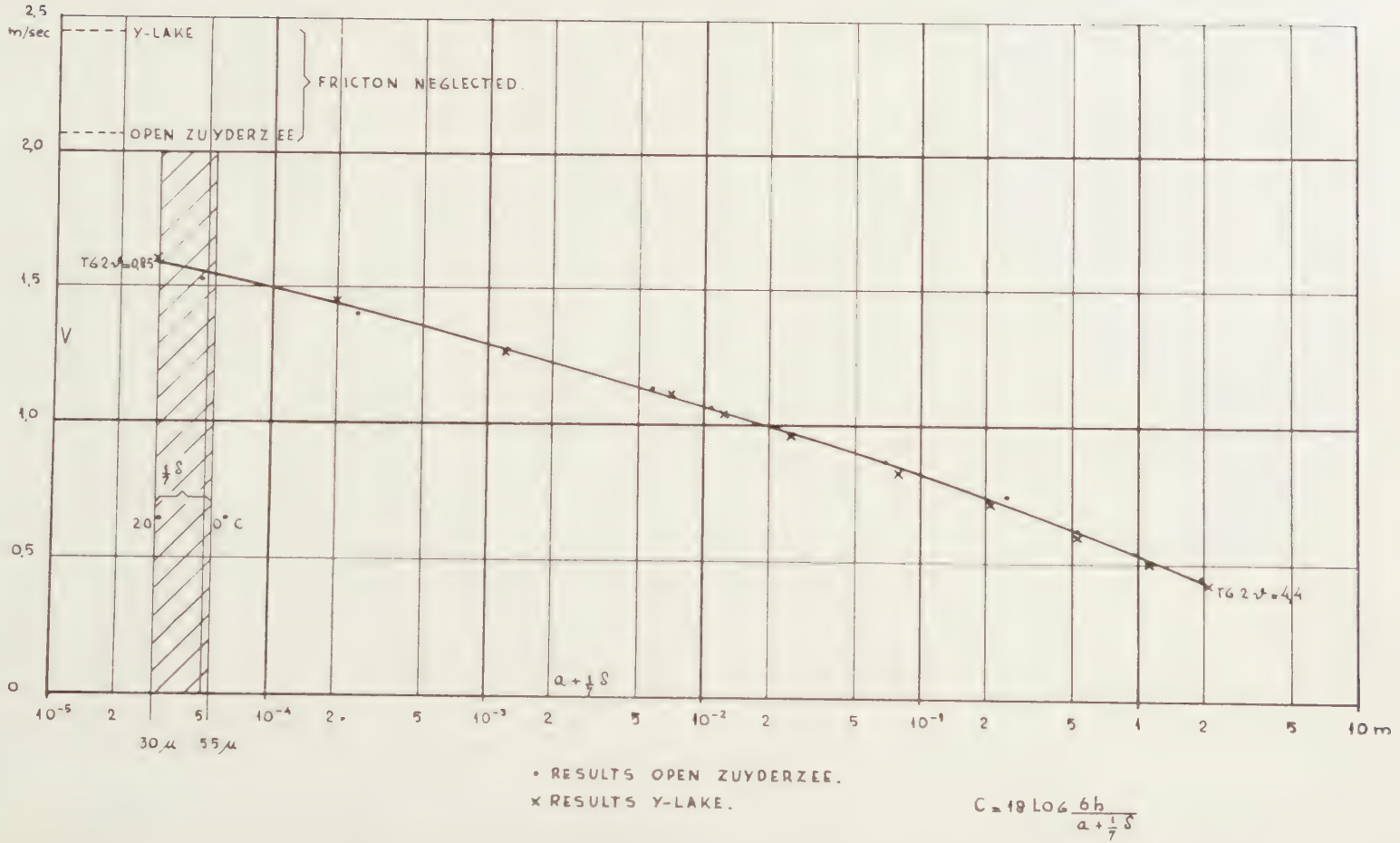

Fig. 3. Relation between roughness and speed of tidal currents.

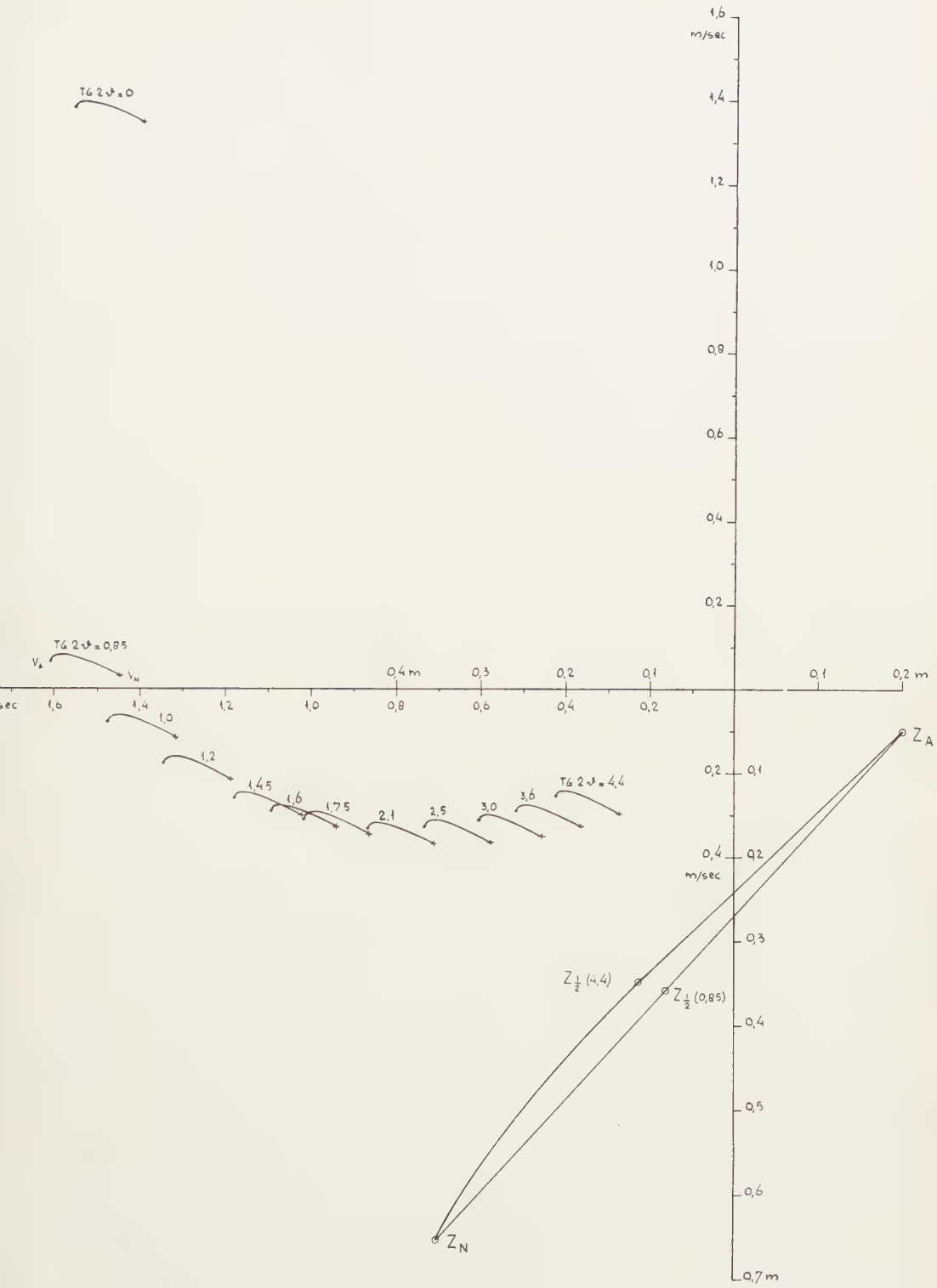

Fig. 4. Open Zuyderzee. Hodographs (levels and currents) for various values of the roughness.

the roughness which the canal walls must possess in order to reduce currents to that strength.

We may expect that by increasing the roughness the strength of the currents is diminished.

Each student has done the calculation with his own value for tg 2ϑ. So results were obtained for:

$$\text{tg } 2\vartheta = 0 - 0{,}85 - 1{,}0 - 1{,}2 - 1{,}45 - 1{,}6 - 1{,}75 - 2{,}1 - 2{,}5 - 3{,}0 - 3{,}6 - 4{,}4.$$

Figure 3 gives the relation between v_m and $(a + {}^1/_7\,\delta)$.

The laminar sub-layer has a thickness of 0,2 to $0{,}4 \times 10^{-3}$ m in the conditions present in the canal, depending upon the temperature (viscosity!), so ${}^1/_7\,\delta$ is between 30 and 50×10^{-6} m (μ). This is the limit for a perfectly smooth canal; the maximum tidal currents are about $1{}^1/_2$ m/sec then (3 knots) (result of calculating with tg $2\vartheta = 0{,}85$): too strong for navigation.

By irregular dredging or by revetting the canal with blocks of stone, a can be given any value up to about one meter. So the tidal streams may be reduced to about ${}^1/_2$ m sec (one knot). This may be low enough for safe navigation.

A remarkable item is the great difference between the results for a physically smooth canal ($a = {}^1/_7\,\delta = {}^1/_7\,\delta$) and a mathematically smooth, frictionless canal ($\vartheta = 0$).

In figure 4 the hodographs of v belonging to the various values of the roughness are shown. At the greatest value of the roughness parameter a, hardly or not at all to be realized ($a = 1{,}9$ m), the full tidal flow is only 0,45 m/sec; at the North Sea end somewhat less, at the Amsterdam end a little more. Lower values of a yield stronger currents. Also the phase changes slightly; the smoother the canal the later the moments of maximum current. This goes on until the canal is perfectly smooth and the denominator in equation (c) is only ${}^1/_7\,\delta = 0{,}03$ to 0,05 millimeter. Apart from the factor $e^{i\sigma t}$, the average for the velocity is about $-1{,}55 - 0{,}05\,i$ meters per second.

If we neglect the friction altogether, dropping the third term of the equation of motion, we get the well known linearized equations leading to undamped and undeformed waves. The hodograph for v then jumps suddenly to another corner of the complex plane: $-1{,}50 - 1{,}35\,i$ meters per second. The velocity increases from $1{}^1/_2$ m sec to about 2 m sec, but the most striking result is the change in phase: nearly 45°.

Even the least thinkable friction advances the currents about $1{}^1/_2$ hour. It is evident that in our conditions (depth of the order of ten meters, velocity of the order of 1 m/sec, tidal frequency of the order of 10^{-4} radians per second) the omission of a friction term leads to unacceptable results.

The question arises now, what would have happened if, the Noordzee-kanaal being open, the enclosure and partial reclamation of the Zuyderzee

would have been effectuated. In the final stage the Noordzeekanaal would have been in open connection, at Amsterdam, with a lake of moderate dimensions, the Y-lake (Ymeer). The area of this lake may be assumed to be 100 square kilometers $= 10^8$ m$^2 = A$.

Theoretically the tidal wave leaving the Noorezeekanaal at A spreads out over the lake and is reflected along its boundaries, a complicated phenomenon. However, the time of propagation from one side of the

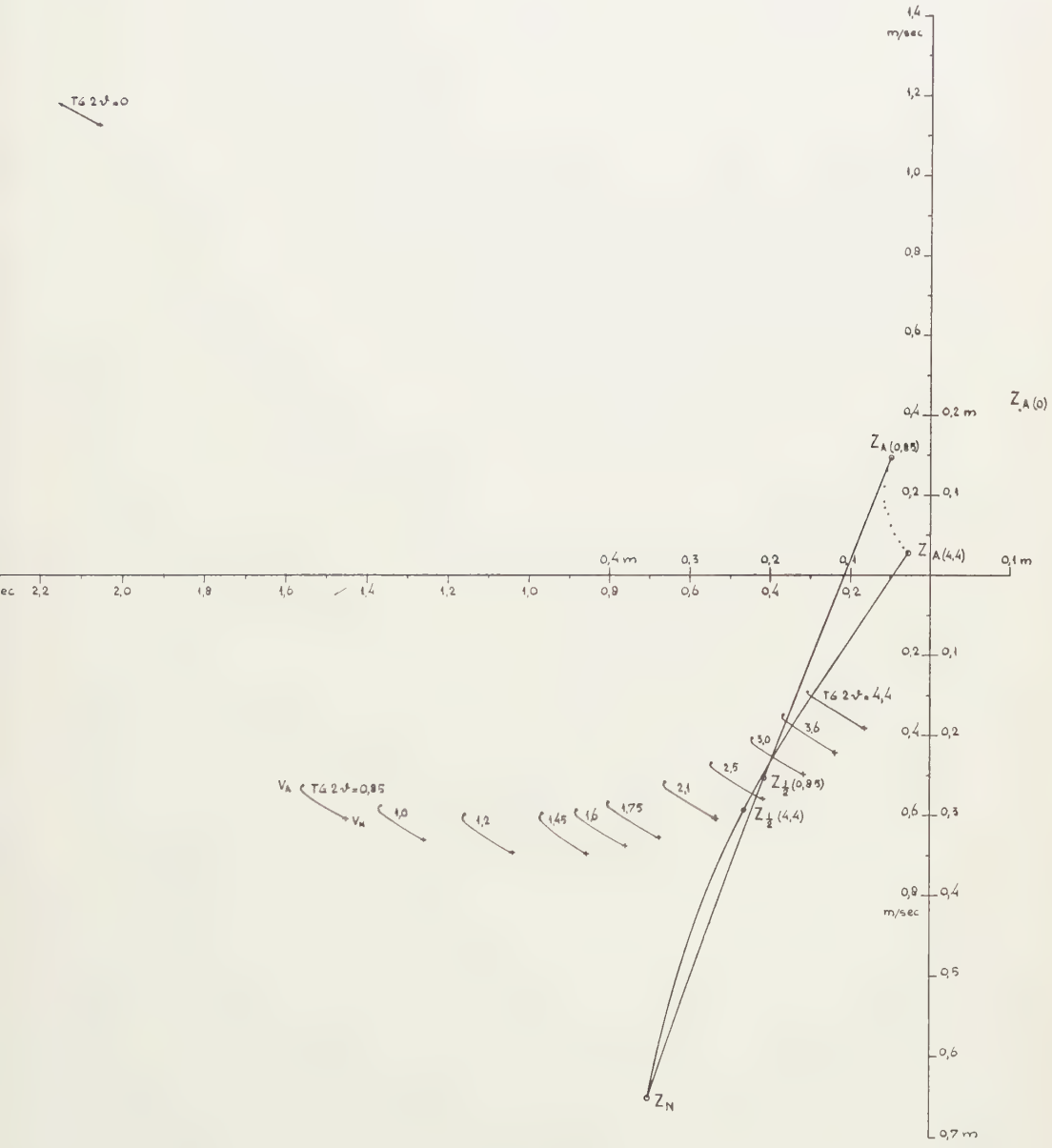

Fig. 5. Zuyderzee reclaimed. Hodographs (levels and currents) for various values of the roughness.

lake to the other side being short, a satisfactory approximation is got by assuming that at every moment the mean level of the lake is equal to z_A. This may be expressed as

(d) $$\frac{Bh}{A} v_A = \frac{dz_A}{dt} = i\omega z_A,$$

B being the width of the canal.

A second group of students has calculated v_N, v_A and z_A, starting from the tide in the North Sea z_N and equation (*d*). The same values for the roughness parameter tg 2ϑ as before have been used.

Figure 5 shows the result. The velocities are equal to those of the former boundary condition (open Zuyderzee), but the phase of the currents is different. The effect of roughness is the same as that in the open-Zuyderzee problem. The great difference between a physically smooth channel and no friction at all is even more pronounced.

The result of the study may be summarized as follows.

The tidal currents in an open Noordzeekanaal could have been reduced to about one knot by making the bottom and the slopes of the canal very rough. This is true for the former conditions with the Zuyderzee in open connection with the North Sea as well as for the future conditions after completion of the Zuyderzee-works, when only the small *Y*-lake exists near Amsterdam.

Even in a perfectly smooth canal the influence of friction is so great that it may not be neglected. This is true for depths of the order of 10 m, currents of the order of 1 m/sec and tidal periods of the order of 1 day.

REFERENCES

1. Verslag van de Staatscommissie inzake hoge waterstanden in verband met de afsluiting van de Zuiderzee.
's-Gravenhage, Algemene Landsdrukkerij, 1926.
2. C. F. Colebrock. Turbulent flow in pipes, with particular reference to the transition region between the smooth and rough pipe laws.
Journal of the Institution of Civil Engineers, 1939.

REPORT OF THE NETHERLANDS EXPEDITION FOR THE OBSERVATION OF THE TOTAL SOLAR ECLIPSE ON OCTOBER 2, 1959

BY

J. HOUTGAST

(Communicated by Prof. M. G. J. MINNAERT at the meeting of June 25, 1960)

Introduction

A preliminary program of observations for the 1959 eclipse was presented already on June 19th, 1956 to the Eclipse Committee of the Academy. In view of the rather favourable prospects, it was decided to organize an expedition of some size. An important subsidy, necessary for this aim, was granted by the Netherlands Organization for Pure Research (Z.W.O), so that the construction and the acquisition of the instruments could be started at the beginning of 1957.

The Canarian Islands and the western coast of central Africa were primarily considered for the observation of the eclipse. In view of the communications and meteorological circumstances [1] the island Fuerteventura seemed to be the most favourable place. The report of Professor H. VON KLÜBER [2] contained most important information concerning the circumstances on the island.

We also took into account the advantage to be obtained by performing observations from a point near the limit of the belt of totality, and decided to set up our camp in the surroundings of the little port of Gran Tarajal, 6 km within the zone of totality, of which the total width amounted to 111 km. The data corresponding with the site of our camp, as they were determined later on in Gran Tarajal are as follows:

geographical position, latitude 28°.2064 N, longitude 14°.0200 W;
moment of 2nd contact, $11^h46^m29^s$ U.T.;
moment of 3rd contact, $11^h47^m40^s$ U.T.;
altitude of sun at mid-totality, 53°;
position angle of 2nd contact, 54°;
position angle of 3rd contact, 3°.

The instruments and the program of observation

Ultimately the program of the expedition consisted of four observations:

1. Photography of the chromospheric spectrum between λ 3885 and λ 4120 Å with a slit-spectrograph, equipped with glass prisms;

2. Photography of the chromospheric spectrum between λ 3400 and λ 4050 Å with a slitless grating spectrograph, provided with a concave mirror;
3. Photoelectrical measurements of the brightness distribution at the extreme limb of the sun in four wavelength regions;
4. Photographical observations of prominences in continuous light and in Hβ with a double camera.

1. The *prism spectrograph* was provided with a wide, semi-circular slit with a central narrow part. A series of spectra of the extreme limb of the sun and of the chromosphere were to be taken in the wavelength region λ 3885 λ 4120 Å, on films of a width of 14 cm. The two 45° prisms had a size of 15 cm × 18 cm (lateral area) and had been mounted in autocollimation. A simple lens with a diameter of 15 cm and a focal distance of 296 cm was used. So far the instrument described is the same as that already used for the observation of the eclipse in 1955 on Ceylon [3]. However, some improvements have been introduced: the lens was placed closer to the prisms, so that a better filling up with light was obtained; the exposure mechanism was made automatic by regulating the times of exposure with an electronic relay; the curtain shutter was replaced by a rotating cylindrical screen, which had already been used at the eclipses of Khartoum (1952) and Gotland (1954) with the same instrument.

The spectrograph was to be used in a horizontal position. The short lateral tube, on which the slit had been mounted was inclined at an angle of 4° downwards. The instrument was fed by a 30 cm coelostat mirror, reflecting the sunlight through a photographical objective of Steinheil, diameter 25 cm, focal distance 340 cm, a solar image of 32 mm being formed on the slit plate. The coelostat and the objective had been mounted on a small low table.

The azimuth of the reflected beam had been chosen such that in the image of the sun the line joining the points of the 2nd and 3rd contact was vertical.

In the spectrum, which was, consequently, practically horizontal, the crescents at 2nd and 3rd contact made an angle of 60° with the direction of the disperson (see fig. 3).

During the totality the slit was to be turned around its centre; at the beginning the narrow part of the slit was tangential in the point of second contact, round mid-totality in a point of the limb of the sun half-way the points of contact, and at the end of the totality in the point of third contact. The aim of our observations was to obtain with the broad parts of the slit total intensities, integrated over the height of the chromosphere, while the narrow part of the slit should yield profiles of strong lines in the region observed (see also [3]). The exposures for the calibration could be made either by means of the image of the sun on the slit, or by

placing before the slit a MgO screen as a diffuser, exposed directly to the sun. In both cases on the narrow part of the slit, 7 mm in height, a platinum step-weakener with 7 steps was placed.

2. The *grating spectrograph* was constructed especially for the occasion of this expedition. It was provided with a flat Rowland grating of 5×8 cm^2, 568 lines/mm, borrowed from the solar spectrograph of the Utrecht observatory, and used in the second order. The horizontal beam was brought to a focus by a concave off-axis mirror (diameter 20 cm, $f - 479$ cm), a dispersion of 0.6 mm/Å being obtained. The off-axis mirror was kindly put at our disposal by Professor A. C. S. VAN HEEL of Delft.

In three cameras of the same type as in the prism-spectograph a length of 40 cm of the spectrum could be photographed. The central camera was placed vertically, the left and right one were mounted horizontally behind two flat mirrors at 45° in order to avoid a screening of the light. The spectral area to be photographed extended from 3400 to 4050 Å. The Balmer jump and the last lines of the Balmer series were included in the central camera. To admit only the light of the right wavelengths, close in front of each film a Schott colour filter of 1 mm thickness was placed, from the short to the longer wavelength regions one UG 11, again an UG 11 and an UG 5 filter respectively.

The transport of the films and the operation of the shutters were achieved by means of magnetic couplings and worked independently and separately for the three cameras. The main aim of the observations was to compare the spicular structure of the chromosphere in the different emission lines. Further we hoped to derive from the successive spectral records, absolute intensities and gradients of weak lines and the wings of the H and K lines, as a function of the height, at several places along the chromospheric area. Finally we hoped to get information about the Fraunhofer spectrum of the extreme limb of the sun.

The optical pieces of this spectrograph were mounted in an open frame of Dexion aluminium strips. The instrument was made light-tight by means of black canvas. The protection against heating by the sun was achieved by a shelter of white canvas, set up over the instrument.

The testing of the instrument in the limited space of the Utrecht Observatory was not a simple operation. The instrument had been mounted in the meridian room and the sunlight was admitted to it via an outside- and inside mirror. In this way the Fraunhofer spectrum could be recorded and an estimate be obtained for the times of exposure, necessary for the chromospheric spectrum. Besides the sun, also a hydrogen tube and a mercury lamp, placed before an auxiliary slit, were used as sources of light for the focussing and the centering of the optical parts. The light through the slit reached an auxiliary concave mirror ($f - 177$ cm), which was used as a collimator, the parallel beam having the same direction in which the sunlight was expected to come during the eclipse.

The off-axis mirror could be turned round a horizontal axis in steps of 1'/16 by means of an electromagnet. This had to take place during the eclipse at 1/3 and 2/3 of the period of totality in order to keep the spectrum central in the open spaces of the shutters.

The focussing was done by moving the off-axis mirror by means of a motor.

To the left and right of the cameras short parts of the spectrum could be seen through a magnifying-glass. If on the left side the line H_γ was visible in the first order of the grating, we should know that the second order spectrum was at the right place in the cameras.

For the recording of the calibration spectra the slit and the collimator mirror were inserted. In front of the slit we then mounted a MgO-screen and a rotating sector, provided with 7 steps.

This horizontal spectrograph was fed by a coelostat mirror of 25 cm diameter. The orientation of the sun in the reflected beam was almost the same as with the prism-spectrograph, so that the crescents at second and third contact here too made practically symmetrical angles of 60° with the direction of the dispersion.

3. The *photo-electrical observation* of the brightness distribution at the extreme limb of the sun was made in four wavelength regions, transmitted by interference filters of 5×5 cm², centred at 6200 Å, 5500 Å, 4770 Å and 4270 Å with half value widths of 120, 120, 60 and 60 Å.

In each of the wavelength intervals the light of the solar crescent, just before the second and just after the third contact, was admitted on a multiplier connected with a mirror-galvanometer (time of response 1,60 sec, make Stylo, from Kipp). The deflections of the light beams of the four galvanometers were recorded on 2 rotating drums, provided with photographic paper of 24 cm width, which moved with ca. 2 cm/sec. While the illumination decreased (near 2nd contact) the sensitivity could be increased in steps with known factors; after the third contact, these arrangements were reversed. By these means care was taken of rapid recording, careful isolation of nearly monochromatic regions and the possibility of bridging great intensity ratios.

The photocells and filters were placed behind 4 tubes with a length of 40 cm, on a parallactical mounting. On behalf of the calibration, MgO screens could be placed in front of the tubes, and exposed to the sun. To determine in advance the sensitivity during the eclipse, the instrument was directed towards the full moon.

The parallactic mounting was placed under a movable sunshade from where cables led to the recording apparatus in a light-tight space to be occupied by one of the observers. This space, about $2\,\text{m} \times 2\,\text{m} \times 2\,\text{m}$ had been built of Dexion-aluminium and black canvas, over which, with some space in between, a tent of white canvas was placed.

4. *The observation of prominences* was to be made with two parallel horizontal cameras, by photographing (*a*) in continuous light at λ 6200 and (*b*) in the emission line H_β (λ 4861).

The comparison of both emissions would provide direct data for the determination of temperature and electron-density in the prominences. A Zeiss refractor, f = 137 cm, aperture 79 mm and a Rüdersdorf refractor, f = 120 cm, aperture 80 mm, were provided with a Leica 35 mm camera, in which Agfa IFF 13/10 din film was used. Both wavelength regions were isolated by means of Zeiss and Balzers interference filters, placed just in front of the films. The top transmissions of these filters were 39 and 26.5 % respectively; the half widths, 66 and 58 Å. Both refractors were placed close to each other and could be fed through one coelostat mirror with a diameter of 25 cm. The mirror was driven by a Foucault regulator. In order to ensure the sharpest images, a new coelostat mirror of pyrex glass was used (manufacturer Ross, England). Focussing had been made by means of the moon. For the calibration collimators were used, provided with simple lenses of 2 dioptries, and inserted in front of the refractor. A rectangular diaphragm in the focal plane of each collimator, illuminated by a diffusing MgO screen, was photographed as a density mark. The density scale was obtained by means of a rotating sector with 7 steps, placed in front of the diaphragm. During the eclipse both cameras would be exposed simultaneously and a series of records with different exposure times would be made; time marks could be recorded on the same paper strip on which the photo-electrical observations of the limb darkening were recorded.

The coelostats for both spectrographs were driven electrically with synchronic motors, for which the exact frequency was generated by a frequency-standard, constructed at the Utrecht Observatory. By means of direct current motors, the rotation of the mirrors of each of the instruments separately could be slowed down or speeded up.

For recording the times of the exposures made with the spectographs, a 9 pens chronograph was used. Also this instrument was specially constructed at the Utrecht Observatory. The paper strip with a width of 10 cm moved with a velocity of about 20 mm per second; the time marks were written with ball-points; one of them responded to the second marks of the chronometer Nardin, two others to the exposures with the prism-spectrograph and the other six to the exposures with the 3 cameras of the grating spectrograph.

For the electrical feeding of the instruments 20 storage cell batteries had been taken of the brand Prest-O-Lite, which have the advantage that, after being filled with acid, they are instantly loaded for 80 %. The loading could be maintained by 2 petrol aggregates.

Preparations

At the Utrecht Observatory all preparations of the expedition took place, including many discussions, the building and testing of the instru-

ments and the organization of the transport to and the stay at Fuerteventura.

The observers and their tasks were:

Dr. J. HOUTGAST, leader of the expedition, prism spectrograph;
Dr. D. KOELBLOED, grating spectrograph;
T. DE GROOT, photoelectrical measurements and frequency standard;
M. KUPERUS, prominences;
A. SCHADEE, time service;

Professor M. G. J. MINNAERT was to join the expedition ten days before the eclipse and during the eclipse he was to assist Mr. DE GROOT.

Mrs. KOELBLOED was to look after the housekeeping and, if necessary, she was to do medical work; moreover, she could act as an interpreter. Messrs. N. VAN STRATEN and J. VAN DEN BROEK took care of the technical side and of the assistance in operating the grating and the prism spectrograph. For safety every member of the expedition had been inoculated against typhoid fever by Dr. DOORSCHODT and Dr. DE WAARD at the Hygienic Laboratory at Utrecht.

The travel agency "Cook" had been charged with the booking of the passage and the stay over there. The transportation of the instruments from Amsterdam to Las Palmas vice versa was arranged by the V.N.S. (United Shipping Company) in Amsterdam, which obliged the Eclipse Committee by carrying out this transportation free of charge.

The departure of the 8 observers took place on August 13, 1959. They arrived on August 14 by train in Barcelona, where they embarked and arrived on August 19 at Las Palmas via Santa Cruz de Tenerife. Here the necessary formalities, such as the customs and the care of further transportation could promptly be arranged by the intermediary of Mr. E. L. Wood and "Wagons Lits Cook". The next night the observers sailed with a smaller boat to Fuerteventura, where they reached the little port of Gran Tarajal early in the morning of August 20. Five members of the expedition went ashore with small boats, while three of them sailed to Puerto del Rosario, the capital of the island, where the expedition-car, a landrover, would be discharged. They were very pleased indeed to make acquaintance there with the first official authority on the island, Mr. J. M. GONZALEZ, who promised the expedition all necessary help.

The instruments and accessories, packed in 55 cases and bundles, with a total weight of 2500 kg, arrived in Gran Tarajal on August 22 without appreciable damage.

Our stay at Fuerteventura

The members of the expedition were lodged in the boarding-house of Mr. P. REYES. The heat and the unaccustomed food had a rather unfavourable influence on the health of the observers during the 6 weeks

of their stay. The medicines we had taken with us from Holland, which had been kindly placed at our disposal by the firm of Pfizer by the intermediary of Mr. VAN STRATEN, have rendered service many times.

We are very grateful to Dr. GUERRERO for his help and medical assistance as well as for the hospitality shown by him and his family. We are also much obliged to the mayor of Gran Tarajal, Mr. FELIX FUMERO, for his attentiveness and readiness to meet all our difficulties in establishing our camping. The population of Gran Tarajal has met our presence with a very pleasant attitude.

On the day of our arrival I went with the mayor to look for a place for our observation camp. Finally a piece of ground of 25 m × 33 m, surrounded by walls, was placed at our disposal. It was situated at a distance of only 100 m from our boarding house, easily accessible to cars and fairly free from dust. After the mayor had placed some fences and the ground had been cleared it had become an almost ideal place for an eclipse camp.

The instruments were orientated by means of a theodolite put at our disposal by Professor A. KRUIDHOF of Wageningen. For the fixing of the azimuth use was made of the triangulation mark on a hill east of our camp at a distance of 1200 m, the direction of which was fixed via the pole-star and the sun. The coordinates of the camp were read from an ordnance map and verified by measuring longitude and latitude. With these coordinates and the formulas given by Mr. J. MEEUS (personal communication) the eclipse data were obtained, as mentioned in the introduction.

The legs and supports of Dexion aluminium of the tables, on which our instruments were mounted, could easily be driven into the soil of sand and stonegrit. We had some trouble with the big grating spectrograph, as it was very difficult to make the cover of black canvas light-tight. When we had managed this we got the impression that the tables, on which the slit, the grating and the mirrors were mounted, were not entirely free from vibrations. These tables were thereupon successfully replaced by mortared stone blocks.

In the coelostats spare mirrors were used until the day before the eclipse, except for taking the absolute intensity standards. During the weeks of our stay our chronometer Nardin was rated by means of radio time-signals. The apparatus, used for this purpose had been put at our disposal by the Netherlands Postal Authorities. The daily rate varied between $-0^s.5$ and $-1^s.5$ a day and on the eclipse day the time indication could be trusted within 0.2 second.

The development of the films, taken in the course of the photographical preparations, took place in an improvised dark room, a small room of our residence, arranged for this purpose. The water we needed was supplied by our own distillation apparatus; because of the heat it was necessary to cool it with ice and fortunately in the last few weeks of

our stay we could obtain this from a new installation in the town.

Rehearsals, which became more extensive successively, had already been held before every preparation for the observation of the eclipse had been finished. During the last fortnight rehearsals were held at eclipse-time as well as in the evening twilight.

The last few days before the eclipse definite calibration spectra on the eclipse films could be made with both spectrographs under ideal circumstances about eclipse-time. The exposure-times of these spectra were recorded on the chronograph paper.

The cloudiness appeared to be according to our expectation on an average of 40 %: the weathertype was rather constant with a N.E. wind and at eclipse-time rising cumuli. Thirty-three per cent of the days would have been useful for eclipse observations. 19 % useless and 48 % ideal. The cumuli had the tendency to remain floating above the valley, and to expand there. Often the sky above us was heavily clouded, while towards the horizon, especially to the S.W., the sky was cloudless. With some anxiety we looked forward to the circumstances on eclipse-day: however, for the other expeditions on the S.W. part of the island things looked more hopeful.

By car we payed a visit to the other expeditions as far as we could reach them. They were: the little Spanish expedition, where we met Dr. Carasco; the expedition of Professor H. von Klüber, where our expedition made a welcome stay after the long trip through the desertlike country, and the American expedition under the leadership of Dr. Dunn. These expeditions had all settled down near and in the little village Morro del Gable. However, it was not possible to visit Professor Allen on the most southwestern point of the island because of lack of time.

At about a week before the eclipse we visited the camp of the Netherlands amateur astronomers, under the scientific leadership of Dr. C. de Jager from Utrecht, who had mounted an extensive tent-camping at about 10 km from Gran Tarajal, near a small fishervillage, Tarajalejo. Everywhere the instruments were shown and the observational techniques discussed. We could not know then that on eclipse-day compact clouds would extend over the whole part of the island situated to the south-west of Gran Tarajal.

Eclipse-day

On October 1, the weather changed; the wind turned south and depression clouds appeared over the island. In the morning of October 2, even raindrops fell, the first during our stay! The weather conditions were critical but we kept good heart, being used to changing of cloud-formations.

The "Guardia Civil" appeared at our terrain in order to keep the public at a safe distance and to keep them quiet. The instruments were submitted to a last inspection and were put into readiness. Except for

the instruments already mentioned, two filmcameras were also installed. With one of them, a Bell and Howell, filled with 16 mm Kodachrome film, the eclipsed sun would be filmed from just before, until just after totality. For this purpose the camera had been provided with a tele-objective and adjusted at a velocity of 8 images a second. This camera had been placed at our disposal by the firm of Foka in Rotterdam. With the other camera, a Pathé, lent to us by the Foundation Film and Science-University Film (S.F.W.-Unfi) in Utrecht, it was planned to make a picture of the sky along the horizon during totality. For this work we had the help of Mr. Luwis Monreal who, well instructed, operated on the beach, and made a turn of 360° with the camera during the totality.

In the last quarter of an hour before the second contact the clouds changed many times; while the time service called the last few minutes it was not yet to be predicted whether the totality would be observed through the thin clouds or that heavy clouds would prevent any observation.

For the last time the observers inspected whether the sunlight was led to the instruments in the right way. Especially at the slit spectrograph the crescent had to be adjusted exactly to the circular slit. The responsible observer regulated the velocity of the coelostat and the orientation of the slit, while he recorded the course of these corrections in a microphone of a tape recorder. On this tape also the sounds of the exposure mechanism of the prism spectrograph were recorded, as well as the time calling.

The moment zero, the real beginning of the totality, would be called at the moment of disappearance of the crescent on the slitplate. This was especially meant for the observer who regulated the exposure times of the grating spectrograph.

It was planned to begin the observations with the photo-electrical apparatus 40 seconds before second contact and those with the spectrographs about 20 seconds later; the latter at the zero-moment to be switched over to a series of exposure times, which had been planned in advance.

The changing aspect of the swiftly passing clouds, however, made a good fixation of the zero point impossible; when suddenly a dark cloud passed, the zero-signal was called by me, many seconds too early as appeared afterwards. Quite naturally this gave some confusion which was of little influence, however, owing to the training and control of the observers.

During the eclipse observations all instruments worked well, 20 to 30 seconds after the totality the observations were finished.

The situation with regard to the clouds had been such that reasonable results could be expected. However, the determination of absolute intensities had to be abandoned, but the program had been drawn up in such a way, that also relative measurements were valuable. At the end

of the eclipse telegrams were sent to Holland, including Z.W.O. and the Utrecht Observatory, informing them of the circumstances and the course of the observations.

Meanwhile the situation of the weather grew worse. There was no possibility of making a second series of calibration records on the same film in order to enclose the eclipse spectra in between two sets of calibration spectra. So, we immediately could start breaking up camp; packing the instruments was already in full swing at the end of the eclipse-day. During the next night heavy rains and thunders broke out. On October 6, everything was ready for transportation; the instruments were shipped to Las Palmas on October 7, and from there to Amsterdam. On October 30, the whole camp equipment was back at the Utrecht Observatory. Meanwhile also the observers had left the island. Professor MINNAERT left on October 3, by plane; the others on October 6, by boat. Also this time the car was transported via Puerto del Rosario. The 8 members of the expedition passed another 3 days in Las Palmas to wind up business and to pay a farewell visit to the Netherlands consul, Mr. J. MIJERS.

The embarkation took place on October 9, with the boat to Malaga. Here Mr. DE GROOT and Mr. SCHADEE went by train to Holland; the 6 others by car. The eclipse-films and chronograph strips had been trusted to Mr. DE GROOT. On October 17, all were home again.

The results

Mr. DE GROOT was the first who could show the eclipse-results. The paperstrips, 24 cm large and about 4 m long, record the intensity variations of the sun's crescent in the 4 wavelength regions. Though the curves show large fluctuations caused by scintillation and clouds, a comparison of the 4 colour regions can lead to valuable data.

Mr. KUPERUS obtained a number of sharply defined images of the prominences and corona in the continuum at λ 6200 and in Hβ. As exposures of the same duration at both wavelengths always had been taken simultaneously and the various exposures include all degrees of photographic density, the observational aim has been reached.

The film of the prism-spectrograph, 14 cm wide, contained a total of over 100 eclipse and calibration spectra over a length of about 10 m. The film was developed in parts, each part containing 12 or 13 spectra, in plastic trays of 85 cm length and 16 cm width. The development took place in Rodinal 1:75 at 20° C during 15 minutes, moving the bath continually and stirring with a soft camelhair brush. The circumstances of temperature, concentration and duration of development as well as the way of development were always the same within narrow limits.

The 18 spectra taken round second contact show the monochromatic chromospheric crescents in the wide parts of the slit, and to a certain extent the profiles of the emissions in the narrow part, between λ 3885

and λ 4120 Å. The two spectra, recorded at mid-totality from the N. and S. point, halfway between the contact points, show no trace at all of the strongest chromospheric lines, although they were exposed for 10 and 20 sec. The sharpness is reasonable, though not maximal. The self-reversals in the H- and K-lines of Ca II are visible. The spectra round third contact are largely spoiled by clouds and by a missetting of the image on the slit. The calibration spectra are of good quality and free of stray light so that good density curves will be obtained.

Finally Dr. KOELBLOED developed the films of the grating spectrograph, using the same method as with the film of the prism-spectrograph.

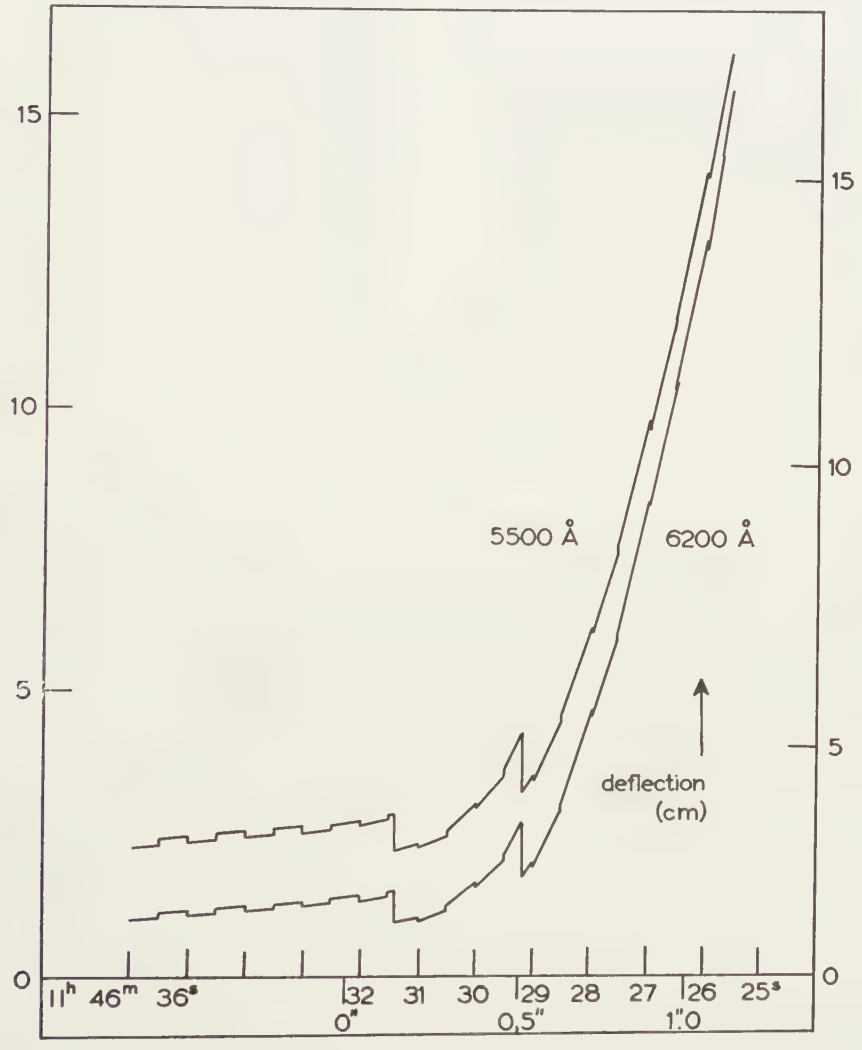

Fig. 1. Photoelectrical records of the intensity of the last crescent at second contact for two wavelength regions, with time marks and jumps in sensitivity, plotted against time and distance in seconds of arc on the sun.

The three films each contain a wavelength region of 200 Å over about 12 cm, together covering the region from 3400-4050 Å. The number of spectra per film amounts to about 90, from which 14 were taken during totality, 70 before and after totality and 5 for the calibration. The spectra of the shortest wavelength region are for the greater part underexposed. Most of the other spectra are of good quality, with only the minor defect of streaks in the middle part spectrum, caused by inhomogeneities in the colour filter that had been placed in front of the film.

The definition of the spectral and chromospheric details is very good, so that e.g. the selfreversals in the H- and K-lines are clearly visible (slitless!) and also interesting details of prominences. Among the features that look most promising for investigation are the reversal of the Fraunhofer spectrum at the sun's limb, the wings of H and K in absorption as well as in emission, the comparison of many weak lines of different atomic origin and the structure of prominences in different emissions.

In the figures 1–6 some of the records of the expedition are reproduced. Figure 1 shows some curves obtained from the photoelectrical measurements of the limb-darkening.

Figure 2 shows a pair of simultaneous exposures with the double camera for prominences.

Figure 3 shows a spectrum near second contact taken with the prism slit spectrograph, in which the spectral strip corresponding with the narrow part of the slit, coinciding with the point of second contact, can be clearly distinguished.

The figures 4–6 show some of the spectra taken with the grating spectrograph. Figure 4 shows the region λ 3400–λ 3600 Å closely before second contact, emitted by a crescent of a maximum width of 4″. In figure 5 two spectra show the region with the higher members of the Balmer series in two stages of the eclipse; it is interesting to note the increasing inhomogeneity of the chromosphere in higher layers. In figure 6 the wings of the H-line and K-line are visible, in 6a in absorption, in 6b in emission.

Concluding it can be said that this expedition has brought home a welcome amount of interesting observational data. The members of the expedition are grateful to all who contributed to the achievement by their help and interest.

LITERATURE

1. Torroja, J. M., Comisión National de Astronomia, Publ. 2, Madrid 1956.
2. Kluber, H. von, Sites for observation of total solar eclipse of 1959, October 2.
3. Houtgast, J., Report of the Netherlands Expedition to Ceylon, Proc. Kon. Ned. Ak. v. Wetensch., Amsterdam, Ser. **B 59**, nr. 4, (1956).

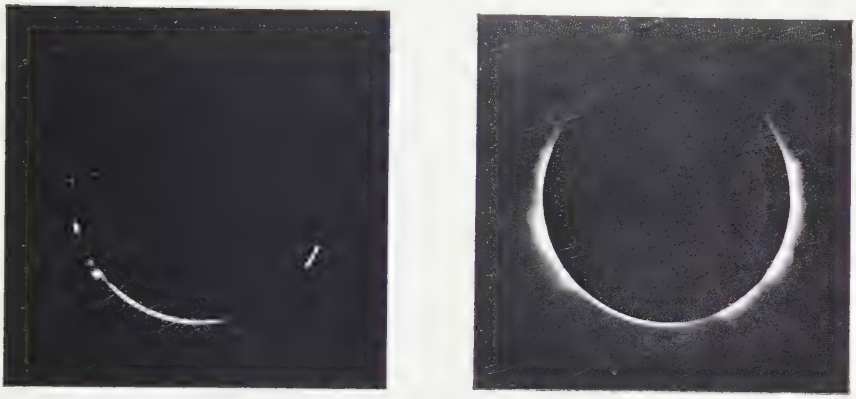

Fig. 2. One pair of the simultaneous exposures in H_β (left) and in the continuum at λ 6200 (right). Exposure from $11^h\,46^m\,43^s.95$ to $47^s.75$. (about two times original size).

Fig. 3. One of the exposures taken with the prism spectrograph at second contact ($11^h\,46^m\,29^s.04$ to $30^s.01$). Wavelength region H 8 (λ 3889) - Hδ (λ 4102); semi-circular slit with narrow central part. (·55 original size).

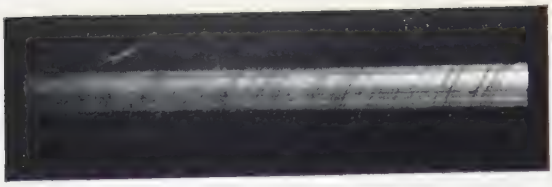

4. wavelength region λ 3400-λ 3600 Å, taken from $11^h\,47^m\,58^s.47$ to $58^s.61$

5. wavelength region λ 3610-λ 3830 Å:
a) $11^h\,46^m\,26^s.54$ to $26^s.97$; *b*) $11^h\,47^m\,24^s.18$ to $27^s.62$.

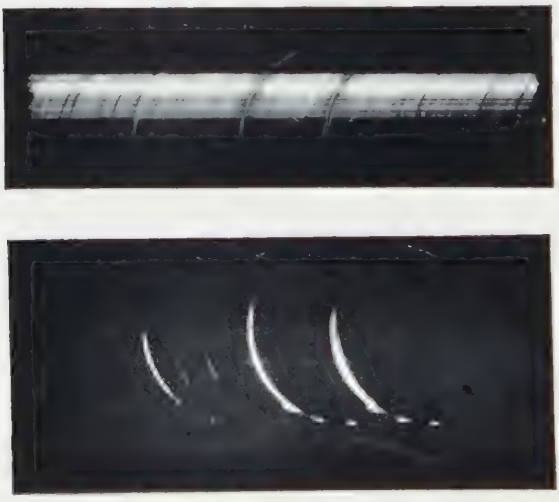

6. wavelength region λ 3840-λ 4050 Å;
a) $11^h\,46^m\,31^s.88$ to $33^s.21$; *b*) $11^h\,47^m\,56^s.92$ to $57^s.03$.

Figs. 4, 5 and 6. Exposures taken with the slitless grating spectrograph. (all figures ·55 of original size).

NOTES ON THE BETIC OF MÁLAGA NEAR VÉLEZ RUBIO (SE SPAIN)

BY

H. J. MAC GILLAVRY, TH. B. ROEP AND T. GEEL

(Communicated by Prof. H. A. BROUWER at the meeting of June 25, 1960)

Abstract

Occurrence of *Novakia sp. indet.* in the Paleozoic of the Betic of Málaga near Vélez Rubio indicates the presence of beds of Devonian age. Detritus in Paleozoic graywackes comprises *a*) crystalline schists; *b*) leucocratic igneous rocks; *c*) non-metamorphic rocks of a eugeosynclinal assemblage. The presence of the crystalline schist material proves the occurrence in the source area of a pre-hercynian metamorphism, which is probably older than the eugeosynclinal suite.

The Mesozoic and Eocene rocks occurring in the same zone are considered to belong with the Betic of Málaga, and not to be penibetic parts of the subbetic realm.

Between the monotonous phyllitic complex of the Sierra de las Estancias in the South, and the subbetic Mesozoic of the Sierras de Orce, de Maria and de la Culebrina in the North, occurs a narrow zone of great tectonic complexity, on which are situated the castillo of Vélez Rubio and the ruins of Xiquena. In his note of 1933 BLUMENTHAL considers the phyllitic complex of the Estancias Mountains to form part of the tectonic complex of the Alpujarrides, while the intermediate zone of the Vélez Rubio castle is considered to form part of the tectonic unit designated as Betic of Málaga, with some elements of doubtful provenance called penibetic. This view is adopted by FALLOT in his work of 1945 on the subbetic between Alicante and the Rio Guadiana Menor. In 1948 FALLOT (p. 46) considers the "penibetic" elements of the zone of the Vélez Rubio castle to belong to the subbetic realm. Both BLUMENTHAL and FALLOT agree, that the Betic of Málaga constitutes the highest tectonic element of the Betic chain (FALLOT, 1948, p. 32). Various other solutions for the structure of the region have been presented in the literature, but a full discussion of these falls outside the scope of this paper.

Field activities of H. A. BROUWER and his students, usually referred to as the Dutch School, were interrupted some twenty-four years ago. Fieldwork was resumed by the Amsterdam University in 1958 by a joint enterprise of W. P. DE ROEVER, C. G. EGELER, H. J. MAC GILLAVRY and a team of students. The stratigraphic group commenced work in 1959 in the neighbourhood of Vélez Rubio (Miss T. GEEL) and of Xiquena (Mr. TH. B. ROEP). New results obtained in the Betic of Málaga zone form the subject of this preliminary note.

The section in the zone under consideration comprises Paleozoic formations, which, though hardly metamorphic, nevertheless show an incipient cleavage; in addition there are various younger formations which do not show any metamorphism at all. Among the latter are described Permotriassic conglomerates, sandstones and dolomites; Liassic dolomites and limestones; light-coloured Tithonian limestones; and Eocene nummulitic limestones. (Blumenthal, Fallot, Llopis Lladó). The tectonical conditions in the zone are exceedingly complex.

The Paleozoic consists of graywacke-like sandstones, intercalated conglomerates, finer-grained sandstones, siltstones, beds of dark limestone, and dark lydite-breccia. The fine-grained sediments show an incipient slaty cleavage, which is the only hercynian influence visible. Fossils have not been reported in the literature from this region in so far as we have been able to ascertain. The age of the complex was, therefore, unknown, and a Paleozoic age was thus far only based upon the lithologic similarity to the Paleozoic in the neighbourhood of Málaga (Blumenthal), and upon the fact that the formations show an incipient slaty cleavage not shown by the Triassic and younger formations. Llopis Lladó considers these rocks as Carboniferous because of their resemblance to the Carboniferous of Asturia. Blumenthal compares the formations with those units in the neighbourhood of Málaga, which have been determined as Upper Silurian to Lower and Middle Devonian (zone of the "calizas alabeadas"), and as Upper Devonian to Lower Carboniferous (zone of the higher graywackes and slates) (cf. Blumenthal, Michelau and Kockel in Kockel, 1958).

One of us (Th. B. Roep) has been fortunate in discovering fossils in the Paleozoic near Xiquena, namely limestone intercalations with *Novakia sp. indet.*, ? styliolines, and a trilobite. Elsewhere occur unidentifiable plant remains, and occasional trochites. The *Novakia* have been identified by Dr. J. E. Hede in Lund, who considers them to be of Devonian age, though not specifically identifiable. In addition a polygenic conglomerate was found, resembling the Marbella conglomerate of the region of Málaga (cf. Kockel, p. 256). The calcareous elements in this conglomerate contain gastropods, corals, and crinoid stems, amongst which one with a central canal in the shape of a five-pointed star. Mr. A. Breimer of Leiden informs me that the latter, though not common, gives no evidence of age. After treatment with monochloric acetic acid, these limestone elements yielded Foraminifera amongst which an involute form, possibly an *Endothyra*? These finds confirm the resemblance in lithology and age of the Xiquena section to that of Málaga.

Owing to the tectonic complexity of the area, it has not yet been possible to unravel the internal stratigraphy of the Paleozoic; however, it would seem that at least the Devonian and possibly the Carboniferous are represented.

The detritus in the graywackes and in the conglomerates associated with them can be roughly classed into three groups:

a) a metamorphic assemblage represented by quartz- and albite-rich schists, schists with chlorite and biotite, garnet-bearing schists, and furthermore frequent detrital garnet. There is furthermore abundant detritic biotite, the origin of which is less clear.
b) leucocratic igneous rocks, consisting of quartz and felspar, with some biotite, which is usually chloritised. Some granophyric detritus has also been found.
c) a eugeosynclinal assemblage, comprising acid volcanics, spilite and black- and light-coloured radiolarite. Some limestone pebbles, which contain unidentifiable organisms, may belong to this assemblage. These rocks may be somewhat strained and veined, but do not show any metamorphism. Some of the quartz phenocrysts in the acid volcanics do not even show wavy extinction.

The schistosities of the metamorphic detritus have different orientations. Accordingly we have clear proof of a metamorphism in the source area. This metamorphism must be pre-hercynian, and, though this cannot be rigidly demonstrated, it seems highly probable that this metamorphism belongs to a tectonic cycle which is appreciably older than the time of deposition of the eugeosynclinal rocks, which yielded the detritus of the third group.

The resemblance of the formation to the Paleozoic of the region of Málaga has already been mentioned. There is also a complete resemblance to rocks found further south near Huercal Overa and in the northern slope of the Sierra Cabrera (De Booy and Egeler, 1960, in press). This resemblance holds both for the assemblage of different rock types and for the detritus contained, the deviations being of minor importance only. As stated by De Booy and Egeler (1960), this makes it very probable that the Betic of Málaga must indeed be a higher tectonic unit than the Alpujarrides, which in turn are underlain by various crystalline formations.

It is to be noted, that a high position for the Betic of Málaga is usually considered to imply a southern derivation of the nappe. Thus the sediments of the zone of the Vélez Rubio castle should have been deposited further south than the Alpujarride basin. In order to find an argument for or against such a derivation one should have some specific indication such as a highly specific kind of detritus, in addition to a full knowledge of the geology of the Iberian and North African Paleozoic, and, worst of all, of those parts which may have disappeared into the present Mediterranean. Such is not the case. The detritus of groups b) and c) (leucocratic rocks and eugeosynclinal assemblage), with the exception of the organic limestone pebbles, is identical in all respects to the detritus found in the Visean graywackes of the Baixo Alentejo in southern Portugal, which, however, do not contain the crystalline elements nor any biotite

(Mac Gillavry, 1961, in press). However, this detritus cannot be considered as specific and the similarity may be merely superficial.

With regard to the Mesozoic and Tertiary formations which accompany the Paleozoic in the zone of the Vélez Rubio castle, great similarities exist both in succession, facies and thickness, with the areas further south to be described by De Booy and Egeler. This suggests that these rocks belong simply to the Betic of Málaga, and that they do not constitute elements torn from the roots of the Subbetic (Fallot 1948, p. 46). It must be admitted, as has been pointed out by Fallot (1945, p. 406), that there are also similarities of facies between the Betic of Málaga and the Subbetic in some stratigraphic units, but there seem to be notable differences of succession and thickness.

Acknowledgements

The authors wish to express their thanks to the Spanish authorities and to the Royal Netherlands Embassy at Madrid, for their cooperation; to Dr. J. E. Hede and Mr. A. Breimer for the examination of some of our fossils; to Professor C. G. Egeler, professor W. P. de Roever, and Dr. T. de Booy for many discussions and suggestions.

BIBLIOGRAPHY

Blumenthal, M. M., Das Paläozoikum von Málaga als tektonische Leitzone im alpidischen Andalusien. Geol. Rundschau, XXIV, 3/4, 170–187 (1933).

Booy, T. de and C. G. Egeler, Occurrence of Betic of Málaga elements in the south eastern part of the Betic Cordilleras (SE Spain). Geol. en Mijnb. 6, 253 (1960).

—— and ————, The occurrence of "Betic of Málaga" in the Sierras Almagro, Cabrera and Alhamilla (SE Spain). In press (1960).

Fallot, P. et R. Bataller, Observations géologiques sur la région de Vélez Rubio. C.R. Séances Ac. Sc. Paris, 187, 988–990 (1928).

————, Estudios geológicos en la zona subbética entre Alicante y el Río Guadiana Menor. Madrid 1945.

————, Les Cordillères Bétiques. Inst. Investigaciones geol. "Lucas Mallada". Estudios Geológicos 8, 83–172 (1948).

Kockel, F., Conodonten aus dem Paläozoikum von Málaga (Spanien). N. Jb. Geol. u. Pal. 255–262 (1958).

Llopis Lladó, N., Observaciones geológicos y morfológicas en el N. de Almeria. Arch. Inst. Aclimatacion, I , 7–55, VIII Pls. (1955).

Mac Gillavry, H. J., The upper Paleozoic of the Baixo Alentejo, Southern Portugal. In press (1961).

THE NATURE OF TOOTH ENAMEL PROTEIN AS SHOWN BY X-RAY DIFFRACTION *)

BY

W. G. PERDOK

(Communicated by Prof. PH. H. KUENEN at the meeting of June 25, 1960)

Introduction

Tooth enamel is the hardest tissue of the human body. It is far more densely calcified than bone, consisting for more than 96 % of orientated hydroxy-apatite crystallites embedded in an organic matrix the weight of which, when dry, amounts to roughly 0.5 %. The enamel being produced by cells of ectodermal origin it was generally believed that the organic matter must be of a keratinous nature, but recent investigations on the amino acids of the enamel protein created some doubts, as its hydroxy-proline content suggested some affinity with collagen. Moreover, the sulphur containing amino acid cystine was present in much smaller amounts than in other keratins.

The great importance of this organic matrix for the properties of the enamel has been pointed out by the author already in 1952 [1]). It was found then, that fluoridized enamel does not show the lattice contraction connected with the transformation of hydroxy-apatite into fluor-apatite as long as the organic matrix is intact. This remarkable fact points to the conclusion, that an intimate connection must exist between the apatite crystal structure and the repeat of molecular building units in the enamel protein. Apart from that, only under these conditions it is plausible, that a mass of very small apatite crystallites can be cemented together to such a rigid texture as tooth enamel shows.

At that time the author also suggested the possibility of epitaxial growth of the apatite crystallites on the protein fibres and emphasized the close agreement between the lattice parameters of apatite ($a = 9{,}4$ Å, $c = 6.9$ Å) and the mean repeat distances in β-keratin (equatorial reflection spacing 4.65 Å $= \frac{1}{2} \times 9.3$ Å and meridional reflection spacing 3.33 Å $= \frac{1}{2} \times 6.7$ Å). These views have been strongly supported by recent electron microscopic evidence obtained by R. FRANK, J. G. HELMCKE, H. LENZ *et al.* [2]), but up to now no X-ray diffraction patterns of tooth enamel

*) The results given in this paper have been communicated at the VII-th ORCA-congress in Hamburg, June 3rd, 1960.

1) W. G. PERDOK, Schweizer. Monatsschrift für Zahnheilkunde 62, 249 (1952).

2) Communications at the VII-th ORCA-congress Hamburg, June 3rd, 1960.

protein could be produced, allowing its nature to be established by measuring repeat distances.

It is true, that S. FEITELBERG and F. MEYER have communicated in a meeting of the American Crystallographic Association (Washington 1951) that tooth enamel gave the diffraction pattern of collagen, but no details have been published afterwards. This observation has probably been erroneous, as only dentin gives a collagen pattern. There is another assertion by Miss K. LITTLE [1]), stating that specimens of tooth enamel "prepared under conditions which would cause the less dense component to dissolve, give a β-keratin X-ray diffraction pattern", but hitherto neither photographs nor further details of how the specimens were prepared, have appeared in literature.

Preparing enamel slabs for X-ray diffraction

As the organic matter in tooth enamel hardly amounts to 0.5 % the chance of getting good diffraction patterns will be the greater the more the sample is decalcified. On the other hand, the organic matrix forms an extremely delicate network that, after complete decalcification, is destroyed by the slightest touching when it is attempted to fix it on a ring or in a capillary. Several discussions with doctor G. GUSTAFSON, head of the histopathological department of the Royal Dental School in Malmö (Sweden) led to a method of decalcification which proved to be successful, the details of which will be published elsewhere. The author is very much indebted to dr. GUSTAFSON for making the enamel specimens that gave the diffraction patterns shown in this paper (fig. 3 and 4).

Discussion of the diffraction pattern of tooth enamel protein

The photographs reproduced in fig. 1–4 have been obtained in a flat plate camera with cobalt radiation (specimen-film distance 50 mm); many details have been lost in the reproduction process.

The tooth enamel photographs are definitely fibre patterns — like those of wool (fig. 1) and calf's tendon (fig. 2) — in agreement with the fibrilar texture of tooth enamel observed in the microscope even at low magnifications. Fig. 3 shows a weak equatorial reflection besides the main spot, indicating that a secondary bundle of fibres is present, making an angle of roughly 30° with the main direction.

The tooth enamel pattern shows an equatorial arc of 13.5 Å and an equatorial diffuse spot of 9.5 Å, these spacings being close to resp. 3 · and 2 · the backbone spacing of the keratins: 4.65 Å. In collagen the corresponding spacings are 12 and 4.4 Å. However, on the tooth enamel pattern the strong and characteristic equatorial reflection of β-keratin at 4.65 Å is missing.

[1]) K. LITTLE, Journal of the Royal Microscopical Soc. **78**, 58 (1959).

Fig. 1

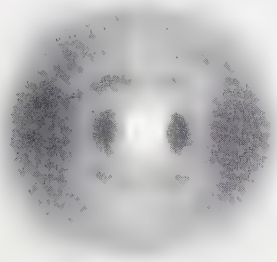

Fig. 2

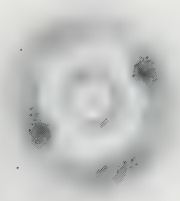

Fig. 3

Fig. 4

Considering the meridional reflections we find a sharp arc indicating a chain repeat of 19,9 Å, almost equal to 6× the characteristic fibre repeat of β-keratin: 3,33 Å and a more diffuse spot around 7.0 Å, close to 2×3.33 Å. Here the strong meridional reflection of α-keratin at 5.1 Å is missing, while the fibre repeats of collagen are 8,9 and 2,87 Å.

From these preliminary X-ray results it can be concluded that the tooth enamel protein indeed has a keratinous and not a collagenous nature, in agreement with histological evidence from enamel development studies. Though the pattern is not identical with that of β-keratin, the close agreement between the spacings found here and the lattice parameters of hydroxy apatite, as predicted by the author in 1952, is striking.

Further work is in progress on preparations with different decalcifying agents and with animal teeth in different stages of development.

As the pattern of tooth enamel protein lacks some characteristic reflections of α- as wel as of β-keratin, the author prefers to call the dental keratin: δ-keratin, of which the structure and its connections to the crystal structure of apatite is the subject of further investigations.

Kristallografisch Instituut der
Rijksuniversiteit, Groningen

CONTENTS

PRINTED IN THE NETHERLANDS
DRUKKERIJ HOLLAND N.V., AMSTERDAM